Concentration of whey proteins using the Pressurized Gas eXpanded (PGX) liquid technology and their characterization

by

Emily Ying Wong

A thesis submitted in partial fulfillment of the requirements for the degree of

Master of Science

in

Food Science and Technology

Department of Agricultural, Food and Nutritional Science

University of Alberta

Abstract

The Pressurized Gas eXpanded (PGX) liquid technology utilizes CO_2-expanded ethanol to simultaneously dry and purify high molecular weight biopolymers, producing micro/nanosized powders and fibrils with low bulk densities and high surface areas. The fractionation, concentration and drying of whey proteins directly from sweet- and acid-type whey was investigated using the PGX technology as a single unit operation to produce concentrated whey protein powders. The feasibility of processing a complex feedstock such as whey was first investigated using sweet whey on a laboratory scale system, followed by a 5× scale up to a bench-scale system and varied mass flow rate ratios (θ_{PGX}). Efficiently defatting and removing > 50% lactose from the dairy waste stream, whey powders containing ≥ 45% protein were obtained through the single-step concentration process. The concentrated whey powders were characterized in terms of their physicochemical attributes, specifically untapped bulk density, particle size distribution, specific surface area and pore size, surface morphology as well as the compositional analysis, protein composition and structure by determining the soluble protein content, analyzing the protein secondary structure, intrinsic protein fluorescence and protein hydrophobicity. PGX whey powders were primarily composed of major whey proteins, β-lactoglobulin, α-lactalbumin, and bovine serum albumin in the presence of amorphous lactose and milk minerals such as Ca, K, Mg, Na, P and S. The physicochemical attributes of the PGX whey powders were affected by the varying θ_{PGX} linked to the anti-solvent interaction with the biopolymer stream at the nozzle. At intermediate θ_{PGX} ratios, the whey proteins had similar protein structures to freeze-dried proteins, indicating that the PGX process is mild. At lower θ_{PGX} ratios, a reduced amount of PGX fluid (the CO_2-expanded EtOH that breaks up the biopolymer stream) limits the anti-solvent-polymer interaction, thereby favouring polymer-polymer interactions, and overall resulting in fewer disruptions to the

protein secondary structures (β-sheet and α-helix). With improved jet breakup at higher θ_{PGX} ratios, protein exposure to the solvent is increased, resulting in rearrangements of proteins to more compact configurations with increased protein hydrophobicity.

To assess the potential of the PGX technology for commercial applications to produce whey protein concentrates, ultrafiltration and spray drying were introduced as reference methods in the second study. To evaluate the versatility of the PGX technology, a second type of whey feedstock was also introduced. The results demonstrated that the PGX technology was comparable to a one-step ultrafiltration process in terms of protein concentration. Whey protein concentration up to 4.4× was achievable utilizing sweet whey, while only 2.7× protein concentration was possible with acid whey feedstocks. Lactose reduction ranged from 25-50% with more effective reduction in sweet matrices compared to acid matrices. This indicated that while it is possible to concentrate whey proteins from various whey feedstocks, obtaining high protein content products from acid whey was more challenging compared to sweet whey due to the high level of ash content and lower amounts of protein in the feed material. Overall, these research findings are significant in the continued application of the PGX technology for the development of value-added ingredients for nutraceutical applications.

Preface

The research reported in this MSc thesis is the original work by Emily Y. Wong, under the supervision of Dr. Feral Temelli, of the Department of Agricultural, Food and Nutritional Science at the University of Alberta. This thesis is comprised of five chapters: Chapter 1 provides background information and presents the research objectives; Chapter 2 is the literature review related to the topics of the two studies; Chapter 3 focuses on the processing of sweet rennet-type whey at two different scales, a laboratory and bench-scale system and characterizing the physicochemical properties of the dried powders; Chapter 4 compares the PGX technology to ultrafiltration using sweet and acid whey feedstocks; Chapter 5 summarizes the key findings and provides the recommendations for future work.

A version of Chapter 3 has been published by Emily Y. Wong, Byron Yépez, Bernhard Seifried, Paul Moquin, Ricardo Couto and Feral Temelli in the *Journal of Food Engineering,* 366 (2024) 111846 (https://doi.org/10.1016/j.jfoodeng.2023.111846). As the first author, I was responsible for the conceptualization, methodology, investigation, formal analysis, visualization, writing of the manuscript draft, editing and reviewing of the manuscript draft. Some of the experiments were completed at Ceapro Inc., supervised by co-author Dr. Byron Yépez who assisted in some of the experiments on the bench-scale system as well as providing research ideas and critical review of the manuscript draft. The other co-authors, Dr. Bernhard Seifried, Dr. Paul Moquin and Dr. Ricardo Couto provided research ideas, as well as contributed to the critical review of the manuscript draft. Dr. Feral Temelli was responsible for supervision, conceptualization, project administration and funding acquisition as well as the critical review and editing of the manuscript.

A version of Chapter 4 is currently under preparation for submission to a peer-reviewed journal by Emily Y. Wong, Byron Yépez, Bernhard Seifried, Paul Moquin, Ricardo Couto and Feral Temelli. I am responsible for the conceptualization, methodology, investigation, formal analysis, visualization, writing of the manuscript draft, editing and reviewing of the manuscript draft. Dr. Byron Yépez, Dr. Bernhard Seifried, Dr. Paul Moquin and Dr. Ricardo Couto contributed to the conceptualization of research ideas, and reviewing and editing the manuscript. Dr. Feral Temelli was responsible for supervision, conceptualization, project administration and funding acquisition as well as the critical review and editing of the manuscript.

Acknowledgements

I would like to express my utmost gratitude to my supervisor Dr. Feral Temelli, for your encouragement, patience and for sharing your immense knowledge. This research and my accomplishments throughout my graduate program would not be possible without your perpetual support and guidance. It was truly a privilege and honour to be a part of your research team as both an undergraduate and graduate student. Thank you for not only celebrating my professional achievements but also my personal achievements over all these years.

Next, my sincere gratitude to my team at Ceapro Inc., starting with Dr. Bernhard Seifried who embraced my addition to the PGX team and for the numerous opportunities he provided me. Thank you to Dr. Byron Yépez, Dr. Ricardo Couto, Dr. Paul Moquin and Javad Mahmoudi for your encouragement, support, and advice throughout my graduate studies.

Thank you to Dr. Lingyun Chen for being my supervisory committee member, for providing the analytical equipment and for your valuable feedback on all the protein characterization assays. Thank you to Dr. Roopesh Mohandas Syamaladevi for being my arms-length examiner and providing feedback for this thesis.

I am grateful for all my labmates and colleagues I've had the privilege to work alongside since 2016. Special thanks to Dr. Ricardo Couto, Dr. Eileen Santos and Dr. Karina Araus Sarmiento for your friendship during my first year in the supercritical lab.

Finally, thank you to my family and friends for their support, patience, and understanding. In particular my sister Amy, husband Alvin and friends Sandra and Steven for your words of encouragement, my source of positive energy and emotional support and unwavering love and support.

Table of Contents

Abstract ii

Preface iv

Acknowledgements vi

Chapter 1. Introduction and objectives 1

Chapter 2. Literature review 4

2.1. Milk proteins 5
2.1.1. Caseins 5
2.1.2. Whey proteins 6
2.2. Whey 13
2.2.1. Sweet whey 14
2.2.2. Acid whey 14
2.3. Membrane and chromatographic separation technologies 16
2.3.1. Microfiltration 17
2.3.2. Ultrafiltration 18
2.3.3. Reverse osmosis 19
2.3.4. Ion exchange chromatography 19
2.4. Whey-derived products 20
2.4.1. Whey protein concentrates 22
2.4.2. Whey protein isolates 23
2.4.3. Whey protein fractions 23
2.5. Drying technologies 24
2.5.1. Spray drying 24
2.5.2. Supercritical fluid processing 25
2.6. Conclusions 32

Chapter 3. Single-step concentration of whey proteins using the Pressurized Gas eXpanded (PGX) liquid Technology: Effect on physicochemical properties and scale-up 33

3.1. Introduction 33
3.2. Materials and methods 36
3.2.1. Materials 36
3.2.2. PGX units: 1 L laboratory-scale and 5 L bench-scale systems 36
3.2.3. Experimental design 38
3.2.4. Sample characterization 42
3.2.5. Statistical analysis 48
3.3. Results and discussion 48
3.3.1. Effect of processing scale (1 L vs 5 L) on whey liquid 48
3.3.2. Effect of θ_{PGX} ratio on whey liquid 66
3.4. Conclusions 72

Chapter 4. The Pressurized Gas eXpanded (PGX) Liquid Technology as a separation and drying technique for acid and sweet whey streams 74

4.1. Introduction 74
4.2. Materials and Methods 76
4.2.1. Materials 76
4.2.2. Experimental design 77
4.2.3. Particle characterization 79
4.2.4. Statistical analysis 80
4.3. Results and discussion 80
4.3.1. Physicochemical attributes 80
4.3.2. Compositional characteristics 85
4.3.3. Protein profile and structure 89
4.3.4. Protein solubility and hydrophobicity 94
4.4. Conclusions 99

Chapter 5. Conclusions and recommendations 100

5.1. Summary of key findings 100
5.2. Recommendations for future work 102

Bibliography 104

Appendix A 117

List of Tables

Table 2.1. Whey protein composition and biological function. 7
Table 2.2. Saccharide chains, N-acetylneuraminic acid (NeuAc), galactosyl (Gal) and N-acetylgalactosamine (Gal-NAc) O-glycosidically linked to Thr residues on glycomacropeptide (GMP) (Thomä-Worringer et al., 2006). 12
Table 2.3. Summary of sweet and acid whey composition on an "as is" basis. 15
Table 2.4. Summary of minerals in sweet and acid whey on a dry weight basis (mg/100g). 16
Table 2.5. Particle formation techniques using pressurized fluids*. 28

Table 3.1. Physicochemical characteristics of whey powders. 51
Table 3.2. Mineral composition (%, dwb) of dried whey powders. 54
Table 3.3. Level of soluble protein in 0.1 M NaCl and water at pH 3 and 7. 64

Table 4.1. Physicochemical characteristics of dried whey powders. 81
Table 4.2. Mineral composition (% dwb) of dried whey powders. 89
Table 4.3. The soluble protein content of whey powders in 0.1 M NaCl and water at pH 3 and 7. 96

List of Figures

Figure 2.1. Molecular structure of major whey proteins obtained from https://www.rcsb.org/..... 7
Figure 2.2. Visualization of sweet and acid whey composition. 13
Figure 2.3. Membrane separation techniques for whey processing.(Shahidi, 2009) 17
Figure 2.4. Whey-derived products and their respective separation technologies are used in their manufacturing. Whey product values increase from left to right and are mainly coordinated with the total protein concentration. 22
Figure 2.5. Pressure-temperature phase diagram for carbon dioxide..... 26

Figure 3.1. Flow chart of the 5 L bench-scale PGX unit. PI: pressure indicator; DI: density indicator..... 38
Figure 3.2. Ternary diagram of water: ethanol: carbon dioxide (mass fractions) with experimental conditions tested. Experimental data for the phase boundary was obtained from(Durling et al., 2007) 40
Figure 3.3. FD-W (left) and PGX-W (right), 0.5 g in each. 49
Figure 3.4. Helium ion microscope (HiM) images of FD-W and PGX-W. 52
Figure 3.5. Compositional analysis of PGX-W and FD-W on a dry weight basis, presented as mean ± SD (n=2) for all groups. Different letters for each component indicate significant differences ($p < 0.05$). 53
Figure 3.6. Normalized x-ray diffraction patterns of FD-W and PGX-W 3.5(5L) powders. 57
Figure 3.7. HPLC chromatograms of protein aggregates: (1) > 250 kDa, (2) BSA, (3,4) β-LG dimer and monomer, (5) α-LA, (6) small molecules < 14 kDa. 58
Figure 3.8. SDS-PAGE patterns of reconstituted whey powders on a 4-20% polyacrylamide gel; Molecular weight standards ladder between bands A. and B.; A) FD-W, B) PGX-W 3.5(1L), C) PGX-W 3.5(5L), D) PGX-W 4.0(5L), E) PGX-W 2.5(5L), F) PGX-W 5.3(5L). 60
Figure 3.9. (1) FTIR-ATR spectra, and (2) second derivative of FTIR-ATR spectra in the wavenumber range of 1580-1720 cm-1 for whey powders obtained using the PGX technology at (A) different scales in comparison to FD-W, and (B) different flow rate ratios. 62
Figure 3.10. Intrinsic fluorescence emission spectra of whey powders reconstituted in PBS, pH 6.8, at an excitation wavelength of 295 nm. 65

Figure 4.1. Scanning electron microscopy images: a) SD-AW; b) SD-AR; c) SD-AP); d) PGX-AW; e) PGX-AR; f) PGX-AP. (1) 5x magnification, scale bar 5 µm and (2) 50x magnification, scale bar 500 nm. 82

Figure 4.2. Scanning electron microscopy images: g) SD-SW; h) SD-SR; i) SD-SP; j) PGX-SW; k) PGX-SR; l) PGX-SP. (1) 5x magnification, scale bar 5µm and (2) 50x magnification, scale bar 500 nm. 83

Figure 4.3. Particle size distribution (PSD) of (A) acid whey and (B) sweet whey powders for (1) spray-dried (SD) and (2) PGX-processed powders. 84

Figure 4.4. Compositional characteristics of whey powders on a dry weight basis (%dwb), (A) acid whey and (B) sweet whey, presented as mean ± SD (n=2). 86

Figure 4.5. Normalized X-ray diffraction patterns of SD- and PGX- whey powders, represented as an average of duplicate scans. 86

Figure 4.6. HPLC chromatograms of reconstituted whey powders: (A) acid whey and (B) sweet whey with peaks (1) BSA, (2,4) β-LG, (3) α-LA, and (5,6,7) small molecules (< 5 kDa). Chromatograms of SD- and PGX-processed powders are represented by solid and dashed lines, respectively. 90

Figure 4.7. Reducing SDS-PAGE patterns of whey powders with lanes (STD), SDS molecular weight standard mixture, (A) SD-AW, (B) SD-AR, (C) SD-AP, (D) PGX-AW, (E) PGX-AR, (F) PGX-AP, (G) SD-SW, (H) SD-SR, (I) SD-SP, (J) PGX-SW, (K) PGX-SR, (L) PGX-SP. 91

Figure 4.8. (1) FTIR-ATR spectra and (2) second derivative of FTIR-ATR spectra in the wavenumber range of 1580-1720 cm-1 for (A) Acid whey matrices, and (B) Sweet whey matrices processed by spray drying (SD, solid lines) and PGX technology (dashed lines). 93

Figure 4.9. Intrinsic fluorescence emission spectra of whey powders reconstituted in PBS, pH 7, at an excitation wavelength of 275 nm for (A) Acid whey, and (B) Sweet whey for (1) spray dried and (2) PGX processed powders..... 98

Figure A1. Particle size distributions of PGX-W 3.5(1L) and PGX-W 3.5(5L).....117

Figure A2. Protein molecular weight calibration curve at 280 nm of whey protein standards: ■:BSA, ■:β-LG and ■:α-LA. 117

List of Abbreviations

A	Absorbance
ASES	Aerosol solvent extraction system
Asp	Aspartate
AW	Acid whey
b	Hunter color index b, yellowness-blueness
BG	Beta glucan
BOD	Biological oxygen demand
BSA	Bovine serum albumin
Ca	Calcium
CMP	Caseinomacropeptide
CN	Casein
COD	Chemical oxygen demand
DELOS	Depressurization of an expanded liquid organic solution
DIAAS	Digestible indispensable amino acid score
ELAS	Expanded liquid anti-solvent
EtOH	Ethanol
FD	Freeze dried
GA	Gum Arabic
Gal	Galactose
GalNAc	N-acetylgalactosamine
GAS	Gas anti-solvent
GMP	Glycomacropeptide
HiM	Helium ion microscopy
IEX	Ion exchange chromatography
Ig	Immunoglobulin
Ile	Isoleucine
K_D	Dissociation constant
L	Path length
Lf	Lactoferrin
LPS	Lipopolysaccharides
MCC	Micellar casein concentrates

MF	Microfiltration
MFGM	Milk fat globular membrane
MPC	Milk powder concentrate
MW	Molecular weight
NeuAc/NANA	N-acetylneuraminic acid
P_d	Particle diameter
PDCAAS	Protein digestibility corrected amino acid score
PGSS	Particles from gas saturated solutions
PGX	Pressurized Gas eXpanded liquid
Phe	Phenylalanine
PKU	Phenylketonuria
RESS	Rapid expansion of supercritical solutions
RO	Reverse osmosis
SAS	Supercritical anti-solvent
$scCO_2$	Supercritical CO_2
SCF	Supercritical fluid
SD	Spray dried
SEDS	Solution enhanced dispersion of solids
SMP	Skim milk powder
T	Temperature
Thr	Threonine
Trp	Tryptophan
Tyr	Tyrosine
UF	Ultrafiltration
UV	Ultraviolet
V	Cross-flow velocity
V_f	Final volume
V_i	Initial volume
VRR	Volume reduction ratio
WL/SW	Sweet whey liquid
WP	Whey protein
WPC	Whey protein concentrate
WPI	Whey protein isolate

XRD	X-ray diffraction
α-LA	α-Lactalbumin
β-LG	β-Lactoglobulin
ΔP	Transmembrane pressure
ε	Molar absorptivity

Chapter 1. Introduction and objectives

Food valorization involves the conversion of food waste or byproducts into value-added ingredients or products that contribute back to the food supply chain. Proper handling and treatment of food waste is important for resource recovery as well as minimizing the economic and environmental burden of the food manufacturing processes. Valorization techniques are unique for byproducts and are dependent on the matrix composition. Common methods include the extraction or recovery of nutrients and valued components as well as the conversion or transformation into biomaterials and renewable energy sources. Recovery of macronutrients such as proteins is critical not only for nutritional applications but also for the exploitation of their functional properties in food product systems. To incorporate these proteins into value-added products, the recovery of the proteins from waste streams should be selective without compromising their physicochemical properties.

The biopolymer(s) investigated in this thesis research are whey proteins recovered from dairy waste streams. This waste stream has received considerable attention due to the continued growth of the dairy product industry, specifically in the manufacturing of cheese and yogurt products. Different types of whey are generated depending on the technique used to precipitate the casein proteins. Sweet whey is the byproduct of manufacturing rennet cheeses and acid whey is separated during yogurt production. Substantial volumes of whey are generated in cheesemaking; for every 10 kg of milk used to create 1 kg of rennet-style cheese, 9 kg of sweet whey is generated. Mechanical, biological, and physicochemical treatments of whey are required to reduce the environmental burden attributed to the large amounts of organic matter (lactose, proteins, minerals and residual milk fat). The utilization of whey *'as is'* is limited due to how diluted its components

are; therefore, separation and concentration techniques are widely applied to recover valuable components from whey. Whey is considered an inexpensive source of nutritious and functional whey proteins. Whey proteins are isolated and recovered from the whey byproduct through the selective removal of lactose and minerals from proteins using sequential membrane separation operations.

A supercritical fluid (SCF) is a pure component (e.g.: CO_2) that is heated and pressurized beyond its critical temperature and pressure. Under these conditions, SCFs have unique properties in between those of gases and liquids, including liquid-like densities with gas-like diffusivity. Leaving no solvent traces in the sample matrix following expansion, SCF technologies are considered green technologies suitable for both food and pharmaceutical applications. SCF technologies have been successfully used for the extraction of valuable components and in the generation of micro/nanoparticles for the development of bioactive delivery systems. Temelli and Seifried (2016) invented the Pressurized Gas eXpanded (PGX) liquid technology to produce micro/nanoparticles, agglomerates, and fibrils, from an aqueous biopolymer solution at mild processing conditions of 100 bar and 40 °C. This technology utilizes a gas-expanded liquid known as the PGX fluid composed of pressurized CO_2 and ethanol (EtOH) as an antisolvent to precipitate, micronize and purify high molecular weight biopolymers such as polysaccharides and proteins.

PGX technology offers great potential for the expansion of SCF technologies to generate value-added ingredients from complex food waste streams. The PGX technology could be considered a single unit operation capable of fractionating, concentrating and drying whey proteins from the dairy effluent whey; however, such an approach has not been reported previously. The selective precipitation of the proteins while continually removing residual fats and minerals could be an alternative to the multiple separation technologies required to recover the whey proteins from

the dilute whey feedstock. PGX-processed biopolymers are characterized by micro/nanoparticle sizes with low bulk densities, exfoliated particle surfaces and high surface areas suitable for the development of bioactive delivery systems.

Therefore, it was hypothesized that concentrated whey protein powders can be generated using the PGX technology, and this technique can be scaled up from a laboratory to a bench-scale system. Additionally, it was hypothesized that the PGX technology can be used as an alternative single-step process to utilize various types of whey. The overall goal of this thesis research was to investigate the unique application and versatility of the PGX technology on a complex feedstock such as whey. To achieve the main objective of this research, the specific objectives were:

i) to evaluate the PGX processing of liquid whey at two different scales: a 1L and 5L system, and evaluate the effect of flow rate ratios on the physicochemical properties of the whey proteins (Chapter 3) and;

ii) to compare the PGX technology to conventional ultrafiltration and spray drying of whey and evaluate the applicability of the PGX technology on different types of whey (acid and sweet whey) (Chapter 4).

Chapter 2. Literature review

Milk contains the principal components required to meet the nutritional needs of mammalian newborns. The composition of milk is reflective of the growth needs of individual species and varies considerably depending on the breed, stages of lactation, feed types, and environmental factors such as climate and season (Roy et al., 2020). While milk from a variety of domesticated animals such as cattle, buffalo, sheep, goat and camel are consumed around the world, the source of 85% of global milk production is bovine (Fox et al., 2015; Gerosa & Skoet, 2012). Aside from water, which constitutes ≥ 85% wt. of bovine milk, lactose, fat and protein are the main components composing 4.6%, 4.0% and 3.3% wt., respectively (Goulding et al., 2019; Walstra et al., 2005). While the nutritional needs of the neonate are primarily met by lactose and fat, milk proteins and peptides have various physiological functions, including enzymatic, antibacterial, and immunological properties as well as growth factors and hormones. Milk is a complex fluid comprised of three phases, including an aqueous phase with dissolved lactose, salts and other small molecules. Milk also contains two other dispersed systems, a suspension of the milk fats and a colloidal system containing the milk proteins and calcium phosphate. Milk proteins can be classified into two groups, curd (caseins) and serum (whey) proteins. Caseins (CN) are present as colloidal aggregates that precipitate upon isoelectric precipitation at pH 4.6 or by enzymatic coagulation, while the serum proteins remain soluble in the aqueous phase. Milk fat globules are dispersed amongst the aqueous phase as globules ranging in diameters of 0.1 - 20 μm (Fox et al., 2015). Milk as a dispersed system exhibits dynamic behaviour due to the unique structures and complex mixture of the various milk components in response to environmental factors, the activity of intrinsic enzymes, and the growth of microorganisms.

2.1. Milk proteins

2.1.1. Caseins

Caseins and serum proteins are classified based on their solubility at pH 4.6 and exist in milk in the proportions of 80:20 for bovine milk (O'Mahony & Fox, 2014). In addition to isoelectric precipitation, caseins are also susceptible to the enzymatic cleavage of rennet. This unique property of casein is widely exploited in the preparation of a variety of cheeses and commercial casein products. The unique micellar structure of CN effectively binds and transports poorly soluble minerals, calcium and phosphate, which are important for the growth and development of the neonate. Caseins can be classified into four different proteins, α_{s1}-, α_{s2}-, β- and κ-CN each with unique amino acid sequences. α- and β-CN are highly phosphorylated, with 8-10 and 5 phosphates, respectively, and have a high affinity for metal ions, specifically Ca^{2+} in milk. CN proteins also contain numerous proline amino acid residues, increasing the rigidity of the overall amino acid chain and limiting the formation of stable protein secondary structures (O'Mahony & Fox, 2014). Consequently, the open, flexible structure of CN makes the proteins susceptible to proteolytic attack. CN proteins also have high surface hydrophobicity due to the lack of shielding hydrophobic amino acid residues. Due to the increased protein hydrophobicity, CN proteins tend to exist in milk as large molecular weight aggregates, ranging from 250-500 kDa. These large aggregates pose challenges for the separation of individual protein components (α_{s1}, α_{s2}, β- and κ-CN). The casein micellar core is composed of α- and β-CNs together with calcium phosphate nanoclusters, while the glycoprotein, κ-CN, forms the outer polar layer. The polar end of κ-CN extends out from the micelle, dubbed the 'hairy layer,' responsible for repelling other casein micelles, thereby stabilizing the CN dispersion. During acid and rennet coagulation in cheese production, the stability of this system is disrupted. The intricate structure of the casein

micelles is disturbed by neutralizing the charges of the κ-CN during isoelectric precipitation or by enzymatic cleavage by chymosin (in rennet) between amino acid residues 105 and 106, phenylalanine and methionine, releasing glycomacropeptide (GMP) into the liquid whey. In the presence of calcium (Ca^{2+}), the now non-polar CN will aggregate forming flocs and eventually forming a continuous gel or coagulum. Compared to whey proteins, CNs are stable due to their lack of tertiary structure and can withstand heating at 100 °C for several hours without considerable effect.

2.1.2. Whey proteins

Whey proteins (WPs) constitute 20% of the milk proteins, which remain soluble following the isoelectric precipitation or the rennet coagulation of the casein proteins. Whey proteins include β-lactoglobulin (β-LG), α-lactalbumin (α-LA), bovine serum albumin (BSA), immunoglobulins (Ig), lactoferrin (Lf), and other minor proteins and enzymes (Fig. 2.1). Whey proteins are globular proteins, which are susceptible to denaturation and aggregation induced by heat and high pressure. WPs have high Protein Digestibility-Corrected Amino Acid Score (PDCAAS) and Digestible Indispensable Amino Acid Score (DIAAS) and are therefore considered excellent sources of amino acids. Depending on the purity of the whey products, including skim milk powder (SMP), milk concentrate powder (MCP), whey protein concentrate (WPC), and whey protein isolate (WPI), the PDCAAS and DIAAS scores range from 97 to > 100, indicating that the processing technique influences the nutritional quality of the proteins (Mathai et al., 2017).

Differing from CN, whey proteins are heat labile, with unfolding and denaturation at temperatures starting at 73 °C (at a heating rate of 1 °C/min). In addition to their nutritive value, whey proteins have received considerable attention because of their unique functional properties attributed to their amphiphilic nature (Table 2.1). The water-binding or hydration behaviour,

foaming, emulsifying, and gelling abilities of the whey proteins make them appealing ingredients for the modulation of food product textures (de Wit, 1998).

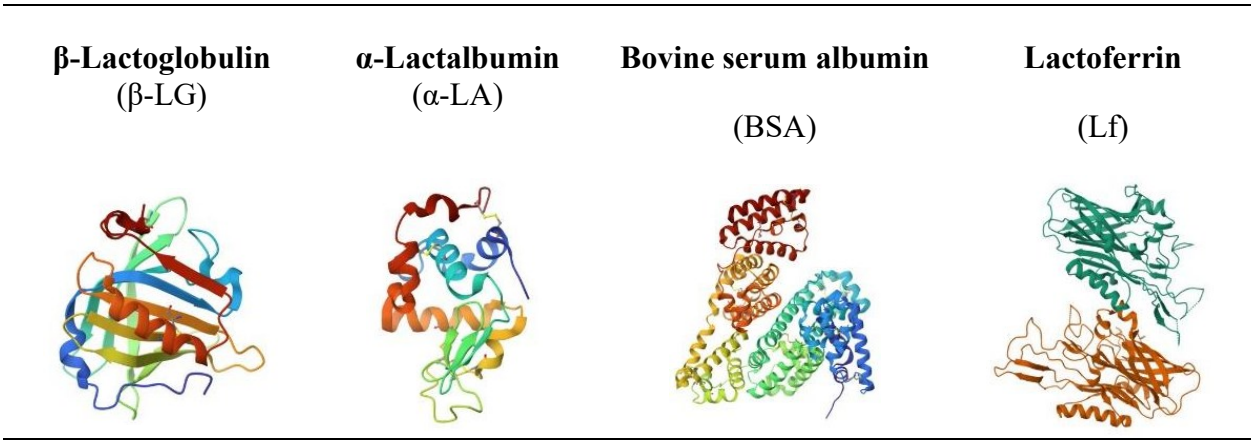

Figure 2.1. Molecular structure of major whey proteins obtained from https://www.rcsb.org/

Table 2.1. Whey protein composition and biological function.

Component	Content†	Biological function‡
β-Lactoglobulin	50-55%	Source of essential and branched amino acids
α-Lactalbumin	20-25%	Source of essential and branched amino acids Primary protein in human breast milk
Immunoglobulins	10-15%	The primary protein found in colostrum; provides passive immunity to neonate
Bovine serum albumin	5-10%	Source of essential amino acids Carrier of lipophilic components
Lactoferrin	1-2%	Antibacterial, antimicrobial, antifungal, antioxidant, immunomodulatory and anti-inflammatory activity; Iron delivery
Lactoperoxidase	0.5%	Antibacterial properties
Glycomacropeptide	10-15%	Source of branched amino acids (lacks aromatic amino acids Phe, Trp, Tyr)

†In rennet-type sweet whey
‡(Kilara & Vaghela, 2017; Madureira et al., 2007, 2010)

2.1.2.1. β-Lactoglobulin

β-Lactoglobulin (β-LG) represents approximately 50% of the whey proteins, equivalent to about 12% of the total milk proteins (O'Mahony & Fox, 2014). While β-LG is the dominant whey protein in bovine, buffalo, sheep, and goat milk, it is absent in human milk and therefore contributes to the allergenicity of infant formulas containing bovine milk proteins. β-LG is a globular protein with a backbone consisting of 162 amino acid residues per monomer and a molecule weight of 18 kDa. Four of the five cysteines (Cys_{66}, Cys_{106}, Cys_{119}, Cys_{121} and Cys_{160}) in each β-LG monomer are involved in two intramolecular disulphide bonds. The presence of such crosslinking greatly adds to the stability of the native protein structure, making it more resistant to unfolding and denaturation. The remaining cysteine residue exists as a free thiol group, forming intermolecular disulphide bonds with κ-CN upon thermal denaturation, with the newly formed β-LG-κ-CN complexes affecting the heat stability and rennet coagulation behaviour of milk (Cho et al., 2003). With an isoelectric point of pH 5.2, β-LG exists as a dimer at physiological conditions of pH ranges 5.5-7.5, as an octamer at pH ranges 3.5-5.5 and as a monomer at pH < 3.5 and > 7.6 (Fox et al., 2015). Extensive hydrogen bonding (H-bonding) contributes to the compact structure with predominately β-sheets, α-helix and unordered structures at 43%, 10-15%, and 47%, respectively (Fox et al., 2015). The parallel and anti-parallel β-sheets of β-LG are arranged in a unique manner forming a ligand-binding cavity known as the calyx or β-barrel. In milk, β-LG binds and transports retinol in the calyx, protecting it from harsh stomach conditions through to the small intestine for absorption as it is required for the growth and development of the calf.

2.1.2.2. α-Lactalbumin

While α-lactalbumin (α-LA) is the principal protein in human milk, it represents just ~20% of the total whey proteins as the second largest fraction of bovine whey. The isoelectric point of

the protein is at pH 4.8. α-LA is composed of 123 amino acid residues with nearly half (54 residues) shared with lysozyme and has a molecular weight of 14 kDa (Fox et al., 2015). The aromatic amino acids tryptophan (Trp) and tyrosine (Tyr) exhibit strong UV light absorption. According to the Beer-Lambert law (A = ε*c*L), peptide and protein absorption at 280 nm have been proportionally correlated to the content of these amino acids. In the protein backbone of α-LA, there are four Trp residues, contributing to the strong UV absorption of these proteins in solution. Biologically, α-LA catalyzes the biosynthesis of lactose and the quantities of the protein are proportional to the lactose quantities in the milk. α-LA is a metalloprotein that can bind one calcium ion (Ca^{2+}) per molecule, coordinated by four aspartate (Asp) residues (Hiraoka et al., 1980). Protein stability is improved following calcium binding through the actual stabilization of the calcium-binding site/loop, and overall it has significant implications on the thermal, solvent and pressure stability of α-LA (Dzwolak et al., 1999). Upon protonation of the Asp residues at pH < 5, the residues and therefore the protein loses the ability to bind calcium thus becoming susceptible to the non-reversible thermal denaturation of α-LA.

2.1.2.3. Bovine serum albumin

Bovine serum albumin (BSA) constitutes ~8% of total whey proteins, the third most abundant whey protein and is presumably present in milk due to the passive leakage from the bloodstream. BSA has a molecular weight of 65 kDa and is composed of 582 amino acids. BSA proteins are heart-shaped and composed of three domains (I, II and III), each with 17 intermolecular disulphide bonds and a free thiol group available for intramolecular bonding (H. Deeth & Bansal, 2019). BSA functions to bind and transport lipids, specifically free fatty acids released into the blood from the adipose tissue, as well as controlling the osmotic pressure of blood

(Fox et al., 2015). Due to its low concentration, BSA has little effect on the physicochemical properties of whey protein products.

2.1.2.4. Immunoglobulins

Representing approximately 10% of total whey proteins, immunoglobulins (Igs) are a complex mixture of large globular glycoproteins with immunomodulatory, antimicrobial and anti-inflammatory properties (Fox et al., 2015). The Y-shaped Igs are composed of two domains connected by a disulphide bond, the NH_2-terminal variable domain and ≥ 1 COOH-terminal constant domains, designated as the light and heavy chains, respectively. The molecular weights of Igs range from 150-900 kDa, and the two most common Igs in bovine milk are IgG1 and IgG2 at 163 kDa and 150 kDa, respectively. Each of the Igs is composed of light and heavy chains (22 kDa and 50-70 kDa). There are five classes of Igs in mammalian milk: IgA, IgG, IgD, IgE, and IgM. Differences between these isotypes are attributed to the variable length of the heavy chains, the location of the intermolecular disulphide bond(s) and the number of attached oligosaccharide moieties. IgG proteins may further be categorized into subclasses IgG1 and IgG2 with IgG1 being the principal Ig in bovine milk. The biological function of IgGs is to provide passive immunological protection against microbial pathogens and bacterial infection in the neonate.

2.1.2.5. Lactoferrin

Lactoferrin (Lf) is an 80 kDa glycoprotein found in both human and bovine colostrum and milk. Lf is a single-chain protein composed of 689 amino acid residues with two globular (N- and C-) lobes connected with an α-helix (Baker & Baker, 2004). Only a few of Lf's biological functions include antimicrobial, antiviral, anti-inflammatory, anti-cancer, and immunomodulatory properties (Brock, 2012; Drago-Serrano et al., 2012; Legrand et al., 2005; Pan et al., 2007). Many

of the biological functions of Lf are attributed to the high binding affinity for iron coupled with a low dissociation constant ($K_D \sim 10^{-20}$M) (Baker & Baker, 2004). LF can bind one ferric ion in each of its two lobes. The binding of iron to LF is a dynamic process in which carbonate ions first bind to their respective sites in the lobe through electrostatic interactions thereby priming the site for iron binding. Upon iron binding in the respective lobes, a conformational change occurs and the protein takes on a more compact structure. The protein can retain iron down to pH 3, which is significant for the delivery of iron through the gastrointestinal tract. Iron that is bound and sequestered by Lf deprives bacteria of the iron required for metabolism. Lf may competitively bind to the receptor sites on cellular membranes thereby preventing the adhesion of other molecules to the host cell. Alternatively, the adhesion of Lf to the lipopolysaccharides (LPS) of the cellular membrane may cause the destabilization and increased permeability of the cell membrane, thereby facilitating the functionalities of antimicrobial agents such as lysozyme (Drago-Serrano et al., 2012). In addition to the numerous biological functions of Lf as an intact protein, peptides derived from gastric and duodenal digestion, as well as enzymatic treatment of Lf can be more active than the parent protein.

2.1.2.6. Glycomacropeptide

The enzymatic cleavage of CN produces para-κ-casein (residues 1-105) and caseinomacropeptide (CMP) (residues 106-169), referred to as the glycomacropeptide (GMP) which is the heterogeneously glycosylated peptide fraction released into (sweet) whey. Two genetic variants exist depending on the residue at position 136, threonine (Thr) or isoleucine (Ile) in variants A or B, respectively (Thomä-Worringer et al., 2006). CMP is characterized by O-glycosylation and phosphorylation, which are post-translational modifications. Approximately half of the CMPs are O-glycosylated with N-acetylgalactosamine (GalNAc), galactose (Gal) and

N-acetylneuraminic acid (NeuAc), NANA, or better known as sialic acid. The degree of glycosylation was reported to affect the susceptibility of CN to enzymatic cleavage by chymosin, trypsin, α-chymotrypsin, and plasmin, with the highly glycosylated protein being less susceptible to hydrolysis. Five saccharide units commonly attached to Thr of GMP are listed in Table 2.2. The isoelectric point of GMP is at pH 3.5 and therefore remains negatively charged under acidic conditions. In sweet whey, GMP constitutes ~20-25% of the total whey proteins. The natural absence of Phe in GMP makes this peptide suitable as an alternative protein source for individuals who suffer from phenylketonuria (PKU) and lack phenylalanine hydroxylase to metabolize Phe (Ney et al., 2009). The molecular weight of GMP is pH dependent due to its tendency to self-associate at higher pH; therefore, resulting in a theoretical molecular weight range from 7-10 kDa, but a range of 20-50 kDa at pH 5 and a range of 10-30 kDa at pH 3.5 (Deeth & Bansal, 2019). Due to the heterogeneity (degree of glycosylation, molecular weight, etc.) of the GMP, it is challenging to analyze the protein fraction.

Table 2.2. Saccharide chains, N-acetylneuraminic acid (NeuAc), galactosyl (Gal) and N-acetylgalactosamine (Gal-NAc) O-glycosidically linked to Thr residues on glycomacropeptide (GMP) (Thomä-Worringer et al., 2006).

Carbohydrate moiety	Saccharide length	Occurrence
GalNAc – O – R	Monosaccharide	0.8%
Gal β1 → 3GalNAc – O – R	Disaccharide	6.3%
NeuAc α2 → 3Gal β1 → 3GalNAc – O – R	Trisaccharide	18.4%
Gal β1 → 3 (NeuAc α2 → 6) GalNAc – O – R	Trisaccharide	18.5%
NeuAc α2 → 3Gal β1 → 3(NeuAc→α26) – O – R	Tetrasaccharide	56%

2.2. Whey

Whey or milk serum is the yellow-green liquid that remains following the removal of the casein proteins (Fig. 2.2). Aside from the manufacturing of dried commercial casein products, the most prevalent application of casein proteins is the production of dairy products such as semi-hard and hard cheeses. Proportionately, there is a significant amount of whey coproduct generated from cheese production, yielding 9 L of whey for every 10 L of milk used for cheese production. Worldwide whey production reported in 2011 totalled 180-190 x 10^6 metric tonnes of whey generated from the cheese manufacturing industry (Tsermoula et al., 2021). The composition of whey is determined by the method of protein coagulation, acidic or enzymatic coagulation generating acidic or sweet whey, respectively.

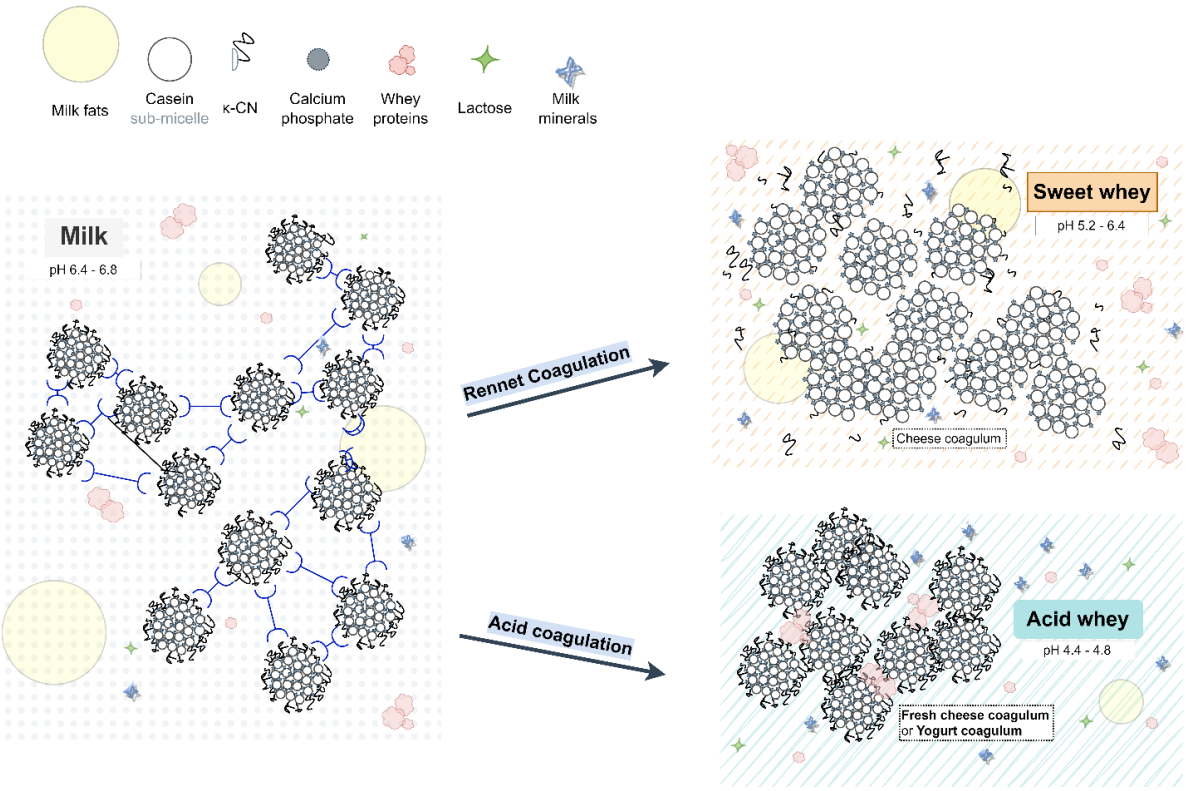

Figure 2.2. Visualization of sweet and acid whey composition.

2.2.1. Sweet whey

Since sweet whey has similar compositional characteristics (Table 2.3) to the physiological characteristics of milk, the physicochemical properties of the whey proteins are not affected by changes in acidity and/or alkalinity. Formerly, handling such volumes of whey involved the direct disposal of the untreated whey into nearby waterways, bodies of water or sewer systems, resulting in rapid pollution. Since whey retains more than half of the nutrients in milk, lactose makes up 70-75% of the total solids in cheese (sweet) whey and contributes to the high biological oxygen demand (BOD) and chemical oxygen demand (COD) of whey, 30-50 and 60-80 g/L, respectively (Chatzipaschali & Stamatis, 2012). Due to its high nutritive value, an economical use for sweet whey has been for swine feed. Feed replacement at levels > 30% has been attributed to gastrointestinal disruption and diarrhea due to excessive fermentation of lactose. The combination of changes in regulations and the isolation of the valuable whey components have rewritten the story of whey from 'gutter-to-gold' (Smithers, 2008).

2.2.2. Acid whey

In the production of fresh-type cheeses such as cottage cheese, quark, and cream cheese, acid whey is generated as the byproduct of the acid coagulation of milk proteins by the addition of organic or mineral acids such as citric, acetic or lactic and hydrochloric acid. The charges on the hairy κ-CN are neutralized, thus disrupting the overall micellar structure. As a result of acidification, shifts in the ionic equilibrium also result in additional minerals being present in acid whey compared to sweet whey (Table 2.4). Lactic acid coagulation in the homolactic fermentation of yogurt products also results in a similar effect, inducing the coagulation of the milk proteins. The resultant gel retains water, milk proteins, lipids and sugars in addition to capturing flavour

compounds such as acetaldehyde. Syneresis is the separation of whey from the yogurt curd. The typical composition of sweet and acid whey is outlined in Table 2.3. Acid whey contains lower protein and lactose content, is more acidic and contains a higher ash content (Rocha-Mendoza et al., 2021). The residual lactic acid content and low pH of acid whey pose additional challenges in the repurposing of the byproduct compared to sweet whey. In recent years, Greek style also known as strained yogurt has increased in popularity due to its perceived health benefits compared to other yogurt styles (Verlagsgesellschaft, 2012). Greek yogurt manufacturing requires an additional straining step following the break up of the coagulum, which encourages further separation of whey (Gyawali & Ibrahim, 2016); this produces a thicker yogurt with a higher total solids content. Excessive acid whey generation coincides with increased Greek yogurt production. In 2015, 2.1 x 10^6 metric tons of yogurt were produced, with 771,000 metric tons of it attributed to Greek yogurt (Erickson, 2017). Per kilogram of Greek yogurt produced, a total of 2-3 kg of acid whey is separated. Therefore, in 2015, > 1.5 x 10^6 metric tons of acid whey was generated. In 2020, it was estimated that the cheese manufacturing industry in the European Union generated ~ 40 x 10^6 metric tons of acid whey (Rocha-Mendoza et al., 2021).

Table 2.3. Summary of sweet and acid whey composition on an "as is" basis.

Component	Sweet whey	Acid whey
pH	5.2 – 6.4	4.4 – 4.8
Total solids (g/L)	64 – 70	63 – 70
Lactose (g/L)	45 – 52	44 – 46
Protein (g/L)	11 – 16	6 – 8
Ash (g/L)	5 – 10	8 –12

*data compiled from (Barukčić et al., 2019; Glass & Hedrick, 1977; Jelen, 2002)

Table 2.4. Summary of minerals in sweet and acid whey on a dry weight basis (mg/100 g).

Mineral	Sweet whey	Acid whey
Ca	395 – 1600	1340 – 3210
P	563 – 1900	888 – 2094
Na	525 – 2910	529 – 1805
K	1460 – 2520	1600 – 2240
Mg	125 – 260	175 – 300
Zn	0.2 – 4.2	4.9 – 10.2
Fe	0.6 – 1.4	0.6 – 3.4

*Data compiled from (Pearce, 1992; Zadow, 1992)

2.3. Membrane and chromatographic separation technologies

To overcome the environmental challenges and financial burden of liquid whey, different approaches to whey utilization have been widely adopted, including direct conversion of whey liquid, biological and chemical conversion into biochemicals, etc., and the isolation of whey components to recover value-added products. Concentrating and drying whey are common processing techniques to eliminate the water, improving the handling, shelf life, storage, and transportation of large quantities of this cheese manufacturing byproduct. In the early 1970s, membrane filtration was introduced into the dairy industry as an alternative to thermal evaporation to concentrate whey liquid before drying. Cross-flow microfiltration, ultrafiltration, diafiltration and nanofiltration are commonly applied in the utilization of whey. These membrane technologies can be used for bacterial removal, clarification, pre-concentration, demineralization and protein separation among many other applications. These separation technologies are non-thermal treatments and therefore the integration of these unit operations in the dairy processes has been instrumental in the recovery of valuable whey proteins. Fig. 2.3 summarizes the various membrane separation techniques used in whey processing.

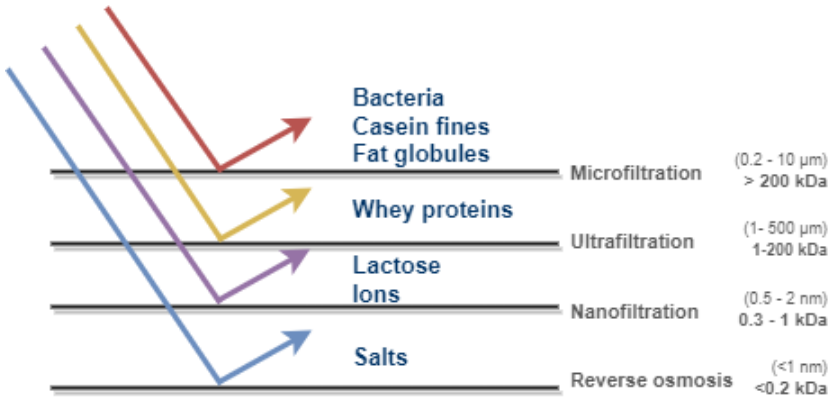

Figure 2.3. Membrane separation techniques for whey processing (Shahidi, 2009).

2.3.1. Microfiltration

Whey liquid is commonly pretreated by microfiltration (MF) to remove suspended casein solids, milk fats, and spoilage microorganisms (de Wit, 2001). The permeate contains the whey proteins, lactose and minerals to be further fractionated with additional separation technologies. Low transmembrane pressures (< 2 bar), and moderate temperatures of 37-55 °C are used in MF to separate components > 200 kDa, concentrating whey by a volume reduction ratio of 2. Volume reduction ratio (VRR) is defined as ($VRR = V_i/V_f$), where V_i is the initial volume and V_f is the final volume after filtration. Micellar casein concentrates (MCC) are separated from skim milk using MF and are commonly used as high-quality proteins for food fortification applications (Carter et al., 2021). MCC contains casein and small quantities of large whey proteins (e.g.: BSA, IgG) retained by MF, lactose and milk minerals. With a cumulative protein content of ~85%, MCC are used in food formulations for calcium delivery. MCC has also been proposed as an innovative feedstock for the preparation of cheese and yogurts with implications for reduced whey generation. Another application of MF for cheese products is for the removal of norbixin, a colourant used in the formulation of cheddar cheeses. Following rennet coagulation, it associates with residual milk

fat globule membrane (MFGM) in whey due to its amphiphilic nature. Qiu et al. (2015) studied the decolouration of cheddar cheese whey using MF and reported the effects on colour, flavour and protein functionality of WPC80. MF (with a molecular weight cutoff of 80 kDa) effectively defatted and reduced the yellowness (*b value) of whey by ~40%, compared to a 93% reduction using the traditional bleaching agent, lactoperoxidase (Qiu et al., 2015).

2.3.2. Ultrafiltration

Another pressure-driven (< 10 bar) separation technique widely used in the dairy industry is ultrafiltration (UF), which is commonly employed for the retention of high molecular weight components such as proteins, < 200 kDa, while low molecular weight components mono- and disaccharides, select peptides and amino acids, minerals, organic acids etc., pass freely through the membrane. UF is the established industrial process used to concentrate whey protein to 35-85% of the total solids. However, the major whey proteins β-LG and α-LA contribute to the fouling of the membrane surfaces (Kumar et al., 2013). Moreover, the adsorption of protein-calcium complexes into the membrane pores contributes to pore blockage. Operating parameters such as the whey feedstock concentration (C), temperature (T), transmembrane pressure (ΔP), and cross-flow velocity (V), all have significant effects on the rejection of total solids, affecting the permeate flux. Various combinations of interactions between these operating parameters had different effects on the permeate flux, protein retention, membrane fouling, ash rejection and overall filtration performance (Kelly, 2019). Pretreatments such as clarification by centrifugation or MF, pH and temperature adjustments as well calcium chelation techniques have been reported to improve the overall flux. Diafiltration is a variation of UF whereby the retentate fraction is diluted with water throughout the filtration process. The diafiltration step is continued to increase the concentration of the whey proteins in the retained fraction. By varying the volume of reduction,

the final protein content can be controlled. The separation of similarly sized protein fractions using UF presented challenges since membrane separation technologies operate as molecular sieves.

2.3.3. Reverse osmosis

Reverse osmosis (RO) can be used for the concentration of dilute fluids such as whey. RO membranes contain small pores allowing small molecules (< 200 Da), most commonly water to permeate through (Pearce, 1992). RO is effective for concentrating solids to ~25% and therefore cannot be considered the lone unit operation for concentrating whey components. High transmembrane pressures of 30 – 50 bar are required for economic rates of water removal (Pearce, 1992). Successive stages (usually, 2, 5 or 7) of RO filtration with incremental pressure increases are a common practice for continuous operation to achieve a cumulative concentration effect. Compared to thermal evaporation techniques, which have implications on protein functionality, RO processing is considered a non-thermal process. On the other hand, the investment costs for RO filtration are higher compared to thermal or vacuum evaporation.

2.3.4. Ion exchange chromatography

Ion exchange chromatography may be used to further separate and purify whey proteins based on their charge. Recovery of the proteins is feasible using buffers with varying ionic strengths. Ion exchange chromatography (IEX) is a form of adsorptive chromatography that separates proteins based on their affinity to the charged stationary phase (Zadow, 1992). Selectivity can be controlled by adjusting pH, buffer concentration and/or the ion exchange media (cation or anion resins). Resins with negatively charged functional groups are cation exchangers and anion exchangers have positively charged functional groups. The column is first equilibrated with a buffer containing counterions of opposite charge to the ion exchange media. Proteins dissolved in

the mobile phase displace these counterions and through electrostatic interactions are temporarily immobilized on the column while the remaining proteins are eluted out of the column. Most commonly, retained proteins can be recovered by using a series of buffers of increasing ionic strength, resulting in the elution of the proteins in order of increasing net charge. With increasing salt concentration in the buffers, there is an increasing number of ions competing with the proteins for the functional groups on the charged resin. Protein fractionation occurs during the elution step as the bound proteins are released separately into different eluent solutions. This reversible adsorption of the proteins is an effective and versatile technique for the demineralization of WPC fractions; therefore, generating WPI fractions containing ~90% protein as well as obtaining individual purified WP fractions through selective elution (Etzel, 2004). Equipment and reagent compatibility for food applications, operational volumes required for economic viability, as well as throughput and protein recovery, need to be considered from the industrial standpoint and application of IEX.

2.4. Whey-derived products

Whey management can be classified into the following four categories (Zadow, 1992):

I. Repurpose the whey as a starting material for producing other food products such as whey beverages and cheeses.

II. Reduce the quantity of whey produced by altering the composition of the milk used in the manufacture of dairy products.

III. Recover the valuable whey components and produce commercially viable products generating revenue from what would be otherwise considered an economic burden.

IV. Treat the whey as waste, reducing the biological- and chemical oxygen demand, BOD and COD, respectively, to minimize the environmental impact of whey disposal.

Whey powder is obtained by drying the dilute (sweet) whey stream. Demineralization of whey through ion exchange chromatography or by electrodialysis and then drying can lead to demineralized whey powder. The next stage of whey processing is to concentrate and recover valuable whey proteins by further reducing the lactose and mineral contents. A variety of ingredients derived from whey and their respective separation technologies are outlined in Fig. 2.4, which include dried whey powder (containing all components of whey but without the water), lactose powder, demineralized whey, WPC, WPI as well as purified protein fractions. A wide number of these whey-derived products have particular importance in nutraceutical applications (de Wit, 1998) due to their high nutritional quality and functionalities. Physicochemical properties such as high protein solubility, acidic pH stability, surface activity (emulsification and foaming capabilities), and gelation capabilities of whey proteins are reasons for their extensive use in a widespread number of applications. As described above, the composition of whey protein products and therefore protein functionality are related to the processing technologies applied. Interactions of the non-protein components such as lactose, minerals and residual lipids present in the whey protein powder matrices with the protein components need to be thoughtfully considered when formulating. In the section below, three main classes of whey protein-enriched, WPC, WPI and whey protein fractions are reviewed.

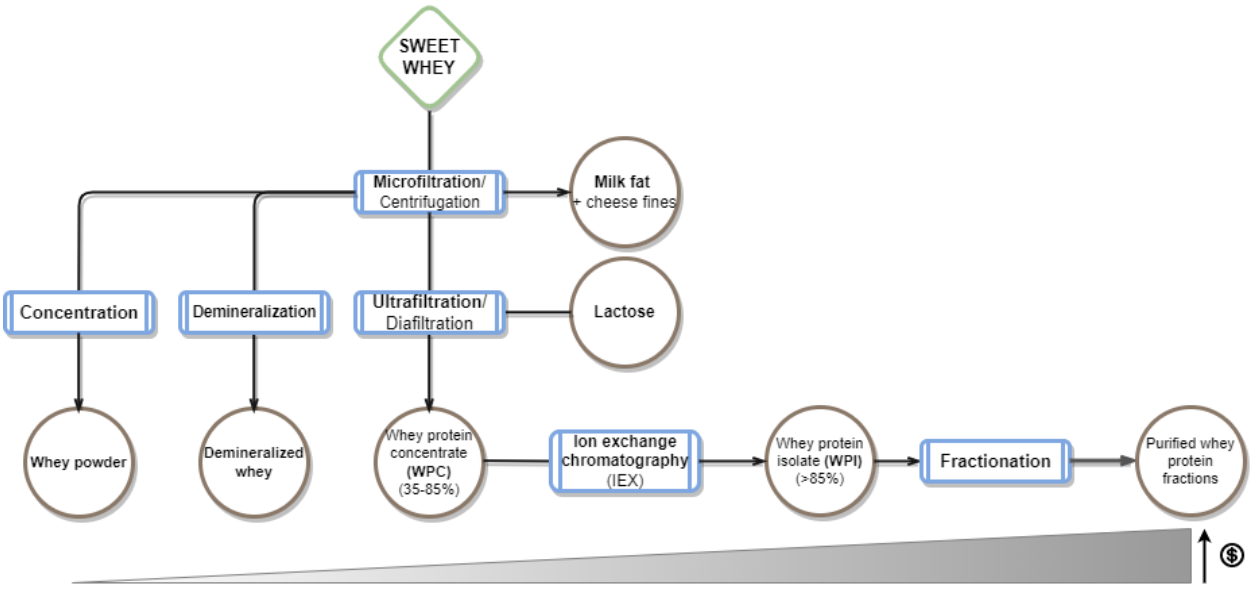

Figure 2.4. Whey-derived products and the respective separation technologies used in their manufacturing. Whey product values increase from left to right and are mainly correlated with the total protein concentration.

2.4.1. Whey protein concentrates

According to the United States Department of Agriculture's (USDA) Code of Federal Regulations (CFR), whey protein concentrate (WPC) is defined as:

"a substance obtained by the removal of sufficient nonprotein constituents from whey so that the finished dried product contains not less than 25% protein…"

However, most commercial WPC products have a protein content in the range of 35-80%, with 35%, 55% and 80% being the most common (Agricultural Marketing Service, 2015). The whey proteins in WPC are made of ~68% β-LG, ~21% α-LA and ~10% BSA with the remaining total solids attributed to lactose and ash (Zadow, 1992). Traditionally, the nomenclature of dairy protein concentrates derived from milk and whey lists the type of protein using a 3-letter code (e.g.: MPC

for milk protein concentrates and WPC for whey protein concentrates) followed by a number that identifies the percentage of protein on a dry weight basis (e.g.: WPC80 for 80% WPC). In food and feed applications, WPC35 is commonly used as a replacement for skim milk (de Wit, 1998). WPC ingredients containing high protein levels are exploited for their functional properties and are more commonly used in confectionary applications and meat formulations. The versatility of whey proteins makes it an economical protein for countless applications. Lactose and milk minerals are the main byproducts of WPC manufacturing. The main application of lactose is as an excipient in the tableting process in the pharmaceutical industry (Shi et al., 2023).

2.4.2. Whey protein isolates

Whey protein isolates (WPI) contain ~90% protein with ash and water constituting the remaining proximate composition. Commercial WPI is widely used in nutritional supplements, specifically protein-fortified beverages, and supplementation for exercise and athletic performance. As described above, IEX is commonly used to concentrate whey proteins through the adsorption of the ions present in whey.

2.4.3. Whey protein fractions

The main proteins in WPCs and WPIs are β-LG, α-LA, BSA, IgG, Lf and GMP. To harness some of the biological functions of these proteins for nutraceutical applications, individual WP fractions are needed. For example, α-LA may be used to enrich infant formulas to have a composition more similar to human milk (Lien, 2003). Another WP fraction of ongoing interest is Lf, the iron-binding milk protein. Based on its unique capabilities to bind iron in the N- and C-lobes, Lf has been evaluated as an iron delivery system to prevent and treat anemia (Martins et al., 2016). Lf nanoparticles (~108 nm) loaded with 2.6 ± 0.7% ferric chloride ($FeCl_3$) were studied as

iron vectors for food fortification (Martins et al., 2016). The nanoparticles remained stable over a temperature range of 4-60 °C, and over a pH range of 2-11 for 76 days. Release of the bound iron at gastrointestinal pH 2 was also investigated, demonstrating the potential application of valuable whey proteins for important nutraceutical applications. The GMP fraction specific to sweet whey proteins has therapeutic applications for phenylketonuria management. Dietary restrictions are required to manage this disorder to prevent toxicity due to unregulated, elevated levels of Phe in the blood (Van Calcar et al., 2010).

2.5. Drying technologies

2.5.1. Spray drying

After considering all the preprocessing steps required to prepare whey for drying, additional parameters need to be considered for the actual spray drying (SD) operation. Lactose in the dried concentrated whey stream precipitates as the highly hygroscopic amorphous lactose. If left unaddressed, whey powders become cakey due to the phase transition of the lactose from a glassy to a rubbery state at the glass transition temperature (T_g), with implications for the recovery, handling, and storage of the powders (Ozel et al., 2022). During storage, the amorphous lactose produced during drying crystallizes into more stable forms of α- and β-lactose (Haque & Roos, 2005; Saito, 1988). Lactose in concentrated whey protein solutions with ~55% solids are rapidly cooled to 30 °C, and crystallization can be initiated by seeding with α-lactose monohydrate (< 10 μm) at concentrations of 0.1-1% with rapid and continuous agitation (Pearce, 1992). Lactose crystallization of the concentrate continues as the solution cools at a rate of ~3 °C/h to reach a final temperature of 10 °C; at that point, the lactose crystals are in the particle size range of 20-30 μm. Infant formula containing 7–24% pre-crystallized lactose showed lower rates of water activity (a_w) increase over 4 weeks (relative humidity of 54%) compared to infant formula prepared with no

lactose pre-crystallization (Saxena et al., 2021). Increases in a_w are related to a drop in the T_g, the point at which lactose is converted from its solid glassy state to a syrup-like sticky liquid, therefore resulting in a cakey powder.

Furthermore, spray drying parameters need to be selected appropriately to minimize the deposition of the newly precipitated hygroscopic amorphous lactose particles on the surfaces of the equipment, which has implications for the economics of the process. High inlet and outlet air temperatures of 180-190 °C and 80-90 °C are required to reduce the viscosity of the feed and prevent the deposition of the hygroscopic powders (Pearce, 1992). Spray-dried powders collected from the cyclone are recovered onto a vibrating fluidized bed for a controlled agglomeration process, known as instantizing, crucial for the generation of whey powders with rapid dissolution properties. Instantized WPCs are generated by exposing dried particles to a controlled humidity environment, promoting particle agglomeration on a fluidized bed, thus increasing particle size, followed by redrying and cooling. Some advantages of instantizing whey protein powders include improved flow behaviour of the powders, increased wettability, improved dispersibility, rapid dissolution and reduction of fine particles and/or dust.

2.5.2. Supercritical fluid processing

Supercritical fluids (SCFs) are pure components (e.g., CO_2) or mixtures of components heated and pressurized beyond their critical temperature (T_c) and pressure (P_c) known as the critical point (Fig. 2.5). The densities of the liquid and gas are the same at the critical point and the distinction between the two phases disappears, forming a supercritical fluid. Neither gas nor liquid, SCFs have unique properties with gas-like viscosity and diffusivity and liquid-like densities. These properties consequently result in improved matrix penetration and therefore enhanced solute solubilization due to near-zero surface tension. The density and viscosity and therefore solvent

properties of the SCF can be 'fine-tuned' by adjusting the operating pressure and temperature. Supercritical CO_2 ($scCO_2$) is the most commonly utilized SCF as it is non-toxic and non-flammable, available in abundance, can be recovered as a gas following depressurization and has a low T_c of 31.1 °C and P_c of 73.8 bar, suitable for processing thermally labile components (Brunner, 2005). Dating back to the mid-1970s, the decaffeination of coffee using $scCO_2$ is one of the most notable applications of SCF technologies attributed to the use of a non-toxic solvent, mild operating conditions, and selectivity to caffeine without disrupting the carbohydrates and proteins that contribute to the flavour of the coffee upon roasting.

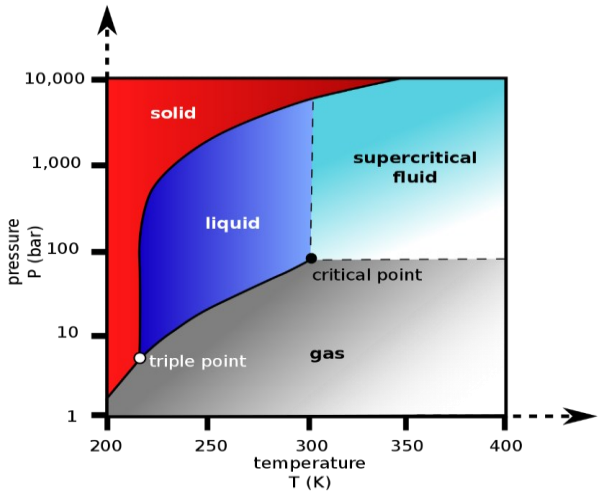

Figure 2.5. Pressure-temperature phase diagram for carbon dioxide.

Over the last several decades, there has been an increasing trend and consumer demand for food and food products that contribute to promoting health and well-being as well as disease risk reduction. Hence the emergence of nutraceuticals and functional foods, generally defined as "*products that are derived from food sources containing extra health benefits in addition to the basic nutritional value of the food*" (Agriculture and Agri-Food Canada, 2009; Shahidi, 2009). Beyond the consumption of whole foods, recent developments include exploiting the bioactive

components naturally occurring in these matrices with health-promoting properties for food product development. The extraction and purification of the said bioactives from the natural protective food matrix affect their chemical stability and their susceptibility to degradation. Extensive research into the design and development of bioactive delivery systems is available in the literature, aiming to protect the integrity of the bioactive, while limiting imparting undesirable flavours, improving the bioavailability and controlling the rate of release in the body (Acosta, 2009). Supercritical fluid technologies are a major focus to reach this goal, considering the numerous advantages they offer as indicated above.

Conventional particle formation techniques can be categorized into "top-down" and "bottom-up" approaches, involving the mechanical reduction in particle size for the assembly of smaller components. Controlling particle size with milling is a challenge and thus more energy is required to achieve smaller particle sizes. Physical processes like milling generate large amounts of heat due to particles colliding with other particles or with grinding media or milling balls, making it unsuitable for heat-labile components. On the other hand, bottom-up approaches involve controlled precipitation/crystallization of the dissolved compounds in solution, followed by evaporation and drying to recover the dried particles. While particle sizes can be better controlled by controlling the rate of crystallization, the use of solvents is not desirable due to the residual solvent in the formed particles or chemical degradation due to prolonged exposure. Alternatively, SCF technologies have gained increasing attention as alternatives to conventional particle design due to their unique solvent capabilities described above (Chafidz, 2018; Bahrami and Ranjbarian, 2007; Jung and Perrut, 2001; Shariati and Peters, 2003; O'Sullivan et al., 2022; Temelli, 2018; Yeo and Kiran, 2005). Table 2.5 is a summary of the common particle formation techniques categorized according to the role of the SCF.

Table 2.5. Particle formation techniques using pressurized fluids.*

Role of CO_2	Technique	Description
CO_2 as a solvent	**RESS**: Rapid Expansion of Supercritical Solutions	Substrates must be soluble in $scCO_2$. The supersaturated, supercritical solution is atomized through a heated nozzle into the atmospheric pressure chamber. Rapid nucleation and precipitation of the solute is achieved during depressurization. This technique is limited to solutes that have reasonable solubility in SCF.
CO_2 as an anti-solvent	**GAS/SAS**: Gas Anti-Solvent/ Supercritical Anti-Solvent **ASES**: Aerosol Solvent Extraction System **SEDS**: Solution Enhanced Dispersion of Solids	$scCO_2$ is used as an anti-solvent resulting in the precipitation of substrates dissolved in an alternative (typically an organic) solvent. Precipitation of the substrate occurs as the SCF dissolves into the organic solvent, reducing the solvation power. Variations of this technique include how the SCF and organic mixture are mixed: **GAS/SAS**: introduce $scCO_2$ into an organic solution **ASES**: pump the substrate + organic solvent into the chamber of $scCO_2$ **SEDS**: coaxial mixing and atomization into a pressurized chamber.
CO_2 as a solute	**PGSS**: Particles from Gas Saturated Solutions	$scCO_2$ is solubilized in melted/molten substrate (such as a biopolymer), making it a gas-saturated solution/suspension. This mixture is sprayed into a chamber under atmospheric conditions. Rapid expansion and cooling aid in the formation of fine particles.
CO_2 as a co-solvent or gas expanded liquid	**DELOS**: Depressurization of an Expanded Liquid Organic Solution **ELAS**: Expanded Liquid Anti-Solvent **PGX technology**: Pressurized Gas eXpanded liquid Technology	A substrate is dissolved in a solvent consisting of $scCO_2$ with a miscible organic solvent. Depressurization of the expanded solution is responsible for solute precipitation. A substrate is dissolved in water and sprayed into a chamber with a CO_2 + organic solvent. The gas-expanded liquid induces precipitation of the solute. Excess water is removed by the gas-expanded liquid and excess organic solvent is removed by pure CO_2. The difference between ELAS and PGX technology is the proportions of CO_2 and EtOH.

*Information compiled from (Bahrami & Ranjbarian, 2007; Chafidz et al., 2018; Jung & Perrut, 2001; O'Sullivan, 2011; Shariati-Ievari et al., 2016; Temelli, 2018; Yeo & Kiran, 2005).

2.5.2.1. Gas-expanded liquid processing

Gas-expanded liquids are mixtures of a compressible gas (e.g., CO_2) with an organic solvent (e.g., EtOH) (Jessop and Subramaniam, 2007). By varying the proportions of the compressed gas to the organic solvent, expanded liquids combine the benefits of traditional solvents with the properties of supercritical fluids, resulting in a unique class of tunable solvents. Ethanol addition is important for enhancing the solubility of polar solutes. As CO_2 dissolves into EtOH, a 2-3× volumetric expansion of the EtOH is observed at pressures between 50-60 bar (Jessop & Subramaniam, 2007). Therefore, gas-expanded solvents are advantageous for processing at milder conditions with considerable replacement of the traditional solvents with CO_2. Several particle formation techniques employing gas-expanded liquids are reported, including, DELOS, ELAS, and the PGX technology (Table 2.5). ELAS utilizes a gas-expanded liquid containing organic solvents and $scCO_2$ to enhance the solubility of water in CO_2. In this process, the gas-expanded liquid is miscible with the water and behaves as an antisolvent for the solute, inducing the supersaturation and precipitation of the solute into the pressurized chamber. Residual water is removed by the continuous injection of the gas-expanded solvent through the chamber followed by a final drying step using CO_2 alone to eliminate the residual organic solvent. Prosapio et al. (2014) reported the formation of BSA microparticles from 20 mg/mL protein solutions at 150 bar and 40 °C. Variable co-antisolvent flow ratios of CO_2 to acetone, EtOH and isopropyl alcohol had significant effects on the particle size distributions and morphologies. More specifically, different particle morphologies were observed at varied distances of the operating point from the vapour-liquid-equilibrium (VLE) phase boundary unique to each ternary mixture. As the operating point moves from the supercritical to the expanded liquid region (increasing

proportions of organic solvent:scCO$_2$), BSA microparticles (> 500 nm) are reduced to nanoparticles (< 200 nm) (Prosapio et al., 2014).

2.5.2.2. Pressurized gas-expanded liquid technology

Similar to the ELAS technique, the Pressurized Gas eXpanded (PGX) liquid technology utilizes CO$_2$-expanded EtOH for processing water-soluble compounds. Differing from the ELAS method, the PGX liquid is composed of pressurized CO$_2$ rather than scCO$_2$. Larger amounts of EtOH are used as a modifier or coanti-solvent to facilitate the processing of higher concentrations of water-soluble biopolymers. The first biopolymers investigated using this novel drying technique by Seifried (2010) were barley β-glucan (BG) and gum arabic (GA). These preliminary experiments were conducted at 40 °C and various processing parameters were investigated including pressure, flow rates of CO$_2$, EtOH, and aqueous solution, three different nozzle configurations and aqueous solution solids concentrations. Initially, CO$_2$ was pressurized to the experimental pressure (100 or 240 bar), followed by pumping EtOH at the desired flow rate (12 or 24 mL/min), with sufficient time given for the system to stabilize. After stabilization, the aqueous solution was injected through the inner tube of the coaxial nozzle. GA, BG or a combination (GA+BG) solution was prepared at various concentrations, ranging from 0.5 to 10% wt. After injecting the solution, the remaining aqueous solution in the coaxial tubing was back-flushed to avoid the formation of drops falling from the nozzle onto the dried particles during depressurization of the system. CO$_2$ was continually flushed through the system to remove the residual EtOH, followed by a nitrogen (N$_2$) flush to displace the CO$_2$ in the system. Dried particles were collected upon depressurization of the system. Processed particles were characterized by scanning electron microscopy (SEM), laser diffraction particle size analysis, and bulk density measurements. GA particles were collected as fine, free-flowing fluffy powders, with bulk

densities ranging from 0.017 to 0.042 g/mL; whereas, processed BG was collected as fibril structures (< 100 nm) with cobweb-like appearances, and very low bulk densities of approximately 0.006 g/mL. With lower flow rates, Seifried (2010) reported the formation of rod-like structures due to the highly viscous solutions, which made it difficult to generate a fine dispersion of the solution at the nozzle. It was found that the smallest orifice diameters of 0.51 and 0.89 mm were most effective for processing the highly viscous BG solutions. The processed biopolymer mixtures of GA + BG were collected as powders that resembled the GA particles. However, the SEM images of the co-precipitated mixture showed a combination of the fibril and spherical structures. The GA particles processed at the lower pressure (100 bar) were reported to be in the size range of 1 to 100 μm; whereas, co-precipitation of GA+BG generated particles mostly in the 500 to 1000 μm region.

More recently, the PGX technology has been reported to generate high-value polysaccharide carriers, such as oat beta-glucan (Liu et al., 2018), yeast beta-glucan (Seifried et al., 2022), gum arabic (Couto et al., 2020), and sodium alginate (Muzzin, 2018; Vilchez, 2019; Johnson et al., 2020; Liu et al., 2022). The dried biopolymers have characteristically large specific surface areas and very low bulk densities, making them suitable for the adsorptive precipitation of bioactive compounds. Bioactives loaded onto the open-porous biopolymer networks are the basis for tailor-made delivery systems. Over the years, PGX-generated powders have demonstrated great potential for nutraceutical and biomedical applications. For example, an orange-flavoured functional beverage was successfully formulated with PGX-processed oat beta-glucan loaded with coenzyme Q10 (Liu et al., 2018a; Liu et al., 2018b). Other biopolymers may be crosslinked to prepare water-insoluble scaffolds for various applications, including wound healing and other biomedical applications (Johnson, 2018; Johnson et al., 2020; Muzzin, 2018) . Ibuprofen loaded on sodium alginate scaffolds has been demonstrated to accelerate burn wound healing in mice

models (Johnson et al., 2020). However, the application of PGX technology for the processing of animal-based proteins, and in particular whey proteins, has not been reported previously.

2.6. Conclusions

To contribute to the ongoing efforts for food waste utilization and valorization, the recovery of valuable whey proteins from dairy effluent streams has received substantial attention. Due to the complete amino acid profile and high digestibility, these proteins have been widely used in the development of nutritional supplements for human health. The unique chemical structure of the various whey proteins is directly related to the functional properties of the proteins and therefore enables a plethora of food system applications. However, the recovery of these proteins requires a multitude of processing steps, from the consecutive elimination of unwanted whey components to drying the concentrated solutions to obtain powders for ease of handling and storage, suitable for application as value-added ingredients. Over the past several decades, advances in SCF technologies have significantly contributed to the application of these green technologies for generating value-added ingredients. The PGX technology is capable of simultaneously precipitating, micronizing and purifying high molecular weight biopolymers such as proteins from aqueous feedstocks. While other single biopolymer systems have been investigated with the PGX technology, the application of the SCF technology to complex feed mixtures such as whey has not been explored. Therefore, in this MSc thesis research, PGX processing of whey at variable processing conditions and different scales were investigated first (Chapter 3) followed by its evaluation against conventional processing methods such as ultrafiltration and spray drying as well as studying variable feedstock compositions (Chapter 4).

Chapter 3. Single-step concentration of whey proteins using the Pressurized Gas eXpanded (PGX) liquid technology: Effect on physicochemical properties and scale-up[1]

3.1. Introduction

The annual global bovine milk production grew an average of 3.1% between 2010 and 2015 to meet the growing demand (Bizzarri & Gapon, 2019). At the same time, about 1.3×10^9 tons per year, equivalent to about 1/3 of the food produced for human consumption, was wasted (Food and Agriculture Organization of the United Nations, 2011). As reviewed in Chapter 2, whey watery liquid coproduct that remains after coagulating the casein proteins for dairy product manufacturing, contributes a substantial portion of dairy waste. Whey contains about half the total solids in milk, nearly all its lactose, ~20% of the milk proteins, some enzymes, minerals, and small amounts of fat. Hence, the efforts to utilize and valorize dairy manufacturing waste have increased. (Brazzle et al., 2019; Chatzipaschali & Stamatis, 2012; Macwan et al., 2016; Mirabella et al., 2014; Panghal et al., 2018; Ryan & Walsh, 2016; Smithers, 2008; Tsermoula et al., 2021; Yadav et al., 2015). Smithers (2008) reviewed how the combination of changes in regulations and the recognition of the valuable whey components have rewritten the story of whey from 'gutter-to-gold'.

Physical methods such as membrane filtration techniques have been applied to produce whey protein concentrates (WPC) and whey protein isolates (WPI) containing 35-90% and > 90% protein, respectively (Baldasso et al, 2011; Argenta & Scheer, 2020) Despite these efforts, only

[1] A version of this thesis chapter has been published as Emily Y. Wong, Byron Yépez , Bernhard Seifried, Paul Moquin, Ricardo Couto, and Feral Temelli. Single-step concentration of whey proteins using the pressurized gas eXpanded (PGX) liquid technology: Effect on physicochemical properties and scale-up. *Journal of Food Engineering,* 366 (2024) 111846, https://doi.org/10.1016/j.jfoodeng.2023.111846

about half the total whey volume is utilized to generate whey products. Therefore, technologies capable of processing whey liquid into value-added functional powder directly or with a minimum number of steps are required.

Among the proteins, β-lactoglobulin (β-LG), α-lactalbumin (α-LA), immunoglobulins (Ig), bovine serum albumin (BSA), lactoferrin (Lf), lactoperoxidase (LPO), glycomacropeptide (GMP) and proteose-peptone (PP) compose the major and minor constituents of whey protein (Madureira et al., 2007; Mehra et al., 2021). Currently, whey-derived protein products are widely available on the market as functional food ingredients and products (de Wit, 1998). Whey proteins are also used in infant milk powders (Jost et al. 1999), sports nutrition protein supplements (Devries & Phillips, 2015), and in the preparation of active food packaging for the extension of product shelf life (Catarino et al., 2017; Daniloski et al. 2021).

Supercritical carbon dioxide ($scCO_2$) has been applied to concentrate, precipitate, and fractionate whey proteins, specifically β-LG and α-LA, from whey liquid or concentrated whey protein solutions (Tomasula, 1999; Bonnaillie & Tomasula, 2012; Yver et al., 2012). Whey proteins are fractionated through their selective precipitation due to the formation of carbonic acid in the presence of CO_2 and water. As a result, the two major whey proteins are separated: β-LG remains soluble in the supernatant fraction, and α-LA is collected as a precipitate. The fractionated whey proteins can be collected by decantation or filtration and must still undergo a drying step before further use in formulations. $scCO_2$ has also been used to dry WPI hydrogels, forming a porous aerogel with a 3D network of interconnected particles with a good oil-holding capacity of up to 75% w/w oil/aerogel (Manzocco, 2021). Others utilized the unique physicochemical attributes of proteins to prepare bioactive delivery systems for anti-inflammatory drugs such as ketoprofen (up to 9.5% w/w) using $scCO_2$ impregnation (Betz et al., 2012). The functionalization of WPC and

WPI with $scCO_2$ was achieved through multiple steps, including but not limited to the preparation of hydrogels, solvent exchange, drying, and adsorption of active materials (Betz et al., 2012; Manzocco, 2021).

This study focused on the continued exploration of the potential applications of the Pressurized Gas eXpanded (PGX) liquid technology, expanding beyond the numerous polysaccharides studied. Proteins, more specifically, of animal origin have not been investigated. Whey is a readily available feedstock suitable for PGX processing with minimal preprocessing, and its complex composition presents unique opportunities to generate value-added ingredients and products.

Novel techniques involving green solvents, such as $scCO_2$, to process whey liquid have been previously reported (Tomasula, 1999), but they still require multi-step processing first to purify and separate desirable proteins, followed by network formation and drying. Therefore, the overall objective of this study was to evaluate the drying and purification of sweet cheese whey in a single step using the PGX technology to generate a protein-rich, free-flowing, low bulk density powder. The specific objectives were to (a) investigate the PGX processing of whey liquid on two different scales, using a 1 L and a 5 L system, and (b) evaluate the effect of flow rate ratio on the physicochemical properties of the powders obtained.

3.2. Materials and methods

3.2.1. Materials

Sweet whey liquid (WL) was purchased from a local cheddar cheese producer (The Cheese Factory, Edmonton, AB, Canada). The yellow-green milky whey liquid (pH 5.6) had an average of 7% total solids, composed of 8% ash, 9% fat, 11% protein, and 72% lactose, determined by an ISO/IEC 17025:2017 accredited milk testing lab. Standard Methods for the Examination of Dairy Products, 15.086, 15.114, 15.040, 15.132, were used for fat, total solids, ash, and protein content determination, respectively (Wehr & Frank, 2004). As the primary carbohydrate component, lactose content was calculated after subtracting fat, ash, and protein from the total solids. WL was utilized 'as is' as the feedstock for PGX processing and freeze drying to generate PGX-W and FD-W powders, respectively. For the 1 L system, CO_2 (99.9% purity, < 3 ppm H_2O) was purchased from Praxair Canada Inc. (Mississauga, ON, Canada), and anhydrous ethanol (> 99.5%) was from Greenfield Global Inc. (Brampton, ON, Canada). For the 5 L system, CO_2 (≥ 99.8% purity) was purchased from Messer Canada Inc. (Mississauga, ON, Canada), and anhydrous ethanol (> 99.5%) was purchased from Permolex Ltd. (Red Deer, AB, Canada).

3.2.2. PGX units: 1 L laboratory-scale and 5 L bench-scale systems

The 1 L PGX system, herein denoted as the laboratory system, is located at Agri-Food Discovery Place, University of Alberta and was previously described in detail by Couto et al. (2020) as a Thar SFE 500 unit (Waters, Milford, MA, USA) modified to include a third liquid pump (LDB1/K210/5, LEWA-Nikkiso America, Inc., Holliston, MA, USA) for aqueous polymer

solution injection. The 1 L vessel was fitted with a custom-made basket, equipped with a stainless-steel filter plate and two 5 μm felt filters at the bottom for collecting the dried whey protein concentrate (PGX-W) powders. The lid of the 1 L collection vessel was modified to include a coaxial nozzle setup where the PGX fluid (CO_2 + EtOH) and aqueous polymer are introduced in the outer and inner tubes, respectively. An O-ring was placed around the top of the basket to ensure the flow of fluids through the basket. The pressure of the system was controlled downstream of the collection vessel with a back pressure regulator (EQ-9609, Equilibar, Fletcher, NC, USA) controlled by a pilot pressure regulator (PCD-3000PSIG-D-PCA13-G, Alicat Scientific, Inc., Tucson, AZ, USA). A separation vessel allowed the collection of liquids at ambient pressure from the processing fluid stream. The whole system was controlled using Thar Instruments Process Suite software (SuperChrom SFC Suite v5.9, Thar Technologies, Pittsburgh, PA, USA).

The 5 L bench-scale PGX unit (Fig. 3.1), herein denoted as the bench system, located at Ceapro Inc. is a custom-built setup equipped with a dual piston pump (SFE Pump HPP400–B, SFE Process, Villers-lès-Nancy, France) for CO_2, a Hydra Cell MT8 Metering Pump (Wanner Engineering, Inc., Minneapolis, MN, USA) to deliver EtOH at flow rates of up to 200 g/min and a pneumatically operated piston pump (P750V400 Series, Williams Milton Roy, Ivyland, PA, USA) to deliver the aqueous biopolymer stream. A coaxial nozzle positioned at the top of the collection vessel allowed the injection and mixing of the two streams (CO_2 + EtOH and WL). The collection vessel of this system is composed of a 5 L high-pressure vessel (Fluitron Inc., Ivyland, PA, USA) with an internal diameter and length of 9.8 cm and 68.0 cm, respectively. The collection vessel was fitted with a basket equipped with a stainless-steel filter plate at the bottom to support stainless-steel meshes and 5 μm pore diameter felt filters to collect the PGX-W dried

powder. The pressure of the collection vessel was controlled by a back pressure regulator (EQ-9609, Equilibar, Fletcher, NC, USA), which is controlled by a pilot pressure regulator (PCD-3000PSIG-D-PCA13-G, Alicat Scientific Inc., Tucson, AZ, USA). A 500 mL separation vessel collects and removes the PGX effluent (EtOH and H_2O) at ambient pressure. The density of the PGX effluent was determined using a FlexCOR® series mass flowmeter (CMF-A, Fluid Components International, San Marcos, CA, USA).

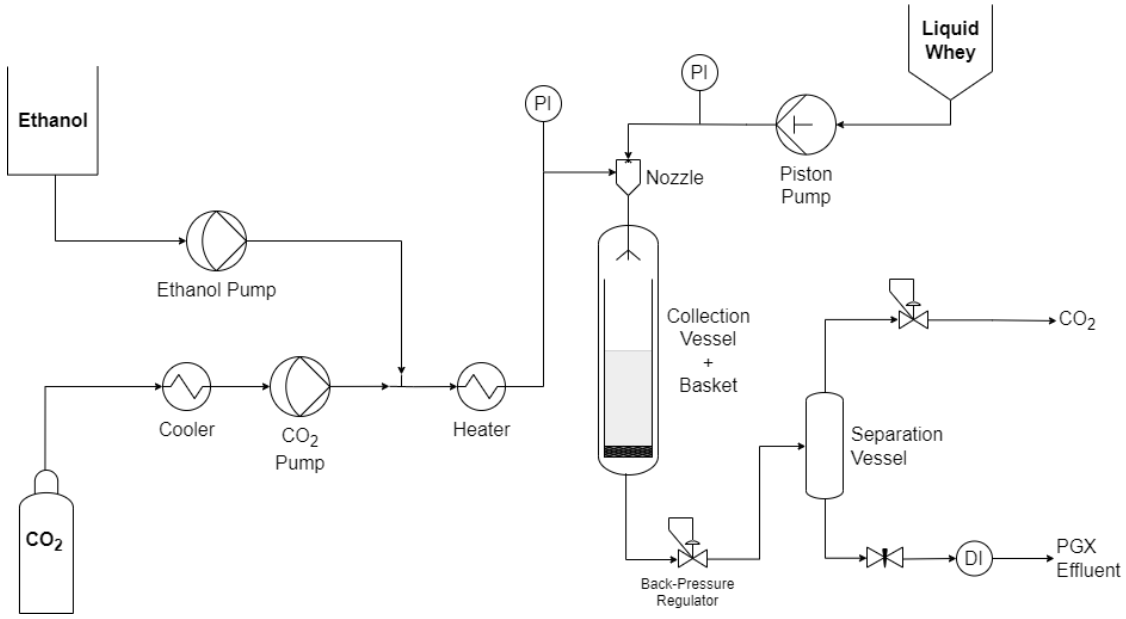

Figure 3.1. Flow chart of the 5 L bench-scale PGX unit. PI: pressure indicator; DI: density indicator.

3.2.3. Experimental design

Two sets of experiments were performed in this study. In the first set, the effect of the PGX process scale was evaluated using the laboratory and bench systems at a specific mass flow ratio θ_{PGX}, as defined in Eq. (3.1), which was kept constant at $\theta_{PGX} = 3.5$. In the second set, the impact of varying the mass flow rate ratio, θ_{PGX}, was investigated using the bench system. The

ratio of CO_2 to EtOH in the PGX fluid (the mixture of CO_2 + EtOH) was kept constant at 1:3, and θ_{PGX} was varied at 5.3, 4.0, 3.5, and 2.5 as shown on the ternary phase diagram of H_2O-EtOH-CO_2 in Fig. 3.2. Equilibrium data for the phase boundary of the ternary phase diagram is from Durling et al. (2007).

$$\theta_{PGX} = \frac{\text{Flow rate of PGX fluid } (CO_2+\text{EtOH})}{\text{Flow rate of water in polymer soln.}} \qquad (3.1)$$

All experiments were performed in duplicate at 40 °C and 100 bar. The mass flow rate ratio, θ_{PGX}, selected for the first set of scale tests (1 L vs 5 L) was $\theta_{3.5}$ following successful initial trials on the laboratory system. Similar θ_{PGX} conditions ($\theta_{PGX} = 4.0$) employed in previous studies (Couto et al., 2020; N. Liu, Couto, et al., 2018; Z. Liu, 2019) on oat beta-glucan, gum arabic, and sodium alginate were selected to expand the investigation of PGX processing on water-soluble biopolymers. Additional θ_{PGX} ratios, generated by utilizing larger and smaller quantities of PGX fluid, were selected to evaluate the effects of the processing parameters on PGX-W powders.

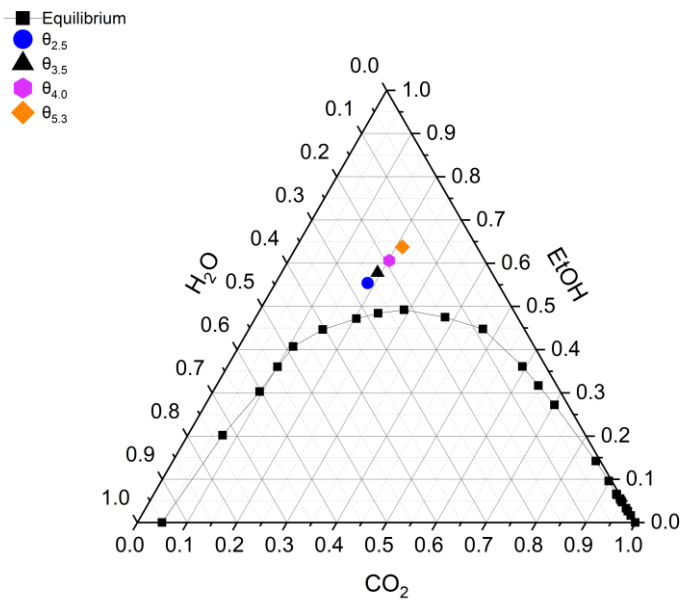

Figure 3. 2. Ternary diagram of water: ethanol: carbon dioxide (mass fractions) with experimental conditions tested. Experimental data for the phase boundary was obtained from (Durling et al., 2007).

3.2.3.1. PGX drying protocol

Regardless of the PGX unit used, the system was initially heated and allowed to stabilize at 40 °C. Meanwhile, WL was heated to 40 °C on a stirring hot plate.

3.2.3.1.1. 1 L laboratory system

The system was pressurized to the target pressure by pumping PGX fluid (CO_2 at 10 g/min + EtOH at 30 g/min) at the experimental conditions. WL was injected into the stabilized system at a flow rate of 11.5 g/min through the inner tube of the coaxial nozzle to achieve θ_{PGX} of 3.5, where the polymer was precipitated upon contact with the PGX fluid, which acts as an anti-solvent. The PGX effluent was collected every 10 min from the separator vessel. Upon completing the injection of 250 mL of WL, the aqueous solution pump was stopped, and the PGX

fluid continued to flow through the collection vessel to remove residual water from the collection vessel. The absence of water in the PGX effluent was confirmed by UV-Vis spectroscopy (FLAME-S-XR1-ES Assembly from 200-1050 nm, Ocean Optics, Dunedin, FL, USA), corresponding to a calibration curve previously acquired at 203 nm. After the complete removal of water, residual EtOH was removed by pumping only CO_2 through the system. Once no more EtOH was detected at the separator, the CO_2 flow rate was increased to 40 g/min to have at least 3x the volume hold-up of the collection vessel flow through to sufficiently dry the PGX-W. Finally, the system was slowly depressurized to ambient pressure to recover the dried PGX-W biopolymer collected on the felt filters.

3.2.3.1.2. 5 L bench system

The bench system is a 5x scale-up of the laboratory system in terms of the collection vessel volume, while the WL feed flow rate increased from 38 to 80 g/min to achieve the targeted θ_{PGX} values of 5.3, 4.0, 3.5, and 2.5. The pressurization of the system was achieved similarly by feeding the PGX fluid (CO_2 at 50 g/min + EtOH at 150 g/min) at the experimental conditions to achieve the target pressure. The aqueous solution (1 L) was injected, and the PGX effluent was collected every 3-4 min at the separator outlet. The water mass fraction of the PGX effluent was calculated from the density and temperature of the liquid measured by the mass flow meter using the model proposed by Danahy et al. (2018). Once the effluent was confirmed to consist of only pure EtOH, EtOH removal by pumping CO_2 only proceeded. CO_2 injection was continued until the EtOH flow rate at the separator outlet reached ≤ 0.1 g/min. The system was depressurized, and the PGX-W powder was collected, similar to the laboratory system.

3.2.3.2. Freeze-dried whey

WL feedstock was lyophilized to obtain freeze-dried whey (FD-W) using a LABCONCO Freeze Zone Plus 12 (Kansas City, MO, USA) freeze drier at < 80 °C and < 40 x 10^{-3} bar. The resulting FD-W was used as reference material to which PGX-processed materials were compared using the analytical methods.

3.2.4. Sample characterization

3.2.4.1. Physicochemical attributes

3.2.4.1.1. Bulk density

Bulk density measurements of FD-W and PGX-W were performed by introducing 0.5-1 g sample into a 25 mL graduated cylinder and recording the volume filled and weight of the untapped powder on an analytical balance (AB204-S, Mettler Toledo Ltd., Leicester, UK).

3.2.4.1.2. Particle size distribution

Particle size was determined using the LS 13 320 Laser Diffraction Particle Size Analyzer (Beckman Coulter, Brea, CA, USA) equipped with a Tornado dry powder system. While particle size distributions were obtained, results were expressed as a mean particle diameter (P_d).

3.2.4.1.3. Specific surface area and pore size

Surface area and pore size were determined using NOVA 4200e (Quantachrome Instruments, Boynton Beach, FL, USA) based on a nitrogen adsorption/desorption isotherm. Samples (around 0.05 g) were degassed at room temperature (22-23 °C) for 24 h. The data were analyzed by the Quantachrome NovaWin software using the Brunauer-Emmett-Teller (BET)

method and the Barrett-Joyner-Halenda (BJH) method to determine specific surface area and pore size, respectively.

3.2.4.1.4. Helium ion microscopy

Particle morphology and surface features of FD-W and PGX-W were examined using a Zeiss Orion Helium Ion Microscope (HiM) (ORION NanoFab, Carl Zeiss Microscopy GmbH, Jena, Germany). Secondary electron images were collected at 30 kV accelerating voltage and 1.5 pA beam current. HiM allows the direct imaging of insulating materials without the need for any coatings, as positive charges are neutralized by an electron gun.

3.2.4.2. Compositional analysis

3.2.4.2.1. Proximate composition

Proximate compositions of FD-W and PGX-W were determined by the following methods: moisture loss was determined gravimetrically after heating for 2-4 h at 110 °C (Wehr & Frank, 2004). Ash content was determined gravimetrically after heating for 48 h at 500 °C in a muffle furnace (AOAC, 2012). The crude protein content of FD-W and PGX-W was determined using a Flash 2000™ Elemental Analyzer (Thermo Fisher Scientific, Waltham, MA, USA), which operated based on a modified Dumas method known as dynamic flash combustion (ISO, 2002). The nitrogen conversion factor of 6.38 for dairy proteins was used to calculate the crude protein content. Crude fat was determined using a hexane extraction method in a test tube. Powdered samples (0.5 g) were dispersed in 10 mL hexane, agitated, and left to stand overnight (approx. 16 h) at room temperature (23 °C). A sample of the supernatant was obtained after

centrifugation for 10 min at 500×*g*, and the solvent was evaporated with a gentle stream of N_2. Crude fat was determined gravimetrically based on the extract in the test tube.

3.2.4.2.2. Elemental analysis

A Thermo Fisher Scientific iCAP 6300 (Thermo Fisher Corp., Cambridge, United Kingdom) Inductively Coupled Plasma – Optical Emission Spectroscopy (ICP-OES) was used to determine the elemental profile of FD-W and PGX-W (Kira et al., 2004). Powdered samples (50 mg) were digested in 5 mL Trace Metal Grade nitric acid (HNO_3) and then diluted to 25 mL with Milli-Q water. Samples were aspirated by a nebulizer into an argon plasma, where they were atomized at temperatures between 5227 – 7727 °C. Analyte atoms are excited, producing characteristic emission patterns unique to each element. These emission lines are detected by a spectrometer, permitting the simultaneous analysis of several elements at once. The elements reported included Ca, K, Mg, Na, P, and S.

3.2.4.2.3. Lactose content determination

Lactose contents of FD-W and PGX-W were determined using Megazyme's Sequential / High Sensitivity Method (K-LOLAC) (Megazyme, Lansing, MI, USA) suitable for the detection of lactose in both low-lactose and lactose-free products as well as in conventional dairy products. MZ104 β-galactosidase hydrolyzed lactose into its monosaccharide constituents, galactose, and glucose (Ivory et al., 2021). The lactose content was calculated by the difference in D-glucose released after the enzymatic hydrolysis and the amount that existed freely in the sample prior to hydrolysis. Sample preparation was performed as per the protocol for "Regular Dairy Samples, Non-Low-Lactose." Briefly, powdered samples were prepared at a concentration of 0.4% w/v in

deionized water, heated to 50-60 °C, and agitated until dissolved. All other assay procedures were followed according to the protocol.

3.2.4.2.4. X-ray diffraction

X-ray diffraction (XRD) patterns of FD-W and PGX-W were measured using a Bruker D8 Discover diffraction system (Bruker, Billerica, MA, USA), equipped with Cu-source and high throughput LynxEYE 1-dimensional detector. The diffractometer was operated with an accelerating voltage of 40 kV and an anode current of 30 mA (Nijdam et al., 2007; Fan & Ross, 2015). Samples were prepared by pressing them into a polymethyl methacrylate (PMMA) powder sample holder. Samples were exposed to CuKα radiation at diffraction angles (2θ) from 5 to 30° at a step size of 0.1° per 5 s time step. Sample data were analyzed using JADE 9.6 software.

3.2.4.3. Protein profile and structure

3.2.4.3.1. Sodium dodecyl sulphate polyacrylamide gel electrophoresis

Sodium dodecyl sulphate polyacrylamide gel electrophoresis (SDS-PAGE) was used to separate proteins in the whey powders according to their electrophoretic mobility. FD-W and PGX-W were reconstituted as 5 mg protein/mL water solutions (Feng et al., 2016). The resulting solutions were mixed with sample buffer at a ratio of 1:1, containing 0.125 M Tris–HCl pH 6.8, 4% w/v SDS, 20% v/v glycerol, 0.5% w/v 2-mercaptoethanol and 1% w/v bromophenol blue in water and heated at 100 °C for 2 min and then allowed to cool to room temperature. Sample aliquots of 10 μL were loaded onto Tris–HCl 4–20% gradient polyacrylamide gels, and electrophoresis was performed with 1x Tris/glycine running buffer at a constant voltage of 80 V for 105-120 min on a Mini-PROTEAN® II electrophoresis cell (Bio-Rad, Mississauga, ON, Canada). After electrophoresis, the gels were stained with 0.1% w/v Coomassie Brilliant Blue G-

250 in an acetic acid/methanol solution (ratio of methanol: acetic acid 1:1 v/v) for 30 min, followed by destaining in an acetic acid/methanol solution (10% v/v methanol) for 20-24 h.

3.2.4.3.2. Soluble protein

Soluble protein contents of FD-W and PGX-W were determined by adapting the method described by Morr et al. (1985). Briefly, a 0.5 g powdered sample was dissolved in 0.1 M NaCl, forming 0.01 g/mL dispersions at pH 3 and 7. FD-W and PGX-W dispersions, 0.01 g/mL in water at pH 3 and 7, were also prepared. Dispersions were prepared at room temperature and constantly agitated at 500 RPM for 1 h. Ten millilitre aliquots were centrifuged at 2500 $\times g$ at room temperature for 10 min. The protein concentration of the protein dispersion as well as the 0.45 µm filtered supernatant were determined as described in section 3.2.4.2.1. Supernatant samples required an additional drying step in a 110 °C oven for 10-15 min before combustion. Soluble protein content was calculated using Eq. (3.2).

$$\text{Soluble Protein (\%)} = \frac{\text{Supernatant protein concentration } \left(\frac{\text{mg}}{\text{mL}}\right) \times 10 \text{ mL}}{\text{Sample weight (mg)} \times \frac{\text{Sample protein content (\%)}}{100}} \times 100 \qquad (3.2)$$

3.2.4.3.3. Size exclusion high-performance liquid chromatography

Average molecular weight (M_W) of FD-W and PGX-W was determined by size-exclusion high-performance liquid chromatography (SEC-HPLC) (Agilent series 1100, Palo Alto, CA, USA), equipped with a TSKgel® G3000 SW XL column (5µm, 7.8 mm ID x 30 cm; TOSOH, Bioscience LLC, Yamaguchi, Japan) where the eluted components were detected by UV absorption at 280 nm (Barry et al., 1988; Dissanayake & Vasiljevic, 2009). Protein solutions (0.1 mg/mL PBS, pH 7) were filtered through a 0.45 µm filter before loading onto the column with an injection volume of 20 µL. The mobile phase was 0.1 mol/L phosphate buffer (pH 7) with 0.1

mol/L NaCl at an isocratic flow rate of 0.5 mL/min. Protein standards β-LG from bovine milk (≥ 90%), α-LA from bovine milk (≥ 85%) and BSA (≥ 98%) (Sigma-Aldrich Co., Oakville, ON, Canada) were used for protein quantification. A standard protein mixture containing 5 mg/mL PBS, pH 7 of each standard (β-LG, α-LA and BSA) were injected into the same column and analyzed under the same conditions as the whey samples. The retention time of each protein in the standard mixture was obtained from the chromatogram and plotted against the logarithmic molecular mass to obtain a calibration curve (Fig. A1, Appendix A). The apparent molecular weights of the whey samples were calculated from the calibration curve.

3.2.4.3.4. Fourier-transform infrared spectroscopy

Fourier-transform infrared (FTIR) absorption spectra were collected using a Thermo Scientific™ Nicolet™ iS50 10 FTIR (Thermo Electron Scientific Instruments LLC, Madison, WI, USA) spectrometer equipped with an attenuated total reflectance (ATR) accessory. The 16 scans were acquired at 4 cm^{-1} resolution for a measurement time of 20 s at a spectra range of 500-4000 cm^{-1}. The spectra were collected and displayed by OMNIC™ spectroscopy software. Data were analyzed with OriginPro 2022b (OriginLab, Northampton, MA, USA).

3.2.4.3.5. Protein intrinsic fluorescence

Right angle intrinsic fluorescence intensities (IFI) of FD-W and PGX-W were determined at 0.1 mg protein/mL phosphate buffer saline, PBS (pH 6.8) using a spectrofluorometer (SpectraMax M3, Molecular Devices, San Jose, CA, USA) at room temperature. The excitation wavelength was 295 nm and the emission spectra were recorded from 260 to 435 nm.

3.2.4.3.6. Protein hydrophobicity

Protein surface hydrophobicity was determined according to Yang et al. (2021) by assessing the extrinsic binding of a fluorescent probe 1-anilinonaphthalene-8-sulfonate (ANS). FD-W and PGX-W were reconstituted to prepare 12.5, 25 and 50 mg protein/L PBS (pH 6.8). The excitation and emission wavelengths were 390 and 470 nm, respectively. The hydrophobicity of the protein was reported as the slope of the plot of relative fluorescence intensities (RFI) vs protein concentration (mg/mL).

3.2.5. Statistical analysis

One-way analysis of variance (ANOVA) and Tukey's test with a 95% confidence interval ($p < 0.05$) were used to determine the statistical differences between the characteristics of samples obtained by freeze drying and under different PGX processing conditions. Statistical analysis was performed using Minitab® Statistical Software (Version 21.3.1.0, Minitab Inc., State College, PA, USA).

3.3. Results and discussion

3.3.1. Effect of processing scale (1 L vs 5 L) on whey liquid

Effect of the processing scale at 1 L vs 5 L was evaluated in the first set of experiments, and the resulting PGX-W was characterized and compared to FD-W. All the experiments in this section were performed at a constant θ_{PGX} value of 3.5. The recovery of the whey solids from the sweet whey solution at the two processing scales, 1 L and 5 L were 6% and 9%, respectively.

3.3.1.1. Physicochemical attributes

FD-W powders were clumpy, yellow-hued flakes and crystalized flecks (Fig. 3.3) with a volume-weighted mean particle diameter (P_d) of 94.3 µm, a bulk density of 177 g/L (Table 3.1) and a faint sweet scent. While both the lab- and bench-scale PGX-W samples were odorless, free-flowing fine white powders with a low bulk density (74 g/L and 35 g/L, respectively) and a similar P_d value (10 mm), their particle size distribution (PSD) differed, with the bench-scale sample having a higher proportion of particles ranging from 20-25 µm. The PSD showed a bimodal distribution in both cases, with peaks at 10 µm and 25 µm (Fig. A2, Appendix A). This may be a result of the particle bed formation and physical association of smaller particles forming larger particle aggregates. Large aggregates in bench-scale PGX-W were most probably physical agglomerations with voids.

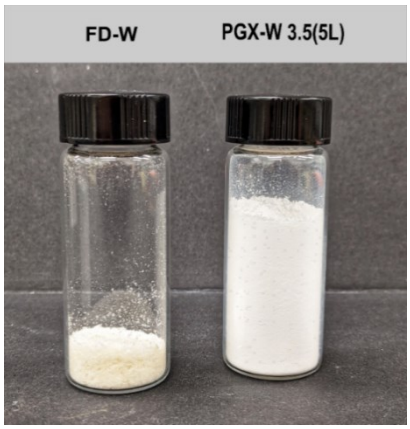

Figure 3.3. FD-W (left) and PGX-W (right), with 0.5 g in each vial.

FD-W had limited surface features with a minimal number of visible pores, while PGX-W were characterized by many distinguishable microscopic features as shown in the HiM images (Fig. 3.4). The PGX process effectively precipitated and micronized whey solids from the sweet whey liquid, producing nano- and micro-scale fused globular morphologies and an overall porous

polymer matrix. HiM images of PGX-W powders had heterogeneous particle sizes, with 100 nm – 2 µm spheres and clusters with nano-sized features. The specific surface area (SSA) of FD-W was not detectable with the analysis method employed (Table 3.1), and consequently, the detection limit of 5 m^2/g was considered for statistical purposes. PGX-W had significantly larger surface areas of 20-28 m^2/g, at least 5-6x larger than that of FD-W (Table 3.1), with the lab-scale sample having the highest surface area at 28.2 ± 1.3 m^2/g. The pore size of these powdered samples was in the range of 16-19 Å and, therefore, are classified as micropores (< 2 nm) (Bardestani, 2019).

Table 3.1. Physicochemical characteristics of whey powders.

	Moisture (%)	Mean P_d (μm)	Bulk density (g/L)	SSA (m^2/g)	Pore size[x] (Å)	Hydrophobicity (a.u)
FD-W	5.2 ± 0.5	94.3 ± 1.9	177 ± 1[a]	< 5[e]	18.6 ± 0.2[a]	429 ± 23[d]
Effect of scale						
PGX-W 3.5(1L)	7.5 ± 0.2	10.5 ± 0.4	74 ± 1[b]	28.2 ± 1.3[a]	18.4 ± 0.2[a]	888 ± 9[b]
PGX-W 3.5(5L)[y]	9.1 ± 0.6	10.9 ± 0.1	35 ± 1[d]	20.1 ± 1.4[b,c]	16.0 ± 0.1[a]	1127 ± 27[a]
Effect of θ_{PGX}						
PGX-W 2.5(5L)	9.4 ± 0.5	14.3 ± 0.5	66 ± 1[b,c]	12.7 ± 3.8[d]	18.0 ± 1.3[a]	712 ± 14[b,c]
PGX-W 3.5(5L)[y]	9.1 ± 0.6	10.9 ± 0.1	35 ± 1[d]	20.1 ± 1.4[b,c]	16.0 ± 0.1[a]	1127 ± 27[a]
PGX-W 4.0(5L)	9.1 ± 0.3	11.2 ± 0.7	38 ± 2[d]	17.7 ± 0.9[c,d]	18.9 ± 0.7[a]	619 ± 26[cd]
PGX-W 5.3(5L)	9.9 ± 0.7	14.3 ± 0.7	57 ± 2[c]	25.7 ± 0.9[a,b]	17.5 ± 1.9[a]	836 ± 72[c]

Data presented as mean ± SD (n=2).

[x] Mean value reported for particle size (% volume), complete particle size distribution presented in Appendix A.

[y] Repeated for ease of comparison

[a-e] Different lowercase letters in each column represent a significant difference ($p < 0.05$).

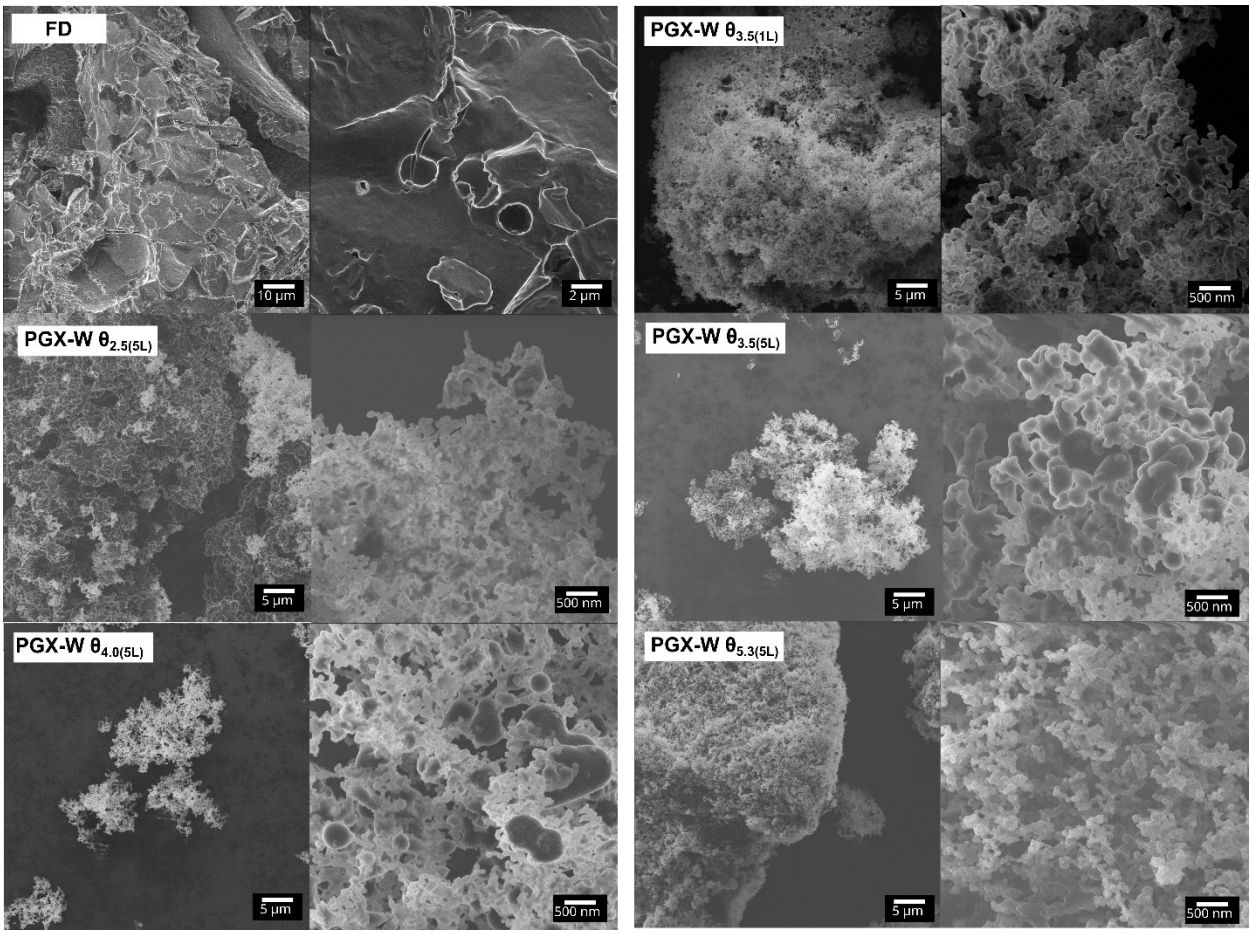

Figure 3.4. Helium ion microscope (HiM) images of FD-W and PGX-W.

3.3.1.2. Compositional analysis

Proximate composition of FD-W and PGX-W is reported in Fig. 3.5. FD-W had a typical composition containing mainly lactose at 65.1 ± 4.2% followed by protein, ash, and fat levels of 10.6 ± 0.4%, 7.3 ± 0.1%, and 3.3 ± 0.8% dwb, respectively (Morr & Ha, 1993). PGX-W 3.5(1L) and PGX-W 3.5(5L) had similar protein, lactose, ash, and fat contents, which suggested that the PGX process was reproducible at two different scales (1 L and 5 L). The average protein content of 44% was significantly higher in both PGX-W than that in FD-W, with proteins being concentrated by > 4x. PGX-W obtained at both scales had significantly lower fat (< 0.5% dwb)

contents but higher ash (~2x) levels compared to FD-W. During PGX processing, the protein, ash, and lactose components were precipitated while the residual milk fat was extracted by the PGX fluid. The smaller lactose particles were also washed out in addition to partial solubilization of lactose, therefore, resulting in the concentration of the protein and ash contents in the dried powder.

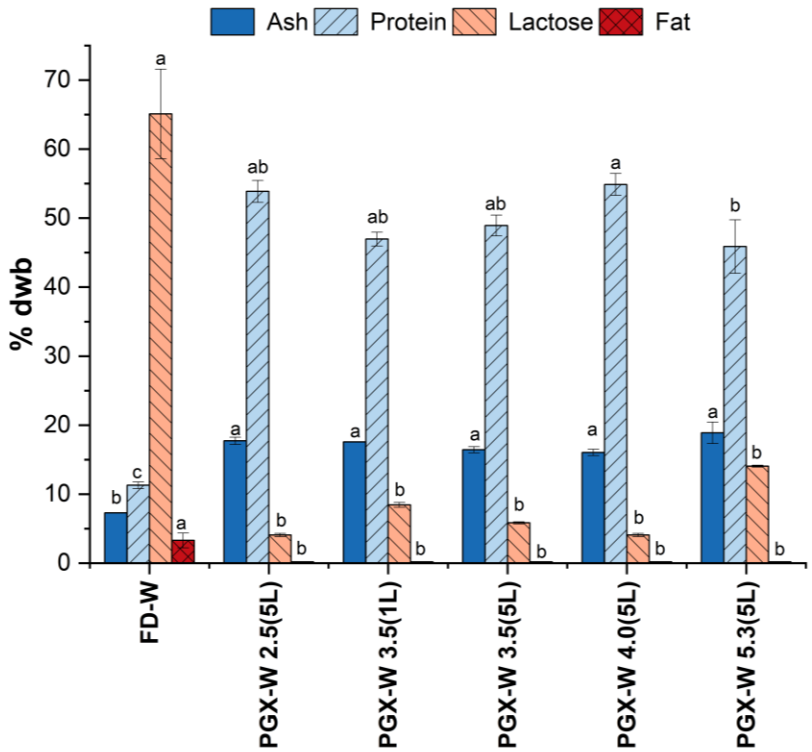

Figure 3.5. Compositional analysis of PGX-W and FD-W on a dry weight basis, presented as mean ± SD (n=2) for all groups. Different letters for each component indicate significant differences ($p < 0.05$).

Table 3.2. Mineral composition (%, dwb) of dried whey powders.

	Ca (%)	K (%)	Mg (%)	Na (%)	P (%)	S (%)	Total (%)
FD-W	0.62 ± 0.07^{c}	$2.44 \pm 0.30^{a,b}$	0.13 ± 0.02^{c}	0.60 ± 0.08^{a}	0.73 ± 0.12^{b}	0.20 ± 0.01^{c}	4.73 ± 1.20^{b}
Effect of scale							
PGX-W 3.5(1L)	3.24 ± 0.02^{b}	3.13 ± 0.08^{b}	0.55 ± 0.01^{b}	$0.51 \pm 0.02^{a,b}$	2.43 ± 0.04^{a}	$0.90 \pm 0.01^{a,b}$	10.75 ± 0.34^{a}
PGX-W 3.5(5L)[y]	3.33 ± 0.13^{b}	$2.47 \pm 0.03^{a,b}$	$0.61 \pm 0.02^{a,b}$	$0.43 \pm 0.01^{a,b}$	2.27 ± 0.05^{a}	$0.93 \pm 0.03^{a,b}$	10.04 ± 0.53^{a}
Effect of θ_{PGX}							
PGX-W 2.5(5L)	3.94 ± 0.06^{a}	2.03 ± 0.01^{b}	$0.60 \pm 0.01^{a,b}$	0.33 ± 0.01^{b}	2.31 ± 0.01^{a}	$0.92 \pm 0.01^{a,b}$	10.14 ± 0.19^{a}
PGX-W 3.5(5L)[y]	3.33 ± 0.13^{b}	$2.47 \pm 0.03^{a,b}$	$0.61 \pm 0.02^{a,b}$	$0.43 \pm 0.01^{a,b}$	2.27 ± 0.05^{a}	$0.93 \pm 0.03^{a,b}$	10.04 ± 0.53^{a}
PGX-W 4.0(5L)	3.49 ± 0.06^{b}	2.19 ± 0.18^{b}	$0.58 \pm 0.03^{a,b}$	0.38 ± 0.03^{b}	2.24 ± 0.04^{a}	0.94 ± 0.01^{a}	9.82 ± 0.68^{a}
PGX-W 5.3(5L)	3.40 ± 0.05^{b}	3.15 ± 0.0^{a}	$0.65 \pm 0.01^{a,b}$	$0.50 \pm 0.01^{a,b}$	2.40 ± 0.01^{a}	0.86 ± 0.01^{b}	10.96 ± 0.19^{a}

Data presented as mean ± SD (n=2).

[y] Repeated for ease of comparison

[a-d] Different letters within each column indicate significant differences ($p < 0.05$).

Ca, K, Mg, Na, P, and S represented over half of the ash content in the FD-W and PGX-W (Table 3.2), which are typically found in milk. Calcium in the ash included calcium liberated from casein proteins and the $CaCl_2$ added to improve curd strength (Schultz & Ashworth, 1974). The unique ability of milk proteins to bind, transport, and deliver these minerals has been previously reported (Gaucheron, 2013). Most notably, the casein micelle structure contains calcium phosphate, which contributes to bone health and required by the neonate. During cheese production, most of the calcium is retained by the casein, and the phosphates are released into the whey stream and concentrated together with the other serum ions, such as potassium and magnesium, during PGX processing.

Amorphous lactose is produced during spray drying and FD-W. However, due to the hygroscopicity and instability of amorphous lactose, its crystallization into the stable forms of α- and β-lactose during storage has been reported (Saito, 1988; Jouppila et al., 1997; Haque & Ross, 2005). Lactose crystallization in FD-W powders was previously reported by Haque and Ross (2005) to be dependent on the relative humidity with rapid crystallization of lactose from anhydrous β-lactose to the more stable form, α-lactose with increasing relative humidity (54.5% > 65.6% > 76.1%). XRD analysis results in this study (Fig. 3.6) confirmed that the lactose in FD-W was composed of the crystallized α-lactose monohydrate and anhydrous β-lactose identified at diffraction angles (2θ) of (12.4°, 16.4°, and 19.9°) and (20.8° and 21.2°), respectively (Haque & Ross, 2005). Mixtures of α- and β-lactose in molar ratios of 5:3 and 4:1 were identified at 19.1° as well as at 19.9° and 19.5°, respectively, which are typical of other freeze-dried powders stored at ≥ 54.5% relative humidity. Previously, lactose crystallization was studied by a modified solution-enhanced dispersion by supercritical fluids (SEDS) technique in which an aqueous lactose solution was sprayed into a pressurized chamber with a $scCO_2$-cosolvent mixture with ethanol or methanol,

forming α-lactose monohydrate particles (Palakodaty & York, 1988). Particle size of stable α-lactose crystals (5-31 μm) was affected by the behaviour of the water-ethanol/methanol-CO_2 system due to changes in the CO_2-cosolvent flow rates. Results from the current study differed such that both PGX-W 3.5(1L) and PGX-W 3.5(5L) powders were characterized by amorphous lactose, with no distinguishable peaks in the XRD patterns (Fig. 3.6). Lactose crystallization in mixtures of 50:50 and 70:30 ratios of lactose:protein studied by Fan and Roos (2015) demonstrated that the presence of whey proteins improved lactose solubility, limited the rate of lactose crystallization, and thus the formation of specific crystal types (e.g., α-lactose > β-lactose) could be controlled. Relative to the findings of this study, the combination of the micronization effect during PGX processing, together with the presence of high protein content, resulted in the preservation of amorphous lactose. Although the amorphous lactose is obtained in PGX powders, stability studies under controlled temperature and humidity settings should be considered to investigate the implications on the powders' quality attributes and shelf life as well as product applications.

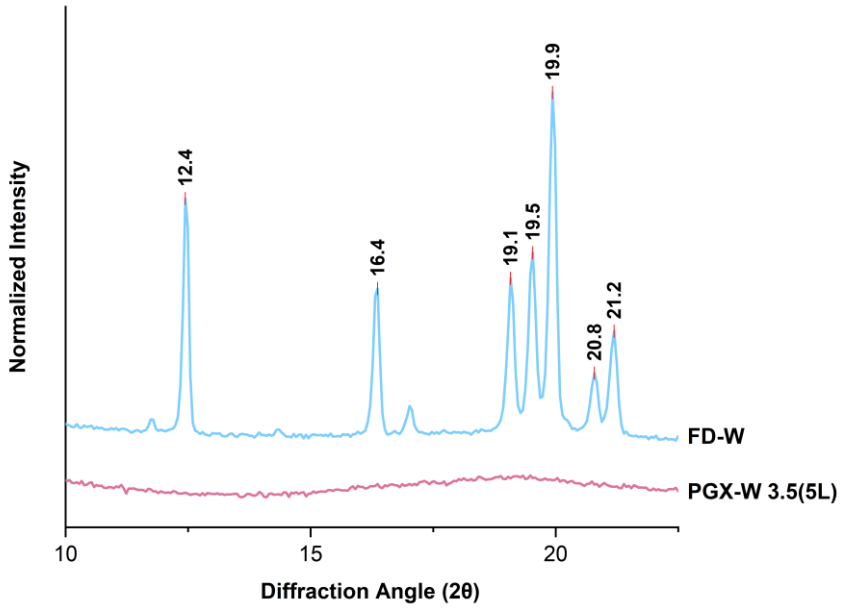

Figure 3.6. Normalized X-ray diffraction patterns of FD-W and PGX-W 3.5(5L) powders.

3.3.1.3. Protein profile and structure

SEC-HPLC was used to analyze the molecular weight distribution of the whey proteins by correlating compounds that were eluted based on their hydrodynamic volume to their respective molecular weights. In this study, BSA, β-LG, and α-LA standards were used as calibration proteins, which eluted at 18.9, 20.7, 21.6, and 22.6 min (peaks 2, 3-4, and 5 in Fig. 3.7), representing MW ranges of 48-67 kDa, 23-37 kDa, and 14-16 kDa, respectively. This elution profile and log(molecular weight) were plotted on a calibration curve, which showed a good linear correlation (R^2=0.89). Thus, the major whey proteins, β-LG, α-LA, and BSA, which encompassed 60%, 20%, and 10% of the proteins, respectively, (Morr et al., 1985) were suitable as standard proteins to generate the SEC-HPLC calibration data.

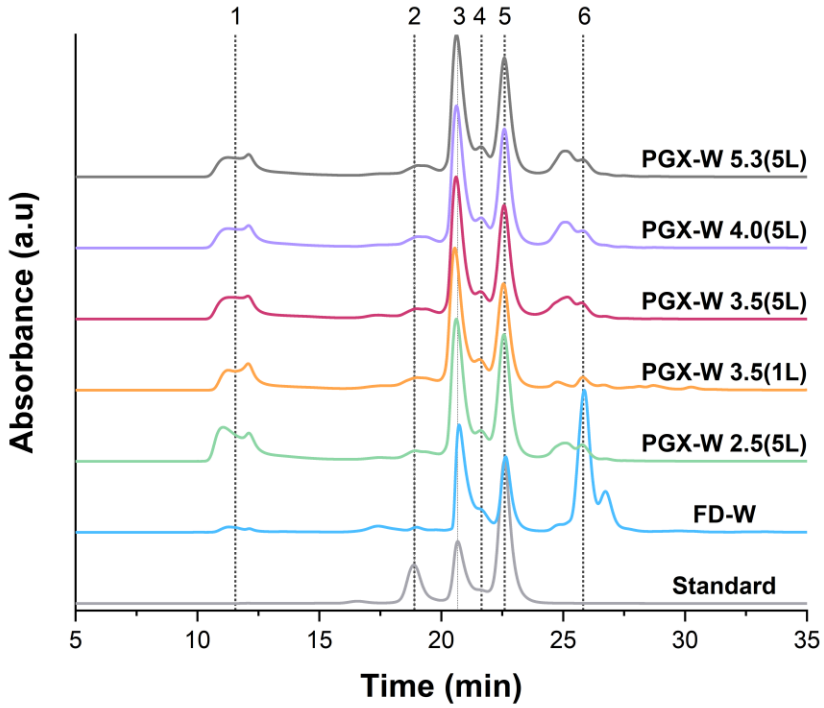

Figure 3.7. HPLC chromatograms of protein aggregates: (1) > 250 kDa, (2) BSA, (3,4) β-LG dimer and monomer, (5) α-LA, (6) small molecules < 14 kDa.

Fig. 3.7 shows the SEC-HPLC chromatograms for the samples obtained in this study. Reconstituted FD-W contained 8% of aggregates, > 250 kDa (peak 1) eluted between 11.3-12.1 min. Consistent with the compositional data (Fig. 3.5), over 64% of the FD-W components were small molecules (peak 6) such as lactose, its respective monosaccharides, and possibly non-protein nitrogen (NPN) compounds. BSA, β-LG, and α-LA constituted 2%, 22%, and 2% of FD-W. The chromatograms for the PGX-W samples were similar to each other. β-LG was concentrated to ~35%, which eluted primarily as the protein dimer (37 kDa) with a small proportion eluting in its monomeric form (18 kDa). α-LA proteins were also concentrated to ~27% in both PGX-W. The proportion of aggregates (peak 1) in the PGX-W increased two-fold compared to that in FD-W, from 8% to 16%, which may be attributed to enhanced interactions amongst the concentrated

proteins. Wang and Lucey (2003) reported molecular weight ranges of proteins in different WPC and WPI samples because of the interactions between whey proteins and other matrix components such as lipids and minerals, notably more in WPC than in WPI matrices. Alternatively, the formation of large MW aggregates may be attributed to the partial unfolding of whey proteins during PGX processing. The significant reduction in low molecular weight components (Fig. 3.7, peak 6), from ~64% to ~11%, may be corroborated by the small particles being washed out and low molecular components being solubilized and extracted during the PGX process.

While SEC-HPLC results reflected the actual behaviour and interaction of the proteins in solution, complementary reduced SDS-PAGE analysis was valuable for identifying individual whey protein fractions in the sample matrix. Fig. 3.8 shows the results of reduced SDS-PAGE analysis. BSA, β-LG, and α-LA bands were most distinguishable in FD-W (lane A). Faint bands representing Lf and IgG were also identified in the SDS-PAGE patterns. After PGX processing, lab-scale PGX-W samples were identified with only β-LG and α-LA bands (lane B).

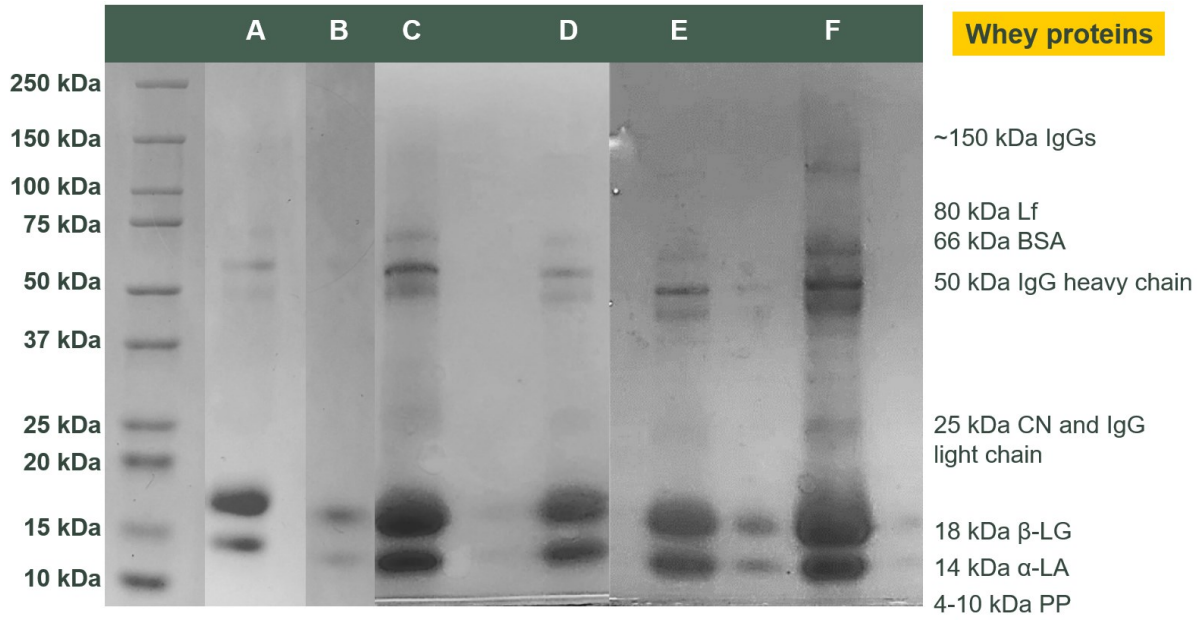

Figure 3.8. SDS-PAGE patterns of reconstituted whey powders on a 4-20% polyacrylamide gel; Molecular weight standards ladder between bands A. and B.; A) FD-W, B) PGX-W 3.5(1L), C) PGX-W 3.5(5L), D) PGX-W 4.0(5L), E) PGX-W 2.5(5L), F) PGX-W 5.3(5L).

The absence of BSA, Lf, and IgG bands in lab-scale PGX-W powders indicated that processing at the laboratory scale was ineffective for retaining minor whey proteins. SDS-PAGE patterns of bench-scale PGX-W were similar to that of FD-W, which demonstrated the retention of the proteins in the dried whey powders from the original whey liquid feedstock. While minor whey proteins (Lf and IgG) in FD-W and bench-scale PGX-W were separated with SDS-PAGE, these proteins were not resolved in the SEC-HPLC chromatograms (Fig. 3.7). Other studies reported that the Lf and IgG proteins are often eluted together with BSA due to their relatively similar molecular weights (Shimazaki & Sukegawa, 1982). Overall, the retention of the minor proteins (Lf and IgG) in bench-scale PGX-W indicated that scale-up processing was favourable. Therefore, further analysis of PGX-whey processing was conducted using the 5 L bench-scale system.

The secondary structure of the protein powders was analyzed using FTIR-ATR. The FTIR spectra of the whey powders obtained at different scales are reported in Fig. 3.9(A1), which featured two regions at 800-1200 cm^{-1} and 1300-1800 cm^{-1}, representing the carbohydrate fingerprint and protein amide I/II/III regions, respectively. The most intense band in the first region is characteristic of the stretching vibrations of C-C and C-O moieties within the glycosidic linkages of lactose (Wiercigroch et al., 2017). The second derivative of the normalized infrared spectra (Fig. 3.9(A2)) was determined to resolve closely located peaks in the amide I region. Beta-structures were identified at 1626 cm^{-1} (β-sheets), 1682 cm^{-1} (intermolecular β-sheets), and 1695 cm^{-1} (β-sheets/turns) (Byler & Susi, 1986; Boye & Ma, 1997; Fang & Dalgleish, 1997) in FD-W, PGX-W 3.5(1L) and PGX-W 3.5(5L) powders.

The peak at 1626 cm^{-1} was more intense in both lab- and bench-scale PGX-W compared to that in FD-W, with intensities PGX-W 3.5(5L) > PGX-W 3.5(1L) >> FD-W. In this region, there are typically two peaks attributed to β-sheets, at 1622 cm^{-1} and 1632 cm^{-1} (Fang & Dalgleish, 1997), and the observation of the enhanced single peak intensity was suggestive of changes in the secondary structures such as increased hydrogen bonding (Boye & Ma, 1997). Protein aggregation due to interactions between the loop/turn regions and amide sidechains affected wavenumber shifts and band intensities. Bands for α-helix and loop and turn structures were specifically identified in the whey powders at 1652 cm^{-1} and 1660 cm^{-1}, respectively (Byler & Susi, 1986). Both PGX-W had similar FTIR spectra, where both had a slightly more intense peak at 1652 cm^{-1} compared to FD-W, which was representative of α-helix structures. The overall increased band intensity of all the β-structures, α-helix, and loops and turns demonstrate the purification and concentration of the whey proteins by PGX processing.

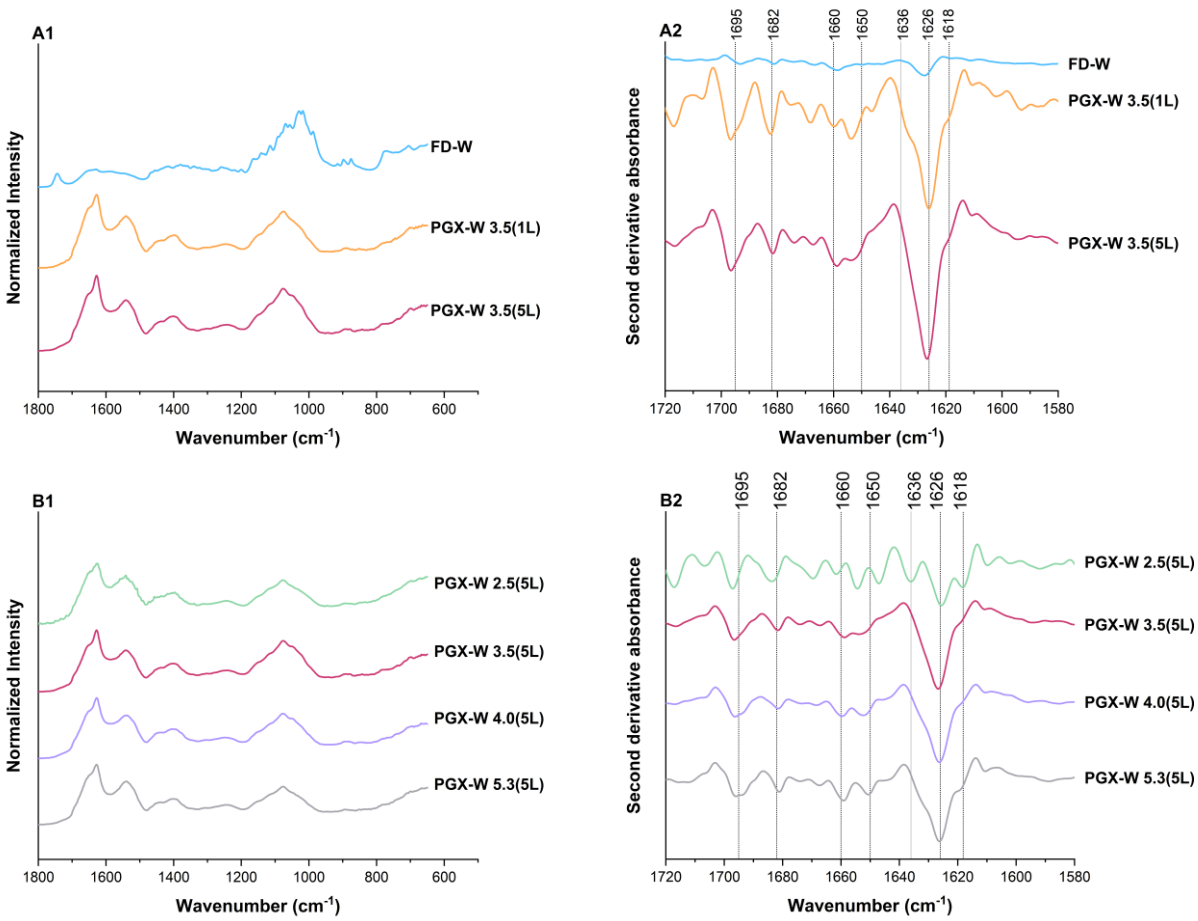

Figure 3.9. (1) FTIR-ATR spectra, and (2) second derivative of FTIR-ATR spectra in the wavenumber range of 1580-1720 cm-1 for whey powders obtained using the PGX technology at (A) different scales in comparison to FD-W, and (B) different flow rate ratios.

3.3.1.4. Soluble protein and aggregation

Physicochemical attributes of proteins affect the functional properties and the overall usefulness of proteins in various food and non-food systems. The level of soluble protein is important for applications involving aqueous environments. Since globulins and albumins constituted the majority of the proteins in the powders, the effect of adding salt and changing pH on the solubility of FD-W and PGX-W was studied. Soluble protein was calculated by determining the total protein in the soluble fraction of protein dispersions relative to the total protein in the dry

powder, and the results are reported in Table 3.3. Changes in ionic strength and solution pH affect the charged amino acid residues on the protein surface. Both pH and ionic strength had a significant effect on the protein solubility in FD-W (Table 3.3). At constant pH, an increase in the ionic strength increased the soluble protein fraction (salting in effect (Carr et al., 2004)), which was more notable at neutral pH. An increase in pH at constant ionic strength, increased the percentage of soluble protein in the saline solution, while reducing the soluble fraction in water (no salt). The highest soluble fraction (96.7 ± 0.9%) was reached at neutral conditions (pH = 7) and in the presence of salt (0.1M NaCl). At pH 3 and 7, away from the isoelectric point of whey (~ 5.2), FD-W soluble protein content in water was 82.2 ± 0.6% and 74.5 ± 1%, respectively. At low ionic strength, the salting in effect was dominant where dissolved ions neutralize surface charges and electrostatic repulsion, thereby, promoting an increase in the FD-W protein solubility (Carr et al., 2004; Dahal & Schmit, 2018). PGX-W 3.5(1L) had the highest soluble protein at 112.6 ± 3.2% in 0.1 M NaCl at pH 7. Despite the large variability in the data, the PGX-W 3.5(5L) sample had a similar soluble protein to that of PGX-W 3.5(1L) (Table 3.3). Having soluble protein levels > 100% for some of the samples (Table 3.3) may be due to the combustion method employed for the determination of crude nitrogen followed by conversion to protein content using a conversion factor of 6.38 for dairy proteins. Thus, any exogenous nitrogen, potentially originating from the solvents used to dissolve the powders, could have contributed to the total nitrogen content detected. In addition, larger uncertainty for some values may be due to variable protein content within the sample matrix.

Table 3.3. Level of soluble protein in 0.1 M NaCl and water at pH 3 and 7.

	Soluble protein (%)			
	Water		**0.1 M NaCl**	
	pH = 3	pH = 7	pH = 3	pH = 7
FD-W	$82.2 \pm 0.6^{A,c}$	$74.5 \pm 1.4^{B,d}$	$91.8 \pm 1.5^{A,b}$	$96.7 \pm 0.9^{B,a}$
Effect of scale				
PGX-W 3.5(1L)	$87.3 \pm 6.6^{A,a}$	$86.3 \pm 0.3^{A,a}$	$103.4 \pm 18.9^{A,a}$	$112.6 \pm 3.2^{A,a}$
PGX-W 3.5(5L)[y]	$78.5 \pm 10.7^{A,a}$	$89.5 \pm 0.5^{A,a}$	$86.9 \pm 1.2^{A,a}$	$91.4 \pm 0.6^{A,a}$
Effect of θ_{PGX}				
PGX-W 2.5(5L)	$83.4 \pm 10.0^{A,a}$	$68.1 \pm 2.5^{B,a}$	$85.5 \pm 4.9^{A,a}$	$84.4 \pm 17.3^{A,a}$
PGX-W 3.5(5L)[y]	$78.5 \pm 10.7^{A,a}$	$89.5 \pm 0.5^{AB,a}$	$86.9 \pm 1.2^{A,a}$	$91.4 \pm 0.6^{A,a}$
PGX-W 4.0(5L)	$62.8 \pm 5.9^{A,a}$	$87.3 \pm 10.1^{AB,a}$	$79.9 \pm 0.5^{A,a}$	$83.3 \pm 5.8^{A,a}$
PGX-W 5.3(5L)	$88.5 \pm 0.5^{A,a}$	$95.4 \pm 5.2^{A,a}$	$102.5 \pm 11.9^{A,a}$	$105.2 \pm 3.84^{A,a}$

Data presented as ± SD (n=2).
[y] Repeated for ease of comparison.
Different lowercase letters represent significant difference ($p < 0.05$) in soluble protein content within each sample.
Different uppercase letters represent significant difference ($p < 0.05$) within each solvent group.

Surface hydrophobicity affects the overall solubility behaviour of proteins and dictates the ability of a protein to adsorb to oil/water and air/water interfaces to behave as emulsifiers and foaming agents. Hydrophobic amino acids tryptophan (Trp), tyrosine (Tyr), and phenylalanine (Phe) absorb UV light due to their aromatic ring structures. As reported elsewhere (Jackman & Yada, 1989), whey proteins absorb strongly at 280 nm, whereas each of the aromatic amino acid residues absorbs strongly at differing wavelengths. Tyr, Trp, and Phe residues absorb at 260 nm, Tyr and Phe at 290 nm, and only Trp absorbs strongly at 295 nm (Hinderink et al., 2021; Jackman & Yada, 1989). Upon excitation at their respective wavelengths, these amino acids also exhibit intrinsic fluorescence properties, which help identify changes in the environment surrounding the protein (Eftink, 2000). Specifically, changes in the fluorescence emission of Trp-19 situated in the hydrophobic core of β-LG (known as the calyx) (Albani et al., 2014) reflected conformational changes in the protein upon subjecting Trp-19 to hydrophilic or hydrophobic environments. FD-W and both PGX-W emitted strongly at 330 nm (Fig. 3.10), between the regions where Trp-19

would be buried (300-320 nm) and exposed (340-355 nm), which suggested that there was a partial unfolding of proteins and the exposure of the hydrophobic groups (Hinderink et al., 2021; Jackman & Yada, 1989).

ANS ligand-protein interactions were evaluated to determine surface hydrophobicity, and values were calculated as the slope of the plot of relative fluorescence intensities vs. protein concentration (ppm). Larger slopes were correlated with increased surface hydrophobicity. FD-W had lower surface hydrophobicity compared to PGX-W (Table 3.1). Dispersions were standardized to obtain the same protein content across the different samples, which was particularly important for FD-W. FD-W powders had significantly larger quantities of lactose relative to protein, thus increasing the overall hydrophilicity of the dispersions relative to PGX-W dispersions.

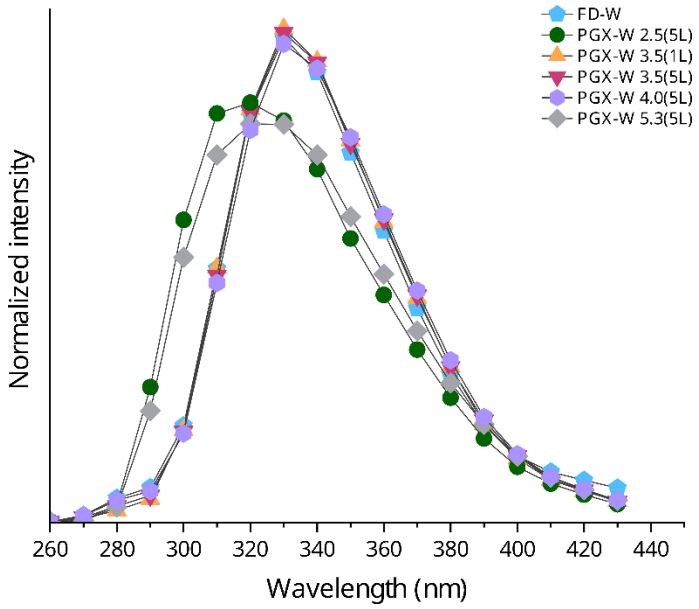

Figure 3.10. Intrinsic fluorescence emission spectra of whey powders reconstituted in PBS, pH 6.8, at an excitation wavelength of 295 nm.

Relative to the processing using the 1 L lab-scale system, PGX-W 3.5(5L) had significantly higher surface hydrophobicity attributed to the prolonged exposure of proteins to ethanol (~120 min vs ~180 min) during PGX processing, causing the rearrangement of hydrophobic sites. Collini et al. (2000) found that the binding of ANS to two different sites, the β-barrel or surface of β-LG, was affected by a range of pH and ionic strength environments. Similar evaluations of ANS and PGX whey protein binding are valuable future considerations to understand better the binding of other hydrophobic molecules, such as bioactive compounds.

Bench-scale PGX-W had intrinsic fluorescence emission behaviour similar to the more hydrophilic FD-W samples yet had the highest surface hydrophobicity (Table 3.1). The fluorescence emission spectra suggested that the FD-W proteins had a hydrophobic or compact conformation with low surface hydrophobicity due to the large quantity and hydrophilicity of lactose. In that sense, bench-scale PGX-W proteins had a less compact structure, which allowed for the increased binding of aromatic residues (Trp-19) to ANS combined with an increased number of exposed hydrophobic regions on the protein surface.

3.3.2. Effect of θ_{PGX} ratio on whey liquid

The θ_{PGX} ratio was varied from 2.5 to 5.3 using the 5 L bench-scale system, and the effects on the characteristics of the dry powders obtained were evaluated. Minimizing θ_{PGX} ratio is important to minimize processing costs; however, it is essential to understand the impact of θ_{PGX} ratio on the protein characteristics.

3.3.2.1. Physicochemical attributes

HiM images (Fig. 3.4) of powders generated at θ_{PGX} of 3.5 and 4.0 showed similar morphologies, but notable differences were observed at θ_{PGX} ratios of 2.5 and 5.3. Similar to other supercritical antisolvent processes (Chávez et al., 2003), larger proportion of the PGX fluid at $\theta_{5.3}$ facilitated the rapid breakup of the aqueous stream at the nozzle, enhancing the transfer of water from the aqueous stream to the PGX fluid, contributing to an overall faster antisolvent precipitation. As a result, PGX-W 5.3(5L) particles had a mean particle size, P_d of 14.3 ± 0.7 μm (Table 3.1), with exfoliated surfaces and fine features in the tens of nm range. PGX-W 2.5(5L) particles were characterized by a mixture of fine nanostructures dispersed on a matrix of mainly 1-5 μm irregular structures (Fig. 3.4). At $\theta_{PGX} = 2.5$, the reduced breakup of the aqueous stream by the PGX fluid permitted extensive interactions between molecules during the antisolvent process, allowing the nucleation sites to grow to larger particles. These microscopic differences in the particle features were not reflected in the particle size distributions since both PGX-W 2.5(5L) and PGX-W 5.3(5L) had a similar mean particle size (Table 3.1). PGX processing generated micronized whey powders at all θ_{PGX} ratios, with characteristically low bulk densities, ranging from 35-66 g/L. At θ_{PGX} ratios of 2.5 and 5.3, bulk densities were higher than those at θ_{PGX} ratios of 3.5 and 4.0 (Table 3.1), demonstrating the fine balance between how quickly the particles are precipitated, growth of particles, and interactions between the particles, as indicated above. The lowest bulk densities were achieved at intermediate θ_{PGX} conditions (θ_{PGX} = 3.5 and 4.0), corresponding to a 5x reduction in bulk density compared to FD-W. Amongst the PGX whey powders, there was considerable variability in the measured surface areas, with a 2-fold increase in the surface area from 13 to 26 m^2/g when θ_{PGX} was increased from 2.5 to 5.3 (Table 3.1).

3.3.2.2. Compositional analysis

PGX-W 4.0(5L) powders had a protein content of 55% dwb, similar to the composition of the other powders generated at all lower θ_{PGX}. At higher θ_{PGX}, PGX-W 5.3(5L) powders had significantly lower protein content at 45% dwb. According to the composition of the dried powders, with concentrated protein and reduced lactose and fat contents, all PGX whey powders may be classified as WPC (Agricultural Marketing Service, 2015). From the processing perspective, PGX-W 2.5(5L) conditions would be desirable to minimize the CO_2 and EtOH resources required to generate a concentrated whey protein product. PGX effectively defatted the aqueous feedstock at all θ_{PGX} ratios evaluated, demonstrating that a centrifugation or microfiltration pre-treatment step could be eliminated when processing whey liquid. The concentration of the ash components with the proteins (as described in section 3.2.4.2.1) was also observed across the different θ_{PGX} conditions. Although the lactose content of PGX-W 5.3(5L) (14.4% ± 0.4% dwb) was higher than that of the other powders generated at the lower θ_{PGX} conditions (~4-9% dwb), the lactose content was not significantly affected by θ_{PGX}. Regardless, higher θ_{PGX} ratios may be required to precipitate small polar molecules such as the disaccharide lactose, while at lower θ_{PGX} ratios, large molecular weight proteins are more efficiently recovered. This conclusion was reflected in the highly exfoliated surface of PGX-W 5.3(5L) consisting of lactose and larger (1-5 μm) irregular structures in PGX-W 4.0(5L). Lactose in the whey powders generated at the various θ_{PGX} conditions were all characterized as amorphous lactose (Fig. 3.6, represented by PGX-W 4.0(5L) spectra) primarily due to the rapid micronization and drying achieved during PGX processing.

3.3.2.3. Protein profile and structure

PGX-W evaluated at all θ_{PGX} ratios (2.5, 3.5, 4.0, and 5.3) had similar protein profiles (Figs. 3.7 and 3.8), indicating that the recovery of all whey proteins on the bench system was very efficient. PGX-W powders had more high molecular weight molecules, > 250 kDa (Fig. 3.7, peak 1), compared to FD-W, possibly due to the formation of protein aggregates. Moreover, 20% of the $\theta_{2.5}$ proteins eluted were > 250 kDa, which supported the formation of larger whey particles due to favoured biopolymer interactions at lower θ_{PGX}. At intermediate θ_{PGX} ratios, proteins in PGX-W 3.5(5L) and PGX-W 4.0(5L) had similar secondary structures as indicated by the FTIR bands (Figs. 3.9(B1) and (B2)). Greater differences in band intensities and broadness were observed at larger θ_{PGX} ratios, specifically in the PGX-W 5.3(5L) sample. At the lowest θ_{PGX} evaluated, PGX-W 2.5(5L), there was the occurrence of an additional peak (1636 cm^{-1}) in the region representing β-sheet structures. While the intensified peaks represented protein aggregation due to increased hydrogen bonding, the resolution of two peaks at 1622 cm^{-1} and 1636 cm^{-1} observed in PGX-W 2.5(5L) proteins (Figs. 3.9(B1) and (B2)) indicated that the reduced solvent interactions at lower θ_{PGX} caused fewer disruptions to the protein secondary structure. Furthermore, in regions representing α-helix and loops and turns, peaks identified at 1647 cm^{-1} and 1654 cm^{-1} were observed with a 5-6 cm^{-1} red shift. Previously, water was reported to strongly absorb in the same region (Byler and Susi, 1986). Therefore, the shift in the peaks representing the α-helix and loops and turns of PGX-W 2.5(5L) proteins were due to residual water. While the CO_2:EtOH ratio was kept constant at 1:3 across all θ_{PGX} ratios and, consequently, no effect can be derived from this parameter, the θ_{PGX} ratio affected the initial precipitation of the biopolymers. At lower θ_{PGX}, precipitation and water removal from the aqueous stream is less efficient due to reduced jet breakup and mixing at the nozzle. Hence, the increased interactions of whey components with

water and the retention of water by the precipitated fractions were apparent at lower θ_{PGX} and, therefore, corroborating the overall hydrophilic environment surrounding the hydrophobic amino acid residues relative to the proteins generated at higher θ_{PGX}.

3.3.2.4. Soluble protein and aggregation

Generally, whey proteins dried at different θ_{PGX} ratios had high soluble protein content ≥ 80% wt. (Table 3.3) and were not significantly affected by the dissolution medium except for PGX-W 2.5(5L), which had a solubility of < 70% wt. in water at pH 7. The reduced soluble protein content of PGX-W 2.5(5L) may be corroborated by the presence of large protein aggregates, > 250 kDa (Fig. 3.7, peak 1). While PGX-W 4.0(5L) had a soluble protein content of 62.8 ± 5.9% wt. in pH 3 water, this was not significantly different from the other PGX-W generated at different θ_{PGX} ratios. The soluble protein content of PGX-W 5.3(5L) was significantly higher (95.4 ± 3.7%) in a neutral dissolution medium, water at pH 7, which was affected by the larger quantity of lactose in the whey powder matrix (Fig. 3.5). This ultimately altered the hydration shell surrounding the proteins in the PGX-W 5.3(5L) matrix, which improved the solubility of water-soluble proteins such as α-LA. Processing at different θ_{PGX} ratios did not significantly affect the solubility of salt-soluble proteins, such as β-LG, as indicated by the high proportion of soluble protein content detected in saline solutions (Table 3.3). Overall, PGX processing did not adversely affect the soluble protein content of the whey powders.

PGX-W 3.5(5L) and PGX-W 4.0(5L) had similar intrinsic fluorescence spectra with a maximum emission at 330 nm (Fig. 3.10). Proteins adsorbed to the surface of the cream layer of an oil-in-water emulsion had similar emission maxima due to increased hydrophobicity experienced by Trp-19 in the hydrophobic core or calyx of β-LG (Hinderink et al., 2021). PGX-

W 2.5(5L) and PGX-W 5.3(5L) were observed to emit most intensely at 320 nm. A 10 nm blue shift indicated that the Trp residues were surrounded by a hydrophobic environment (Jackman & Yada, 1989). Blue shifts and reduced fluorescence intensities can be triggered by globular protein conformational changes and folding, affecting the overall exposure of the non-polar regions to aqueous media. Therefore, the selective binding of the fluorescent probe, ANS was useful in further evaluating changes in the hydrophobicity of PGX-processed whey powders. Moro et al. (2021) evaluated the binding behaviour of aliphatic and aromatic fluorescent probes, *cis*-parinaric acid (CPA), and ANS on heat-treated whey proteins. Heat-treated proteins were reported to have larger surface hydrophobicity with increased binding to ANS due to flexible protein structure and increased access to the β-LG calyx core. Proteins precipitated at the θ_{PGX} conditions of PGX-W 2.5(5L) and PGX-W 5.3(5L) were surrounded by more hydrophilic environments with intermediate surface hydrophobicity values of 836 ± 72 and 712 ± 23 (Table 3.1 and Fig. 3.10). As mentioned above, the reduced breakup of the aqueous solution favoured the association of whey components with water, which increased the hydrophilicity of the protein environment. At PGX-W 5.3(5L), the rapid breakup of the aqueous feedstock, increased exposure to PGX fluid, rapid precipitation of proteins, and exposure of hydrophobic residues all contributed to the rearrangement of non-polar regions and, therefore, affected the increased ANS binding and reduced fluorescence emission.

Nikolaidis and Moschakis (2018) studied the effects of EtOH exposure on WPI denaturation. While WPIs dissolved in 5% EtOH had similar UV-Vis absorbance profiles (and therefore similar denaturation degrees) to that of freeze-dried WPI, WPIs exposed to 50% EtOH resembled guanidine hydrochloride denatured whey proteins with increased exposure of tyrosine and tryptophan to aqueous environments (Nikolaidis & Moschakis, 2018). The denaturation of

whey proteins is well reported in the literature (De La Fuente et al., 2022), such that the partial unfolding or denaturation of proteins is desirable concerning their surface activity and applications as emulsifiers and foaming agents. Recent studies by Feng et al. (2021) demonstrated that WPI treated with different concentration levels of ethanol promoted protein unfolding and subsequent aggregation. By utilizing 40% v/v ethanol to treat WPI, a significant increase in antioxidant activity, the highest emulsifying activity, emulsifying stability, foaming capacity, and surface hydrophobicity compared to native WPI was obtained. This leads to the conclusion that exposure of whey proteins to ethanol during PGX processing partially denatured the proteins, which affected the locations of hydrophobic groups on the protein surface. The high soluble protein content of PGX-processed proteins suggested that the functional properties of whey proteins were not adversely affected; however, further testing of functional properties is needed.

3.4. Conclusions

Pressurized Gas eXpanded (PGX) liquid technology utilizing CO_2-expanded ethanol was employed to dry sweet cheese whey, forming unique morphologies with low bulk density of 35-74 g/L and large surface areas of up to 30 m^2/g. Free-flowing, protein-rich (45-55%) powders with exfoliated surfaces distinguished by interconnected tens of nm particles and porous networks were precipitated and dried in a single processing step. Two different processing scales, a 1 L laboratory system and a 5 L bench-scale system, were evaluated to determine the scalability of this precipitation and drying process. PGX-W had three to six times (3-6x) larger surface areas compared to freeze-dried whey powder. Similar proximate compositions of whey powders with high concentrations of proteins and reduced lactose and fat were reproducible on the 5 L system. Of the whey proteins recovered, β-LG, α-LA, and BSA constituted 35%, 27%, and 5% of the powders, respectively. Amorphous lactose was precipitated in concentrations of 4-14% and

believed to contribute to the high solubility (≥ 80%) of the concentrated proteins in aqueous media. FTIR and fluorescence results indicated that PGX-processed whey proteins at moderate conditions of $\theta_{PGX} = 3.5$ had similar hydrophobicity values to freeze-dried whey proteins which indicated that the PGX technology is a mild process that did not appreciably affect the secondary structure of proteins more so than the initial heat treatment of milk during cheese production. At low θ_{PGX}, the antisolvent breakup of the aqueous solution is low, which favoured the formation of larger particles, limited the exposure of whey proteins to solvent, and lessened the effects on protein secondary structure. At higher θ_{PGX}, smaller particle sizes were obtained due to improved mixing and rapid precipitation, but increased exposure to solvent resulted in compact conformations. Such PGX whey powders are characterized by unique surface functionalities and high solubility and therefore would be suitable for bioactive loading and the development of novel delivery systems.

Chapter 4. The Pressurized Gas eXpanded (PGX) liquid technology as a separation and drying technique for acid and sweet whey streams

4.1. Introduction

Membrane separation technologies have been widely used in the recovery of principal components such as proteins, lactose and minerals of whey, the abundant byproduct of dairy product manufacturing (Ganju & Gogate, 2017; Wen-qiong et al., 2019). The separation of these biomolecules is driven by efforts to reduce the biological and chemical load of the direct disposal of large quantities of whey into the waterways (Smithers, 2008) as well as to recover high-value components and minimize waste. Whey composition varies depending on the dairy product where the effluent is generated as a byproduct. Sweet whey is generated in the production of rennet-coagulated cheeses such as cheddar cheese, while acid whey is produced during the direct acidification of milk in the preparation of mozzarella cheese, or acidification by lactic acid bacteria in yogurt manufacture. A semi-permeable membrane fractionates the whey feed, concentrating large molecules above the molecular weight cutoff (MWCO) in the retentate fraction, while allowing small molecules to move through into the permeate fraction. Supplying all the essential amino acids and offering excellent functional properties, the recovery of whey proteins from the dairy effluent stream is favourable due to their potential use in various product formulations.

Pretreatment of sweet whey using centrifugation and microfiltration (MF) is required to remove suspended particles, followed by ultrafiltration (UF), most commonly with a MWCO of 10 kDa, to concentrate whey proteins. A series of diafiltration steps in tandem with UF effectively improved the separation of other principal whey components during the concentration of whey proteins, by diluting the retentate fraction with fresh water, washing out the lactose and minerals

in addition to limiting membrane fouling (Baldasso et al., 2011). The selectivity of the semi-permeable membranes can be adapted for protein fractionation, as well as increasing the filtration capacity by assembling additional membrane modules in parallel. In contrast, the high mineral content of acid whey poses challenges in the recovery of the whey proteins, requiring additional pretreatments (Heng & Glatz, 1991). Pretreatments typically involve the chelation of calcium, which would otherwise precipitate in the pores of the membrane, reducing the flux and ultimately resulting in the concentration of calcium and other minerals together with the whey proteins, affecting the solubility of the proteins upon reconstitution. While additional treatment of the retentate with diafiltration may be effective in ash removal, the large volumes of water required make the recovery of proteins from acid whey less acceptable. Following concentration by membrane filtration technologies, water is removed, and proteins are dried using spray drying for ease of storage and transport. The cumulative effect of processing and storage on the physicochemical properties of the whey proteins has been well reported (Nishanthi et al., 2017b, 2017a).

Pressurized Gas eXpanded (PGX) liquid technology has the potential as a single step alternative to conventional membrane processing, followed by spray drying; however, such a comparison has not been evaluated previously. PGX technology (Temelli & Seifried, 2016) utilizes a CO_2-expanded organic solvent (typically ethanol, EtOH) as the PGX processing fluid to precipitate and dry high molecular weight biopolymers from aqueous solutions, generating open-porous micro- and nano-structured fibres and/or powders at mild operating pressure and temperature, 100 bar and 40 °C, respectively. In the previous study (Chapter 3), various mass flow rate ratios of the PGX fluid (CO_2 + EtOH) to the aqueous solution were evaluated to achieve the highest protein content of ≥45% from sweet whey to produce free-flowing, high surface area,

protein powders using the PGX technology. In this study, a second variety of whey, acid whey was introduced to better understand the applicability of the PGX process as a single-step process in whey utilization. The specific objectives of this study were to (a) process two different types of whey feedstock, acid and sweet whey using the PGX technology in comparison to conventional techniques, (b) evaluate the PGX technology as a separation technique relative to ultrafiltration with a 10 kDa MWCO, and (c) evaluate the effects of the two different processing techniques on the physicochemical properties of the dried whey powders collected.

4.2. Materials and Methods

4.2.1. Materials

Sweet whey (SW) was purchased from a local cheddar cheese producer (The Cheese Factory, Edmonton, AB, Canada). This sweet whey was the same variety used in the first study (Chapter 3) but from a different batch. The yellow-green milky whey liquid (pH 5.6) had an average of 7% total solids, composed of 8% ash, 9% fat, 11% protein, and 72% lactose. Acid whey (AW) was provided by a Mediterranean cheese and yogurt producer (Chinook Cheese, Calgary, AB, Canada). The yellow-coloured whey (pH 4.1) separated during the production of labneh had an average of 11% total solids, composed of 18% ash, 5% fat, 6% protein and 71% lactose. Feedstock compositions were determined by an ISO/IEC 17025:2017 accredited milk testing lab following the standard Methods for the Examination of Dairy Products, 15.086, 15.114, 15.040, 15.132 for fat, total solids, ash, and protein content determination, respectively (Wehr & Frank, 2004). Total carbohydrates were determined by calculation after subtracting ash, protein, and fat from the total dissolved solids. Whey streams (SW and AW) were utilized 'as is' as the feedstock for ultrafiltration followed by spray drying and PGX processing of their respective fractions.

Spray-dried and PGX-processed fractions are referred to with SD- and PGX- abbreviations, respectively. CO_2 (≥ 99% purity) was purchased from Messer Canada Inc. (Mississauga, ON, Canada) and anhydrous ethanol (EtOH) (> 99.5%) was purchased from Permolex Ltd. (Red Deer, AB, Canada).

4.2.2. Experimental design

Spray drying (SD) and PGX processing were utilized as the drying techniques. In addition to processing SW and AW directly, both feedstocks were pretreated by ultrafiltration (UF) as described in section 4.2.2.1 producing retentate (R) and permeate (P) fractions, then further dried by SD and PGX processing. Dried AW and SW powders, together with their respective UF fractions (R and P) were all characterized according to section 4.2.3 to evaluate the PGX process as a fractionation technique compared to a conventional separation technique, such as UF. PGX processing experiments were performed at a fixed mass flow rate ratio, θ_{PGX}, of 4.0 as defined in Eq. (4.1). All experiments were performed in duplicate at 40 °C and 100 bar. The mass flow rate ratio $\theta_{PGX} = 4.0$ based on the amount of water in the polymer solution was selected as the processing condition that resulted in the highest crude protein content as reported in Chapter 3.

$$\theta_{PGX} = \frac{Flow\ rate\ of\ PGX\ fluid\ (CO_2+EtOH)}{Flow\ rate\ of\ water\ in\ polymer\ solution} \quad (4.1)$$

4.2.2.1. Ultrafiltration protocol

Feedstock, AW and SW were processed by ultrafiltration (UF) through a Pellicon® XL50 Biomax® 10 kDa membrane (50 cm^2 filter area) with a transmembrane pressure of 1 bar. Whey liquid was heated to 50 °C before filtration to ensure a homogeneous solution, minimizing the separation of residual globules. Rathour et al. (2017) reported that pH 5.2 and 50 °C were optimal

feed pH and temperature for higher filtration flux. Acid whey retentate (AR) and permeate (AP) had a solids content of 12.0% and 11.5%; whereas that for sweet whey retentate (SR) and permeate (SP) was 7.5% and 5.3%, respectively. The appearance of both AR and AP fractions was non-turbid and yellow. Alternatively, SR fractions had a milky white appearance while the SP fraction had a yellow, non-turbid appearance attributed to the presence of riboflavin (Durham, 2009). Ultrafiltration fractions (AR, AP, SR, SP) together with their feedstocks (AW and SW) were subsequently processed by spray drying and PGX.

4.2.2.2. PGX drying protocol

The bench-scale PGX unit described Chapter 3 (Fig. 3.1) was used to conduct all the PGX experiments in this study. While the PGX system was heated and allowed to stabilize at 40 °C, the aqueous solution was also heated to 40 °C on a stirring hot plate before injection. The PGX system was pressurized to the target pressure by pumping the PGX fluid at the experimental conditions (CO_2 at 50 g/min + EtOH at 150 g/min). Once the system was stabilized, the aqueous solution (0.5 L) was injected through the inner tube of the coaxial nozzle at a rate of 52.8-56.8 g/min, adjusted to achieve θ_{PGX} of 4.0 based on the water content of the feed solution. The polymer was precipitated upon contact with the PGX fluid, which acts as an anti-solvent. The PGX effluent was collected at the separator outlet every 3-4 min. Upon completing the injection of the aqueous solution, the aqueous solution pump was stopped and the PGX fluid continued to flow through the collection vessel to remove residual water from the collection vessel. The water mass fraction of the PGX effluent was calculated from the density and temperature of the liquid measured by the mass flow meter using the model proposed by Danahy et al. (2018). Once the effluent was confirmed to consist of only pure EtOH, EtOH removal by pumping pure CO_2 proceeded. CO_2 injection was

continued until the EtOH flow rate at the outlet separator reached ≤0.1 g/min. The system was depressurized to ambient pressure to recover the PGX-dried biopolymers on the felt filters.

4.2.2.3. Spray drying protocol

Spray drying is considered to be the standard particle formation technique (Schuck, 2014) to obtain powdered whey product and therefore, was used as a reference technique to which PGX processing was compared to. AW, AR, AP, SW, SR and SP (0.5 L each) were spray dried (LabPlant SD-06A, LABPLANT UK, North Yorkshire, UK) at a rate of 485 mL/h as is without further concentration, at an inlet and outlet temperature of 175 °C and 85 °C, respectively. Dried powders were stored in airtight glass containers at room temperature (22-23 °C) until analysis.

4.2.3. Particle characterization

4.2.3.1. Physicochemical attributes

Bulk density, particle size distribution and specific surface area of the whey powders were determined according to the physicochemical characterization methods outlined in Chapter 3 (section 3.2.4.1).

Particle morphology and surface features of SD- and PGX- whey powders were examined using a scanning electron microscope (SEM) (Zeiss EVO 10, Carl Zeiss Microscopy GmbH, Oberkochen, Germany) operating at 20 kV. Powdered samples were sputter-coated with gold, observed and photographed.

4.2.3.2. Compositional analysis and protein characterization

The proximate composition, elemental analysis, lactose content determination and X-ray diffraction of whey powders were determined according to the methods described for

compositional analysis in Chapter 3 (section 3.2.4.2.). Sodium dodecyl sulphate polyacrylamide gel electrophoresis (SDS-PAGE), soluble protein content, size exclusion high performance liquid chromatography (SEC-HPLC), infrared spectroscopy, protein intrinsic fluorescence and protein hydrophobicity have been analyzed according to the methods outlined in Chapter 3 (section 3.2.4.3.) to characterize the protein profile and structure of the whey powders.

4.2.4. Statistical analysis

All experiments were completed in duplicate and one-way analysis of variance (ANOVA) and Tukey's test with a 95% confidence interval ($p < 0.05$) were used to determine the statistical differences between the characteristics of acid and sweet whey samples obtained by spray drying and PGX processing. Statistical analysis was performed using Minitab® Statistical Software (version 21.3.1.0, Minitab, Inc., State College, PA, USA).

4.3. Results and discussion

4.3.1. Physicochemical attributes

All SD-powders were pale yellow, had a faint milk scent, and settled into the storage jars as clumps within 3 days from the initial drying. Although SD- and PGX- whey powders had similar moisture contents (Table 4.1), PGX-processed whey powders were fluffy, odourless and had a fluid-like flow behaviour when agitated in the storage jars. Compared to the SD-AW and SD-SW samples, all PGX- powders had significantly lower bulk densities, with up to 10x reduction (Table 4.1). While PGX-AP had a reduced bulk density compared to its SD- counterpart, it was significantly higher than those of PGX-AW and -AR, which may be attributed to its lower protein content and higher lactose content as will be discussed later.

Table 4.1. Physicochemical characteristics of dried whey powders.

	Moisture (%)	Bulk density (g/L)	SSA* (m^2/g)	Pore size (Å)	Hydrophobicity (a.u)
Acid whey					
SD-AW	$10.3 \pm 1.8^{b,c}$	237.8 ± 2.7^{b}	$< 5.0^{c}$	20.3 ± 4.1^{a}	2694.4 ± 14.3^{a}
SD-AR	$13.5 \pm 0.7^{a,b}$	260.3 ± 7.8^{a}	$< 5.0^{c}$	32.6 ± 16.5^{a}	2396.9 ± 8.8^{b}
SD-AP	17.6 ± 0.5^{a}	195.6 ± 1.7^{c}	$< 5.0^{c}$	18.8 ± 0.1^{a}	545.4 ± 4.7^{f}
PGX-AW	$13.6 \pm 0.5^{a,b}$	21.2 ± 1.6^{e}	65.8 ± 10.0^{a}	18.8 ± 0.1^{a}	1425.2 ± 30.9^{d}
PGX-AR	$9.6 \pm 0.3^{b,c}$	17.6 ± 0.2^{e}	$22.0 \pm 9.0^{b,c}$	18.8 ± 0.1^{a}	1830.2 ± 50.9^{c}
PGX-AP	8.4 ± 0.3^{c}	142.2 ± 2.5^{d}	$44.6 \pm 2.9^{a,b}$	16.0 ± 0.1^{a}	1016.9 ± 5.8^{e}
Sweet whey					
SD-SW	11.5 ± 1.0^{a}	$230.6 \pm 7.7^{a,b}$	$< 5.0^{c}$	16.1 ± 0.1^{a}	3239.9 ± 5.2^{c}
SD-SR	12.7 ± 0.9^{a}	216.2 ± 4.4^{b}	$< 5.0^{c}$	17.5 ± 1.3^{a}	2068.1 ± 3.0^{d}
SD-SP	6.0 ± 0.1^{b}	241.8 ± 14.8^{a}	$< 5.0^{c}$	17.4 ± 1.4^{a}	331.6 ± 60.5^{e}
PGX-SW	13.6 ± 0.1^{a}	33.8 ± 3.3^{c}	17.7 ± 0.1^{b}	18.9 ± 3.0^{a}	4674.9 ± 25.2^{b}
PGX-SR	12.7 ± 0.9^{a}	25.9 ± 0.8^{c}	$11.0 \pm 0.1^{b,c}$	16.2 ± 0.1^{a}	14671.5 ± 165.4^{a}
PGX-SP	$10.1 \pm 0.9^{a,b}$	23.9 ± 1.2^{c}	36.1 ± 0.5^{a}	16.0 ± 0.1^{a}	2403.0 ± 4.9^{d}

*SSA -specific surface area

Data presented as mean ± SD (n=2).

[a-d] Different letters within each column indicate significant differences ($p < 0.05$).

SEM images of acid and sweet whey powders are presented in Figs. 4.1 and 4.2, respectively. SD-AW and -SW powders were primarily identified by clusters of 1-10 µm smooth spherical particles, some with notable surface depressions or dents. The ability of the PGX process to precipitate and micronize whey solids from their respective feedstocks is exhibited in the SEM images. The fluffy macroscopic appearance of the PGX-processed powders is reflected as 100 nm – 2 µm globular morphologies forming highly exfoliated surfaces. Corresponding to the low bulk densities and nano-sized surface features, PGX- powders had significantly higher specific surface areas, ~13× for acid whey and ~7× for sweet whey permeate, compared to their SD counterparts (Table 4.1). All whey powders were characterized by super-nanopores, typically ranging from 10-100 nm (Mays, 2005), which remained unaffected by the drying technique.

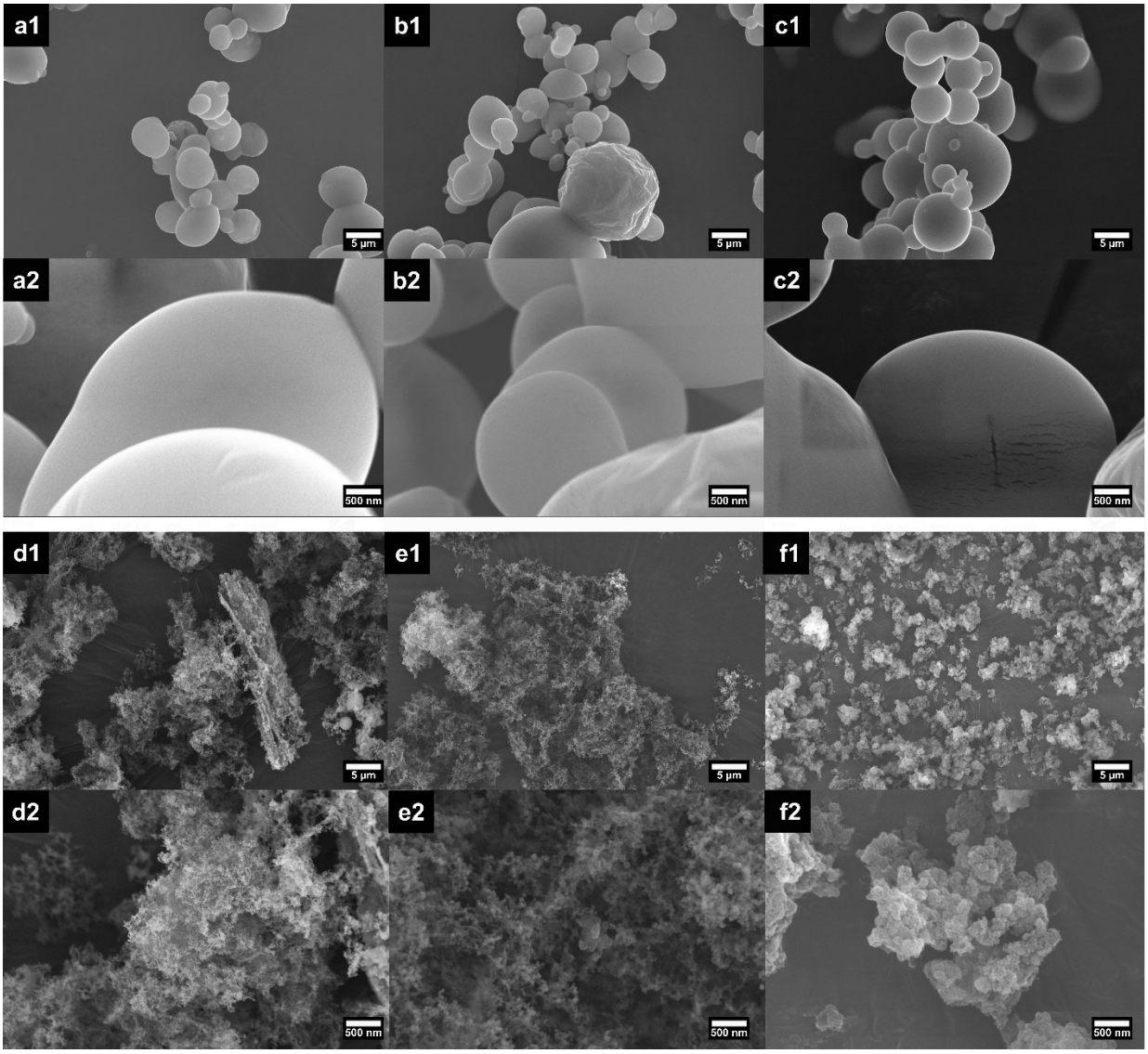

Figure 4.1. Scanning electron microscopy images: a) SD-AW; b) SD-AR; c) SD-AP); d) PGX-AW; e) PGX-AR; f) PGX-AP. (1) 5x magnification, scale bar 5 µm and (2) 50x magnification, scale bar 500 nm.

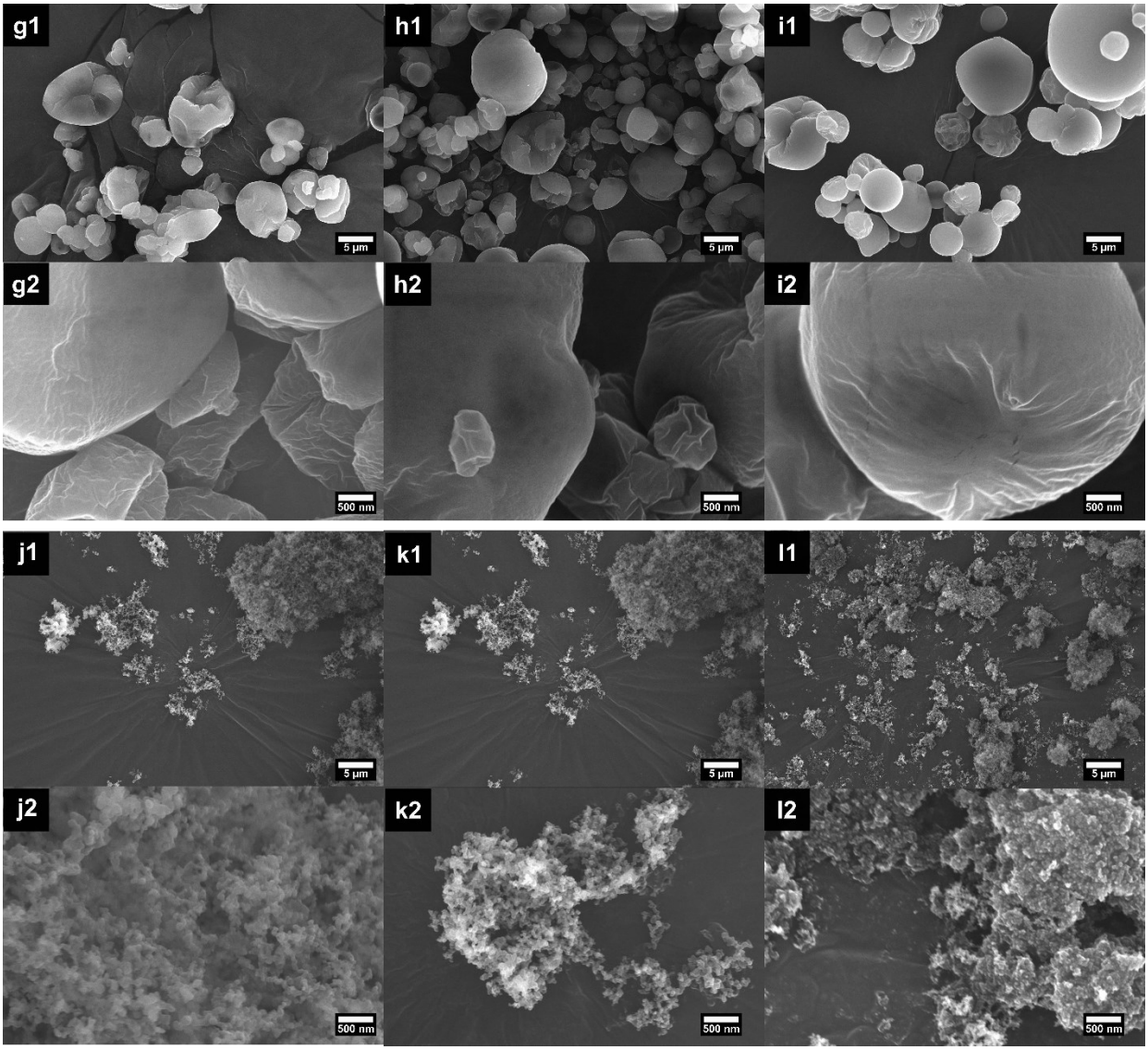

Figure 4.2. Scanning electron microscopy images: g) SD-SW; h) SD-SR; i) SD-SP; j) PGX-SW; k) PGX-SR; l) PGX-SP. (1) 5x magnification, scale bar 5µm and (2) 50x magnification, scale bar 500 nm.

The particle size distributions (PSD) of whey powders are reported in Fig. 4.3, depicting SD- and PGX- whey powders with mean particle sizes (P_d) ranging from 4-18 µm. SD-powders of acid and sweet whey powders (Fig. 4.3A1 and B1, respectively) were characterized by broad distributions, with shoulders resulting in overall non-uniform PSDs. While SD-SP had a larger proportion of small particles (< 5 µm), PGX-SW and -SR had more large particles (20-50 µm).

PGX- whey powders (Fig. 4.3A2 and 4.3B2) had a narrow particle size distribution with a mean P_d of 11-17 µm. While only particles above the filter cutoff (1 µm) were initially collected, smaller particles were collected later by the polymer bed throughout the injection and drying process, which effectively retained particles that would otherwise be washed out.

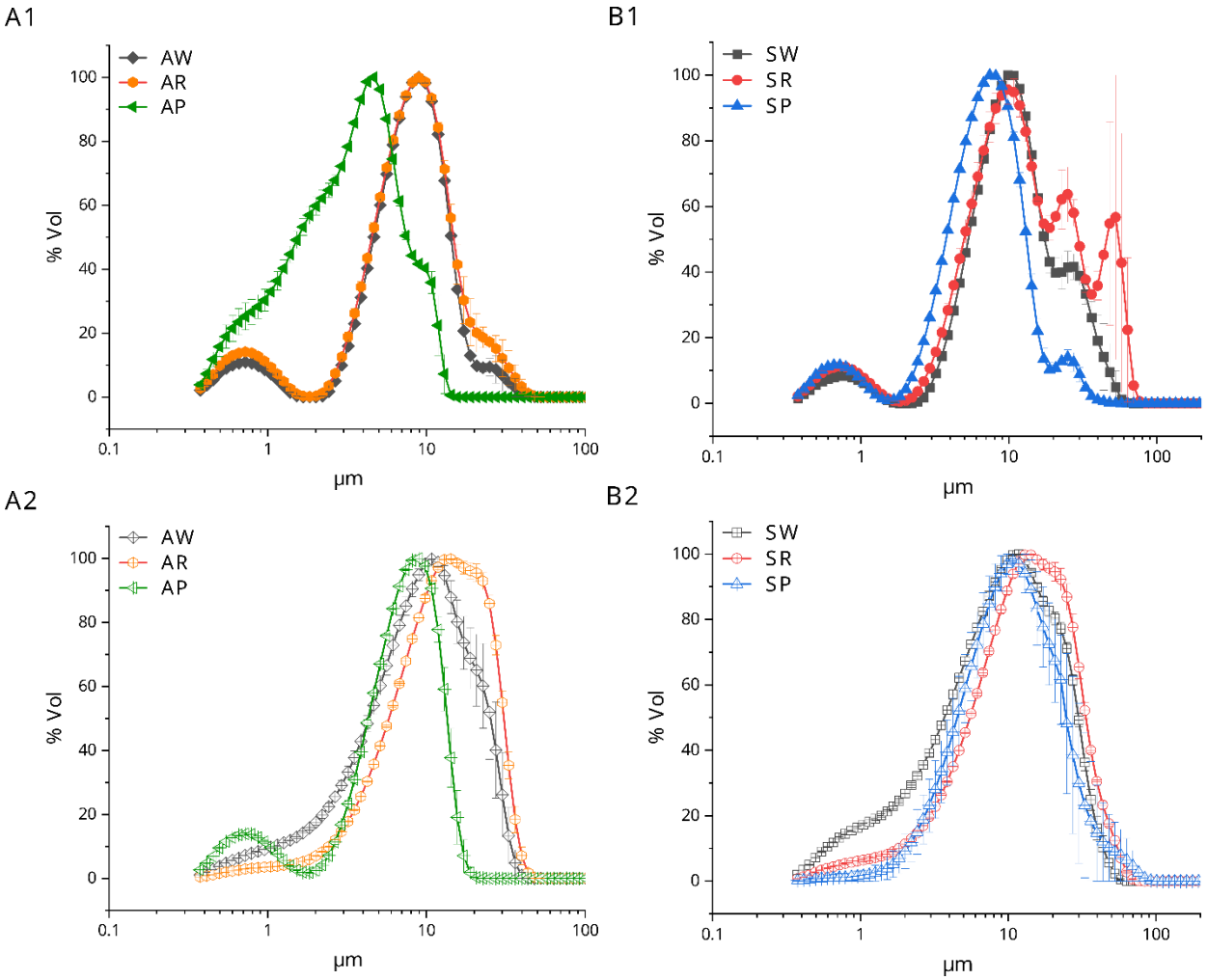

Figure 4.3. Particle size distribution (PSD) of (A) acid whey and (B) sweet whey powders for (1) spray-dried (SD) and (2) PGX-processed powders.

4.3.2. Compositional characteristics

The composition of the spray dried acid (SD-AW) and sweet (SD-SW) whey powders, together with their respective ultrafiltration fractions (SD-AR, -AP, -SR, and -SP) are reported in Figs. 4.4A and B, respectively. Lactose is the primary component of both AW and SW at 68 and 76%, respectively. XRD spectra of SD- powders (Fig. 4.5, solid lines) were characterized with a broad peak around 20°, typical of anhydrous β-lactose with peaks at diffraction angles (2θ) of 20.8° and 21.2°. While β-lactose crystals have sharp peaks, the observation of broad peaks captured the crystallization of amorphous lactose formed during spray drying. Due to the hygroscopicity and instability of amorphous lactose produced during spray drying, it crystallizes into the stable forms of α- and β-lactose during storage (Haque & Roos, 2005; Saito, 1988). The crystallization rate from anhydrous β-lactose to the more stable form, α-lactose is influenced by increasing relative humidity (54.5% > 65.6% > 76.1%) (Haque & Roos, 2005). PGX-processed powders consisted of amorphous lactose, represented by a flat XRD spectrum. The protein and ash contents of the feedstocks had inverse relationships, such that ash content was dominant in acid whey, whereas protein content was dominant in SW at a level of 15%. The remaining proportion, protein in SD-AW and ash in SD-SW comprised ~6% of the dissolved solids. Fat contents of AW and SW were < 2% and < 4%, respectively.

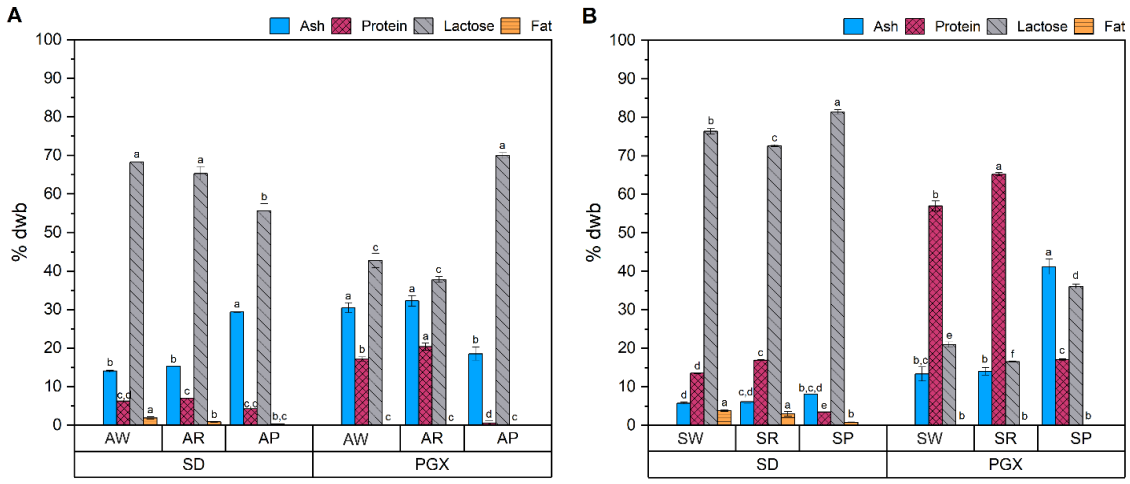

Figure 4.4. Compositional characteristics of whey powders on a dry weight basis (%dwb), (A) acid whey and (B) sweet whey, presented as mean ± SD (n=2).

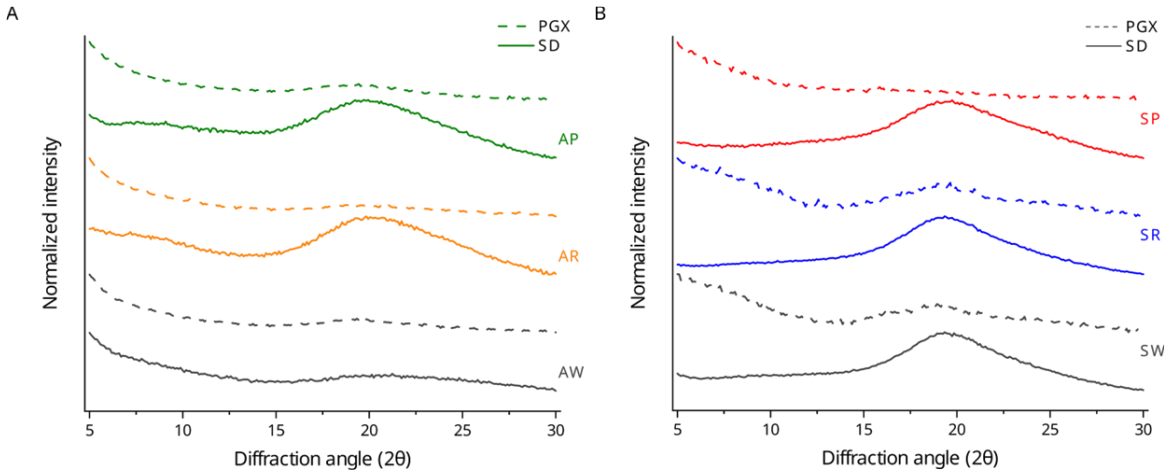

Figure 4.5. Normalized X-ray diffraction patterns of SD- and PGX- whey powders, represented as an average of duplicate scans.

Industrially, whey ultrafiltration is a well-established process for concentrating whey proteins, consisting of multiple filters with successive molecular weight (M.W) cutoffs, as well as integrated diafiltration steps to further concentrate the retentate. However, for the purpose of this study, a simplified UF process consisting of a MW cutoff that would be suitable for retaining the

major whey proteins was selected to compare to the single unit operation of PGX. In this study, following UF, the composition of the retentate fractions shifted to retain the larger MW biomolecules such as proteins and lipids while reducing smaller components such as sugars and minerals. For acid whey matrices (Fig. 4.4A), the composition remained similar between AW and AR, except for the reduced fat content in AR ($p < 0.05$). The AP fraction contained lower amounts of fat and higher amounts of ash compared to SD-AW. Lactose content in AP was lower than that of AW and AR, which may be attributed to the blockage of membrane pores by minerals such as calcium and phosphorus (Heng & Glatz, 1991), reducing the flux of lactose across the membrane. Differing from acid whey, protein levels in sweet whey were concentrated from 14% in SW to 17% in SR (Fig. 4.4B). Small amounts of protein were also recovered in the permeate fraction, SP (3%), which may be due to the presence of low molecular weight glycomacropeptide (GMP) cleaved from the C-terminus of κ-casein during protein coagulation in the cheese-making process. Ash levels remained similar amongst the feedstock and UF fractions of sweet whey. Lactose concentrations were highest in SP > SW > SR and the majority of the lipids in SW were retained in SR.

Following PGX processing, AW and AR had similar proximate compositions, characterized by significant reductions ($p < 0.05$) in lactose levels by 25% and concentrated ash and protein levels compared to spray dried feedstocks (SD-AW) (Fig. 4.4A). PGX-AP contained similar lactose and ash levels to the acid whey feedstock. Ash contents in PGX-AW and PGX-AR were similar to levels of SD-AP. PGX processing of the acid whey feedstock resulted in a powder sample with 17% protein, and further processing of the preprocessed UF retentate fraction (AR) concentrated protein levels to 20%. During PGX processing, protein, lactose and mineral

components were precipitated while the residual milk fat was solubilized and washed out by the PGX fluid.

The proximate composition of PGX-SW, -SR and -SP powders shifted to consist of substantially reduced levels of lactose (45-55% reduction) while retaining more protein and ash (Fig. 4.4B). Protein in PGX-SW and -SR was concentrated ~4×, to impressive levels of 57% and 65%, respectively. PGX processing of SP also resulted in the concentration (2x) of minerals. The large quantities of EtOH used in PGX processing were effective in the lactose content reduction while precipitating the high-value whey proteins. More evident in sweet whey matrices than in acid whey was that minerals were concentrated together with proteins during PGX processing.

Major milk minerals, Ca, K, Mg, Na and P are reported in Table 4.2. Mineral concentrations vary depending on the dairy product from which the whey is separated. The differences in the ash composition of acid and sweet whey (SD-AW and -SW) are attributed to the method of protein coagulation, acid production by lactic acid bacteria (LAB) in yogurt and rennet for sweet whey. LAB produces lactic acid, dissolving casein micelles in milk; therefore, displacing the liberated calcium phosphate into the acid whey phase. Salt added in the production and seasoning of labneh is also reflected in the serum phase. Curtis et al. (2002) discussed the electrostatic interactions between dissolved ions and the peptide groups on proteins, consequently observing a salting-in or salting-out effect in solution. In the present study, salts may negatively impact protein solubility, due to the high ash contents of the whey matrices, specifically, the large proportion of Ca and P may lead to the formation of insoluble calcium phosphate. Chelation of Ca or dialysis was reported to be effective in improving the concentration of whey proteins by limiting membrane fouling during UF (Heng & Glatz, 1991; Morr & Lin, 1970).

Table 4.2. Mineral composition (% dwb) of dried whey powders.

	Ca (%)	K (%)	Mg (%)	Na (%)	P (%)
Acid whey					
SD-AW	2.18 ± 0.07^{d}	2.51 ± 0.04^{b}	0.18 ± 0.02^{e}	3.09 ± 0.02^{b}	1.13 ± 0.02^{e}
SD-AR	2.11 ± 0.02^{d}	2.51 ± 0.02^{b}	0.18 ± 0.02^{e}	3.06 ± 0.02^{b}	1.13 ± 0.02^{e}
SD-AP	3.25 ± 0.04^{c}	3.21 ± 0.02^{a}	0.55 ± 0.02^{c}	3.79 ± 0.02^{a}	1.79 ± 0.02^{d}
PGX-AW	9.62 ± 0.02^{a}	2.06 ± 0.05^{c}	0.62 ± 0.02^{c}	1.73 ± 0.02^{c}	4.68 ± 0.02^{b}
PGX-AR	6.82 ± 0.02^{b}	1.39 ± 0.02^{d}	0.51 ± 0.02^{d}	0.91 ± 0.02^{e}	4.42 ± 0.02^{c}
PGX-AP	6.89 ± 0.02^{b}	1.44 ± 0.01^{d}	1.51 ± 0.02^{a}	1.14 ± 0.02^{d}	6.98 ± 0.02^{a}
Sweet whey					
SD-SW	0.56 ± 0.02^{e}	2.31 ± 0.02^{c}	0.11 ± 0.02^{d}	0.54 ± 0.02^{c}	0.63 ± 0.02^{e}
SD-SR	0.56 ± 0.02^{e}	2.17 ± 0.02^{d}	0.11 ± 0.02^{d}	0.51 ± 0.02^{d}	0.60 ± 0.01^{e}
SD-SP	0.63 ± 0.02^{d}	2.80 ± 0.02^{b}	0.13 ± 0.02^{d}	0.67 ± 0.02^{b}	0.71 ± 0.02^{d}
PGX-SW	3.65 ± 0.02^{b}	2.79 ± 0.02^{b}	0.64 ± 0.02^{b}	0.49 ± 0.01^{d}	2.49 ± 0.03^{b}
PGX-SR	3.13 ± 0.02^{c}	2.04 ± 0.04^{e}	0.58 ± 0.02^{c}	0.38 ± 0.02^{e}	2.35 ± 0.02^{c}
PGX-SP	7.33 ± 0.02^{a}	6.31 ± 0.02^{a}	1.50 ± 0.04^{a}	1.03 ± 0.02^{a}	5.67 ± 0.01^{a}

Data represented as mean ± SD (n=2).
$^{a-d}$ Different letters within each column indicate significant differences ($p < 0.05$).

4.3.3. Protein profile and structure

Proteins from the feedstocks (AW and SW) are concentrated following PGX processing; therefore, the following section focuses on the effects of SD and PGX processing on the profile and structure of proteins in the whey powders. Using SEC-HPLC, the hydrodynamic volumes of the reconstituted macromolecules were correlated to their respective molecular weights using the calibration curve (R^2=0.918) developed using whey protein standards, bovine serum albumin (BSA), β-lactoglobulin (β-LG) and α-lactalbumin (α-LA). BSA, β-LG, and α-LA eluted as peaks 1, 2 and 3, respectively, in Figs. 4.6A and B. While β-LG and α-LA in the standard protein mixture eluted as well resolved peaks, SD-AW chromatograms had only two characteristic peaks, one broad, overlapping peak of β-LG and α-LA, and the other peak representative of small molecules < 10 kDa. Reducing SDS-PAGE results (Fig. 4.7 lane A) corroborated the presence of β-LG and

α-LA monomers, yet these monomers behaved as SD-AW protein aggregates in solution (Fig. 4.6A). Similar observations were made for SD-AR (Fig. 4.7 lane B), suggesting that the components retained during UF had similar behaviour to the proteins present in the starting acid whey feedstock. The UF permeate fraction (SD-AP) had protein levels similar to those of SD-AW and -AR (Fig. 4.4A), and the profile characterization (Fig. 4.6A and 4.7 lane C) results suggested that the nitrogen sources may be attributed to proteose and peptones, a mixture of low molecular weight proteins and peptides as well as non-protein nitrogen (NPN). PGX processing of all acid whey streams (PGX-AW, -AR and -AP) did not affect the protein profile (Fig. 4.6A and 4.7 lanes D-F).

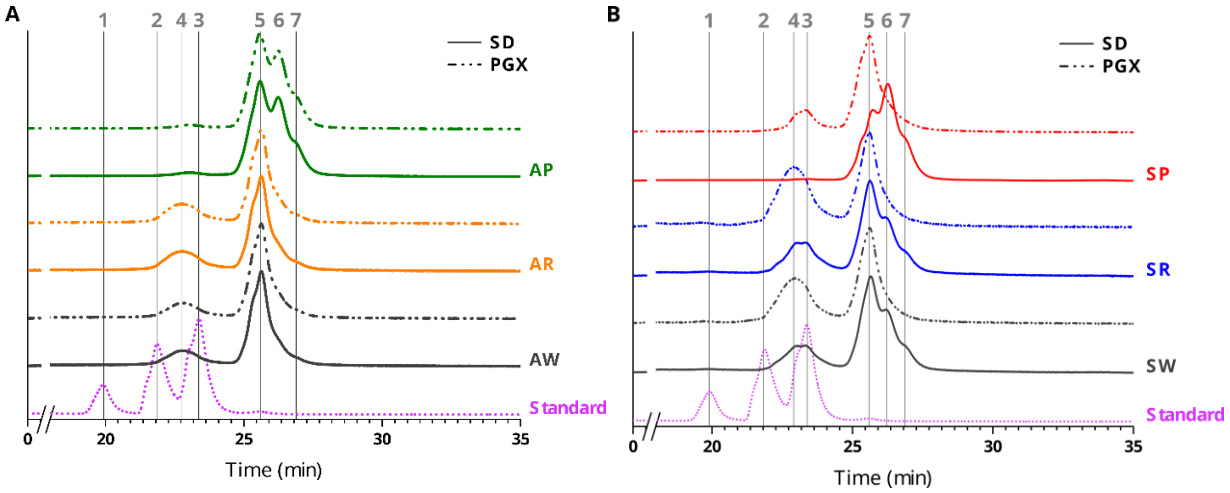

Figure 4.6. HPLC chromatograms of reconstituted whey powders: (A) acid whey and (B) sweet whey with peaks (1) BSA, (2,4) β-LG, (3) α-LA, and (5,6,7) small molecules (< 5 kDa). Chromatograms of SD- and PGX-processed powders are represented by solid and dashed lines, respectively.

In matrices containing higher protein concentrations (SW), BSA (around 66 kDa) and immunoglobulin (IgG heavy chain) (around 50 kDa) were detected with reducing SDS-PAGE (Fig. 4.7 lanes G-L), yet they were absent in the HPLC chromatograms of -SW and -SR (Fig. 4.6B). A plausible explanation would be that aggregates formed by the larger proteins were

physically removed during HPLC sample preparation (> 0.45µm), and therefore not injected into the column. Regardless of the drying technique, β-LG and α-LA proteins in SD- and PGX- SW and SR behaved as aggregates in solution (Fig. 4.6 B). Protein content in the UF permeate fraction was speculated to be attributed to the GMP; however, this peptide (7.5 kDa) is invisible in SDS-PAGE analysis (Fig. 4.7 lanes I-L). Protein separation results indicated that β-LG and α-LA also contributed to the protein content of the whey powders dried from the permeate fractions, specifically the dark SDS-PAGE bands and the appearance of a peak representing the whey protein aggregates compared to its SD- counterpart. The total nitrogen content in cheddar cheese whey (SW) is typically distributed among whey protein nitrogen, proteose-peptone nitrogen as well as non-protein nitrogen sources (Matthews et al., 1976). Fat separation, whey concentration, filtration time and the extent of diafiltration all influence the ultrafiltration process, and therefore the distribution of the nitrogenous components.

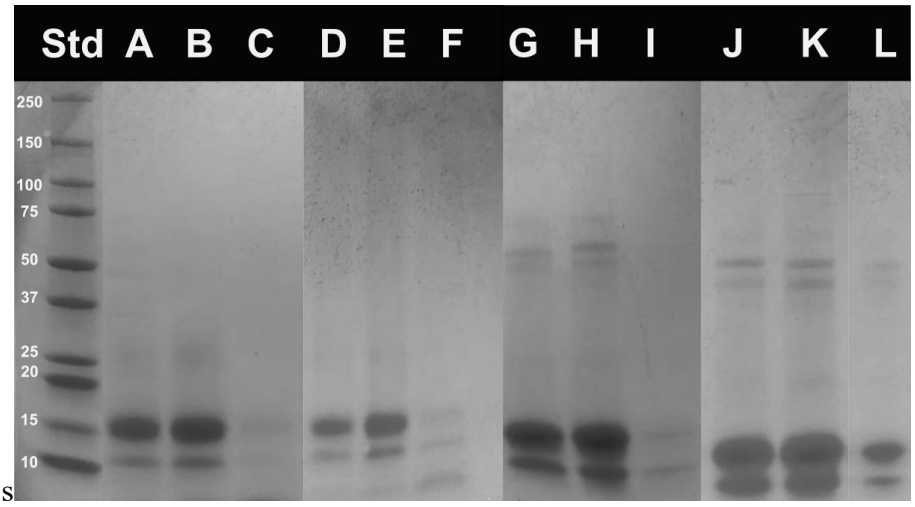

Figure 4.7. Reducing SDS-PAGE patterns of whey powders with lanes (STD), SDS molecular weight standard mixture, (A) SD-AW, (B) SD-AR, (C) SD-AP, (D) PGX-AW, (E) PGX-AR, (F) PGX-AP, (G) SD-SW, (H) SD-SR, (I) SD-SP, (J) PGX-SW, (K) PGX-SR, (L) PGX-SP.

The FTIR-ATR spectra of the protein secondary structure are reported in Figs. 4.8A1 and B1, featuring two regions at 800-1200 cm^{-1} and 1300-1800 cm^{-1}, representing the carbohydrate fingerprint and protein amide regions, respectively. The most intense band in the fingerprint region was between 1190 and 930 cm^{-1}, characteristic of the stretching vibrations of the C-C and C-O moieties within the glycosidic linkages of lactose monohydrate (Wiercigroch et al., 2017). The second derivative (Figs. 4.8A2 and B2) was computed to differentiate the various protein secondary structure components that collectively contribute to the broad peak in the amide I region (1600-1700 cm^{-1}) (Carissimi et al., 2020). The second derivative infrared spectra of SD-AW, -AR and -AP (Fig. 4.8A2, solid lines) were mostly flat while their PGX-processed counterparts had the notable appearance of bands (Fig. 4.8A2, dashed lines) in the amide I region. In addition to the compositional data demonstrating the concentration of proteins after PGX-processing (Fig. 4.4A), the appearance of bands near 1622 cm^{-1}, 1630 cm^{-1}, 1676 cm^{-1} and 1690 cm^{-1} (Fig. 4.8A2) represented increased β-sheet structures (Fang & Dalgleish, 1997; Lefèvre & Subirade, 1999) of PGX-AW and -AR compared to their SD- counterparts. Various secondary structures such as β-sheets (1622 cm^{-1} and 1630 cm^{-1}), intermolecular β-sheets (1676 cm^{-1}) and β-sheets/turns (1690 cm^{-1}) were identified in the PGX-processed whey powders. Lefèvre and Subirade (1999) found that spectra containing one band in the region (1620-1635 cm^{-1}) represented the presence of β-LG in its monomeric form while the observation of two bands in the β-sheet region indicated β-LG present in its dimeric form as a result of increased hydrogen bonding. These findings can be used to support the observation of a broad chromatographic peak and the probable association of β-LG monomers (Fig. 4.6A). Another intense band in the PGX-AW, -AR and -AP spectra is located around 1650 cm^{-1}, representative of α-helical structures. The reduced β-sheets and α-helix bands in the SD-AP spectra had reduced intensities compared to PGX-AW and -AR (Fig. 4.8A2), which

has been previously reported to indicate a lower concentration of β-LG (Lefèvre & Subirade, 1999). Importantly, these findings demonstrate that the low levels of whey proteins (β-LG and α-LA) that passed through UF processing were effectively concentrated and recovered by PGX processing.

Similar trends were observed for sweet whey, such that SD-SW, -SR and -SP powders have spectra with the most intense peak in the carbohydrate fingerprint region. Following PGX processing, intense bands appear in the amide region (Fig. 4.8B1) corroborating the shift in proximate composition. Bands representative of β-sheets are also observed in PGX-SW, -SR and -SP powders; most notably a very intense band at 1622 cm^{-1}.

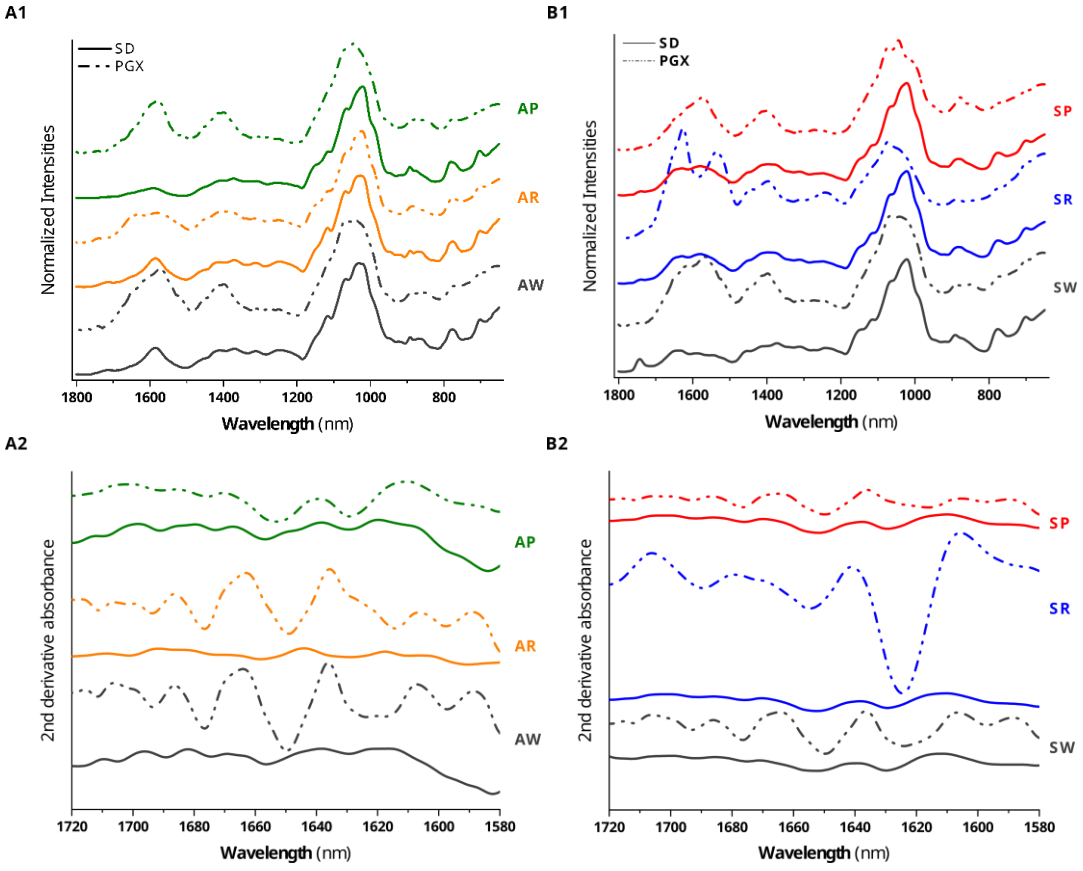

Figure 4.8. (1) FTIR-ATR spectra and (2) second derivative of FTIR-ATR spectra in the wavenumber range of 1580-1720 cm-1 for (A) Acid whey matrices, and (B) Sweet whey matrices processed by spray drying (SD, solid lines) and PGX technology (dashed lines).

4.3.4. Protein solubility and hydrophobicity

Protein solubility is an essential functional property, which determines the applicability of the protein ingredients for formulation purposes. The solubility of the reconstituted whey proteins was evaluated by the addition of salt and pH adjustment. Soluble protein content was calculated by determining the total nitrogen in the soluble fraction of protein dispersions relative to the total nitrogen in the dry powder. Both ionic strength and pH had significant effects on whey protein solubility. SD-AW had good solubility of ≥ 75% in water (pH 3 and 7) (Table 4.3) Amongst the acid whey powders, SD-AW had good solubility in the various media evaluated (~> 75%), with SD-AP having the lowest solubility in water, most likely attributed to the high ash content, specifically Ca and P. The PGX-AP had a low protein content (Fig. 4.4A), which resulted in no detectable protein content upon dissolution (Table 4.3). In salt solutions at pH 3 and 7, away from the isoelectric point of whey (~ 5.2), proteins separated by UF (SD-AR) had soluble protein contents of 83.5 ± 3.5% and 61.2 ± 0.3%, respectively (Table 4.3). At low ionic strength, the salting-in effect (Curtis et al., 2002) was prevalent where dissolved ions neutralize surface charges on the proteins, limiting electrostatic attraction of proteins; thereby promoting protein-solvent interactions leading to an overall increase in the protein solubility (Carr et al., 2004). Following PGX processing, acid whey powders had similar solubility in water and salt solutions, with pH having no noteworthy influence on solubility. Since the ash content of the acid whey powders is significantly higher than that of the sweet whey powders, the salting-in effect was less prevalent after PGX processing. Acid whey proteins concentrated by UF, which were subsequently dried with PGX had significantly reduced solubility in the various dissolution media assessed (Table 4.3).

The broad range (15-58%) of soluble protein reported for each of the sweet whey matrices (SD-SW, -SR and -SP) demonstrates the complex effect of the composition on protein solubility and consequently, protein functionality. SD-SW protein solubility can be manipulated by ionic strength and pH adjustment to achieve ≥ 50% soluble protein content. SD-SR had high solubility in water and the presence of dissolved ions (0.1M NaCl) resulted in a salting-out effect, leading to the aggregation and precipitation of proteins. While the SD-SP has low protein content, there was a moderate level of soluble protein (~70%) in water (pH 7), attributable to significant amounts of lactose in the matrix. Due to the hydrophilicity of lactose, the solubilization of lactose affects the hydration shell around proteins, improving the solubility of water-soluble whey proteins such as α-LA. While PGX-SR had the highest protein content, 65% (Fig. 4.4B), once reconstituted, it had lower soluble protein content compared to PGX-SW. This further established the preference to use PGX technology to directly concentrate and dry the whey proteins from the whey streams. Soluble protein content in this study was evaluated at low concentrations, however, dispersion at concentrations similar to whey or formulations should be further investigated.

Table 4.3. The soluble protein content of whey powders in 0.1 M NaCl and water at pH 3 and 7.

	Soluble protein (%)			
	Water		**0.1 M NaCl**	
	pH = 3	pH = 7	pH = 3	pH = 7
Acid whey				
SD-AW	$79.2 \pm 1.2^{A,a}$	$78.3 \pm 2.4^{A,a}$	$81.9 \pm 3.4^{A,a}$	$73.3 \pm 0.4^{A,a}$
SD-AR	$74.9 \pm 1.1^{AB,\ ab}$	$70.2 \pm 2.2^{A,bc}$	$83.5 \pm 3.5^{A,a}$	$61.2 \pm 0.3^{C,c}$
SD-AP	$72.5 \pm 1.1^{B,a}$	$39.4 \pm 1.2^{C,b}$	$70.2 \pm 2.9^{AB,a}$	$78.2 \pm 0.4^{A,a}$
PGX-AW	$74.1 \pm 1.1^{AB,a}$	$70.3 \pm 0.8^{A,a}$	$62.6 \pm 2.6^{B,a}$	$62.5 \pm 3.6^{B,a}$
PGX-AR	$65.7 \pm 1.0^{C,a}$	$54.3 \pm 1.7^{B,b}$	$27.8 \pm 1.3^{C,c}$	$69.6 \pm 0.3^{BC,a}$
PGX-AP	-	-	-	-
Sweet whey				
SD-SW	$15.0 \pm 0.7^{D,c}$	$48.6 \pm 1.3^{C,b}$	$58.5 \pm 1.5^{AB,a}$	$53.0 \pm 0.3^{C,ab}$
SD-SR	$96.3 \pm 1.4^{A,a}$	$89.7 \pm 1.0^{A,a}$	$54.8 \pm 2.6^{AB,b}$	$67.8 \pm 3.9^{B,b}$
SD-SP	$46.7 \pm 0.7^{C,b}$	$70.1 \pm 2.2^{B,a}$	$62.5 \pm 2.6^{A,a}$	$48.8 \pm 0.2^{C,b}$
PGX-SW	$91.9 \pm 4.2^{A,a}$	$81.3 \pm 2.9^{AB,ab}$	$68.4 \pm 3.9^{A,b}$	$97.8 \pm 2.4^{A,a}$
PGX-SR	$74.7 \pm 3.4^{B,a}$	$74.0 \pm 2.7^{B,a}$	$47.3 \pm 2.7^{B,b}$	$49.8 \pm 1.2^{C,b}$
PGX-SP	$51.7 \pm 0.8^{C,ab}$	$57.8 \pm 0.7^{C,a}$	$23.5 \pm 1.1^{C,c}$	$43.9 \pm 2.6^{C,b}$

Data presented as mean ± SD (n=2).
Different uppercase letters represent significant difference ($p < 0.05$) within each column.
Different lowercase letters represent significant difference ($p < 0.05$) in soluble protein within each row.

Protein hydrophobicity is affected by the spatial arrangement of the hydrophobic and hydrophilic groups at the surface and core of the molecule, influencing the behaviour of the proteins towards the solvent. Upon UV-visible light excitation, hydrophobic amino acid residues exhibit intrinsic fluorescence properties, specifically Tyr, Trp, and Phe absorb starting at 260 nm, Tyr and Phe, at 290 nm, and only Trp absorbing strongly at 295 nm. Shifts in the intrinsic fluorescence (IF) emission spectra attributed to the Trp residues, specifically Trp-19 in β-LG, are indicative of environmental changes surrounding the protein molecules (Eftink, 2000). Acid and sweet whey proteins emitted strongly around 300 nm, with a secondary emission peak between 330-340 nm (Figs. 4.9A and B). The fluorescence of Tyr residues is typically at λ_{EM}= 350 nm in hydrophilic environments; however, the blue shift to λ_{EM}= 300-320 nm indicates that the residue

is in a hydrophobic environment, typically shielded in the core of protein (Hinderink et al., 2021; Jackman & Yada, 1989). Alcohol precipitation of the whey proteins was previously reported to disrupt H-bonding, leading to the reassociation of hydrophobic groups and regions on proteins (Morr & Lin, 1970). Proteins in the permeate fractions had a higher intensity at 300 nm and lower intensity at 340 nm, than their retentate and feedstock counterparts, indicating that the permeate proteins experienced a more hydrophobic environment. Protein hydrophobicity was separately analyzed using the fluorescent probe (ANS) and reporting the slope of the plot of relative fluorescence intensities vs protein concentration (ppm). Increased surface hydrophobicity was correlated with larger slope values. While the hydrophobic amino acid residues were surrounded by more hydrophobic environments, the proteins overall were more hydrophilic compared to the proteins in the retentate and feedstock powders (SD- and PGX-AW and -AR) (Table 4.1). This is attributed to the significant proportion of lactose relative to the protein content of the acid whey powders. Proteins were significantly ($p < 0.05$) more hydrophobic in concentrated protein matrices with reduced lactose content, specifically PGX-SW and -SR.

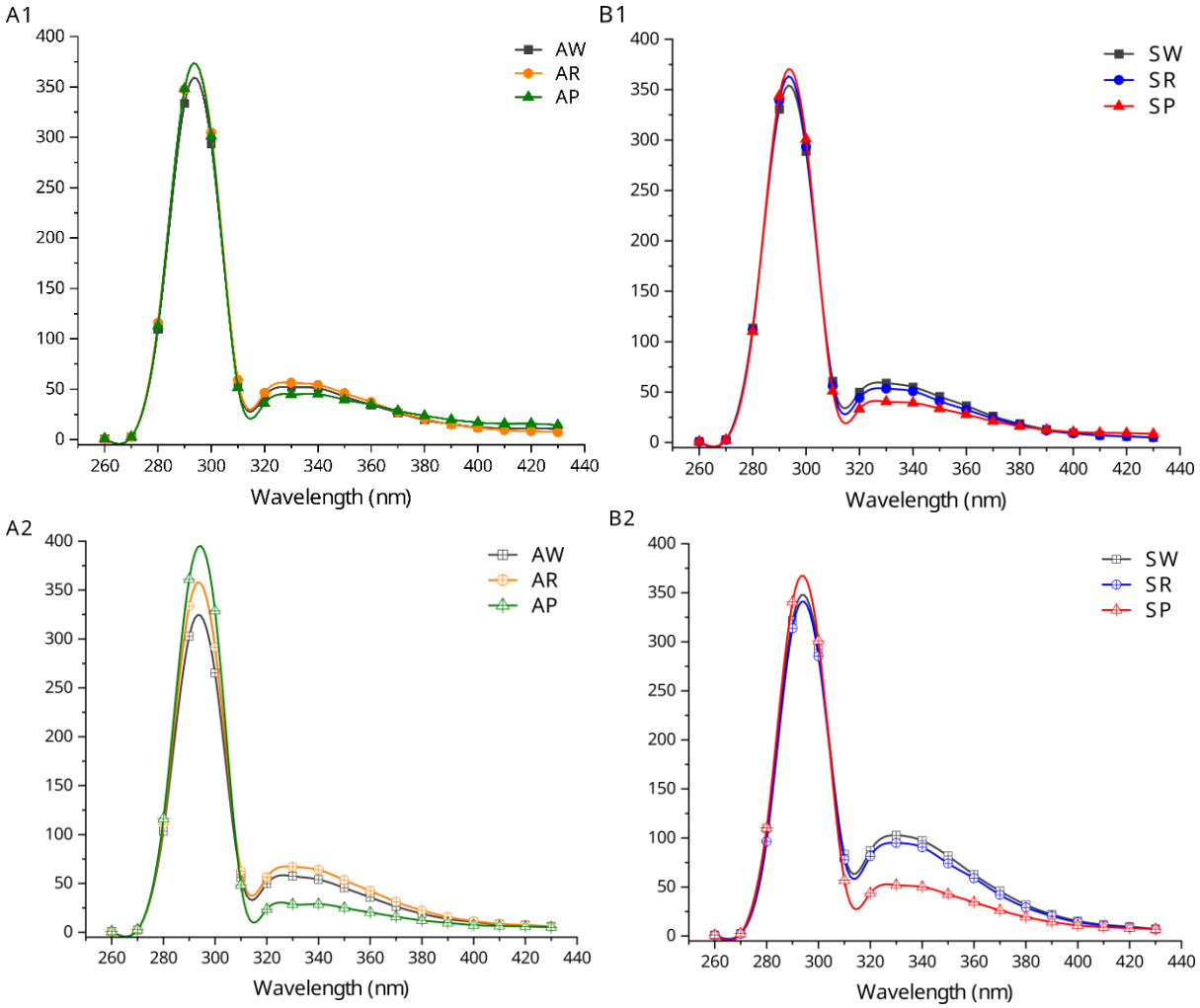

Figure 4.9. Intrinsic fluorescence emission spectra of whey powders reconstituted in PBS, pH 7, at an excitation wavelength of 275 nm for (A) Acid whey, and (B) Sweet whey for (1) spray dried and (2) PGX processed powders.

4.4. Conclusions

Acid and sweet whey matrices were successfully fractionated and dried using the patented PGX technology. PGX processing the feed streams directly resulted in free-flowing powders with compositions, protein profiles and structures similar to the UF-treated fractions. Lactose content was reduced by 25-50% while concentrating valuable whey proteins by 2.7-4.4×. In acid whey, ash and lactose contents were dominant, while whey proteins, such as β-LG and α-LA were concentrated from sweet whey. While Ca and P were both precipitated together with the whey proteins, protein solubility in water and low ionic solutions was only slightly impacted. While protein secondary structure was not significantly affected by PGX processing, exposure to EtOH caused some disruptions to protein tertiary structure, resulting in the rearrangement of hydrophobic groups of whey proteins. Further PGX processing of the UF fractions did not significantly improve the particle attributes. The findings of this study demonstrate that the PGX technology is an effective single-step fractionation and drying technique for direct whey processing applications.

Chapter 5. Conclusions and recommendations

5.1. Summary of key findings

The Pressurized Gas eXpanded (PGX) liquid technology was successfully applied to the fractionation, concentration and drying of whey proteins from fresh whey streams. Up until recently, the PGX technology has been applied primarily to polysaccharides such as oat and yeast beta-glucan, sodium alginate, gum arabic, pectin and starch. Previously, single biopolymer systems were primarily studied, and in this MSc thesis research, whey was introduced as the first complex mixture investigated with the PGX technology. The presence of various components in liquid whey poses several challenges with the direct utilization of whey. Sequential elimination of each component is required to concentrate the target proteins.

In the first study (Chapter 3), initial trials on a 1 L laboratory system were successful in concentrating the whey proteins, specifically, β-LG, α-LA and BSA. In addition to the recovery of the major whey proteins, minor proteins including Lf and IgGs were also recovered from the 5 L bench-scale system. Additional experiments with varied flow rate ratios were conducted to understand the effects of solvent exposure on the physicochemical attributes of the proteins. With varied PGX fluid to whey solution flow rates, the mixing of the biopolymer solution with the anti-solvent affects the precipitation and water removal process. Efficient mixing, rapid precipitation and water removal at higher θ_{PGX} ratios produced smaller more compact particles due to increased solvent exposure. On the other hand, reduced θ_{PGX} ratios favoured whey protein-protein interactions, resulting in larger particle sizes, greater retention of water surrounding the proteins, and fewer disruptions to the protein secondary structure.

In the second study (Chapter 4), two different varieties of whey feedstock, sweet and acid whey were evaluated with the PGX technology, producing free-flowing, microparticles (in the range of tens μm) with nano-scaled surface features. Whey protein powders had characteristically low bulk densities (ranging from 21-74 g/L), equivalent to a 10x reduction compared to conventionally freeze- and spray-dried whey proteins. Proteins in sweet and acid whey powders were concentrated by 4.4× and 2.7× to levels of 65% and 17%, respectively. From sweet whey, proteins were primarily concentrated, while lactose and ash content were concentrated from acid whey matrices. PGX technology was determined to be as effective as conventional ultrafiltration (10 kDa MW cutoff) since further processing of ultrafiltration fractions with PGX did not significantly improve the particle attributes.

Overall, this research extends the applicability of the PGX technology for the development of value-added ingredients by utilizing food waste streams. The research findings demonstrated that this SCF technology is versatile and suitable for processing food manufacturing waste 'as is' without complicated preprocessing steps. While this study utilized processing conditions and parameters similar to those previously applied to polysaccharides, process conditions including temperature, pressure, and PGX fluid ratios (CO_2:EtOH) should be investigated further with considerations for the higher orders (secondary, tertiary, and quaternary) of protein structures compared to polysaccharides. Simultaneous precipitation and concentration of valuable components while removing impurities demonstrated that the PGX technology is suitable as an alternative to and simplification of conventional processing techniques. The extensive characterization of whey protein concentrate powders performed in this MSc thesis research and the findings may be useful in optimizing the generation of value-added ingredients and/or for the potential development of novel bioactive delivery systems.

5.2. Recommendations for future work

Based on the findings of the two studies, it would be worthwhile to investigate the following aspects in future research:

- The optimization of PGX processing parameters (e.g.: θ_{PGX}, feedstock preprocessing) to obtain higher protein content powders (> 65%) by further reducing the levels of lactose and ash.
- Investigate the effect of other processing parameters (e.g.: operating pressure and temperature, PGX fluid (CO_2:EtOH) ratio (outside of 1:3), on the proximate composition, physicochemical properties of the dried whey powders, and the protein composition and structure of the whey proteins.
- The functional properties of whey proteins, including the foaming, gelling and emulsification behaviour. Additionally, understanding how the solubility of the whey proteins is affected by other food system components.
- Evaluate the stability of lactose, specifically by measuring the crystallinity and glass transition temperature (T_g) of lactose over a given storage period and controlled relative humidity conditions and the thermal stability of the whey proteins.
- In order to utilize these whey powders for the development of delivery systems, protein stability needs to be determined. It is recommended to establish water sorption isotherms by using gravimetric methods under controlled relative humidity environments.
- Continue investigating the recovery of proteins from acid whey matrices by incorporating additional demineralization and lactose reduction treatments (e.g.: diafiltration) to obtain results comparable to concentrated whey protein powders from sweet whey.

- Investigate the possibility of fractionating the whey protein mixture to obtain concentrated individual whey protein fractions (e.g.: Lf) or obtain bioactive peptide fractions for novel nutraceutical applications.
- Investigate the possibility of utilizing second cheese whey (whey byproduct from the manufacture of whey-type cheeses, e.g.: ricotta) to generate concentrated whey protein powders.

Bibliography

Agricultural Marketing Service. (2015). *Whey Protein Concentrate (WPC)*. https://www.ams.usda.gov/sites/default/files/media/Whey%20Protein%20Concentrate%20TR.pdf

Agriculture and Agri-Food Canada. (2009). *Market Analysis Report Consumer Trends - Functional Foods*. https://publications.gc.ca/collections/collection_2015/aac-aafc/A74-2-2009-4-eng.pdf

Albani, J. R., Vogelaer, J., Bretesche, L., & Kmiecik, D. (2014). Tryptophan 19 residue is the origin of bovine β-lactoglobulin fluorescence. *Journal of Pharmaceutical and Biomedical Analysis*, *91*, 144–150. https://doi.org/10.1016/j.jpba.2013.12.015

Angel de la Fuente, M., Singh, H., & Hemar, Y. (2022). Recent advances in the characterisation of heat-induced aggregates and intermediates of whey proteins. *Trends in Food Science & Technology*, *13*, 262–274. https://doi.org/https://doi.org/10.1016/S0924-2244(02)00133-4

AOAC. (2012). Solids (total) in milk - By direct forced air oven. In *Official Methods of Analysis of AOAC International: Vol. Method 945.46-1945* (19th ed.). AOAC International.

Argenta, A. B., & Scheer, A. D. P. (2020). Membrane separation processes applied to whey: A review. *Food Reviews International*, *36*(5), 499–528. https://doi.org/10.1080/87559129.2019.1649694

Bahrami, M., & Ranjbarian, S. (2007). Production of micro- and nano-composite particles by supercritical carbon dioxide. *Journal of Supercritical Fluids*, *40*(2), 263–283. https://doi.org/10.1016/j.supflu.2006.05.006

Baker, H. M., & Baker, E. N. (2004). Lactoferrin and iron: Structural and dynamic aspects of binding and release. *BioMetals*, *17*(3), 209–216. https://doi.org/10.1023/B:BIOM.0000027694.40260.70

Baldasso, C., Barros, T. C., & Tessaro, I. C. (2011). Concentration and purification of whey proteins by ultrafiltration. *Desalination*, *278*, 381–386. https://doi.org/10.1016/j.desal.2011.05.055

Bardestani, R., Patience, G. S., & Kaliaguine, S. (2019). Experimental methods in chemical engineering: specific surface area and pore size distribution measurements—BET, BJH, and DFT. *Canadian Journal of Chemical Engineering*, *97*(11), 2781–2791. https://doi.org/10.1002/cjce.23632

Barry, F., Beechinor, F., & Foley, J. (1988). High performance liquid chromatography analysis of whey protein products. *Irish Journal of Food Science and Technology*, *12*(1), 25–39. https://www.jstor.org/stable/25558177

Barukčić, I., Jakopović, K. L., & Božanić, R. (2019). Valorisation of whey and buttermilk for production of functional beverages - An overview of current possibilities. *Food Technology and Biotechnology*, *57*(4), 448–460. https://doi.org/10.17113/ftb.57.04.19.6460

Betz, M., García-González, C. A., Subrahmanyam, R. P., Smirnova, I., & Kulozik, U. (2012). Preparation of novel whey protein-based aerogels as drug carriers for life science applications. *Journal of Supercritical Fluids*, *72*, 111–119. https://doi.org/10.1016/j.supflu.2012.08.019

Bizzarri, G., & Gapon, S. (2019). *Climate change and the global dairy cattle sector -The role of the dairy sector in a low-carbon future*. https://www.fao.org/3/ca2929en/ca2929en.pdf

Bonnaillie, L. M., & Tomasula, P. M. (2012). Fractionation of whey protein isolate with supercritical carbon dioxide to produce enriched αlactalbumin and β-lactoglobulin food ingredients. *Journal of Agricultural and Food Chemistry*, *60*(20), 5257–5266. https://doi.org/10.1021/jf3011036

Boye, J. I., Ma, C.-Y., Ismail, A., Harwalkar, V. R., & Kalab, M. (1997). Molecular and microstructural studies of thermal denaturation and gelation of lactoglobulins A and B. *Journal of Agricultural and Food Chemistry*, *45*, 1608–1618. https://doi.org/https://doi.org/10.1021/jf960622x

Brazzle, P., Bourbon, B., Barrucand, P., Fenelon, M., Guercini, S., & Tiarca, R. (2019). *Wastewater treatment in dairy processing - innovative solutions for sustainable wastewater. Bulletin of the International Dairy Federation, No. 500*. www.fil-idf.org

Brock, J. H. (2012). Lactoferrin-50 years on. *Biochemistry and Cell Biology*, *90*(3), 245–251. https://doi.org/10.1139/o2012-018

Byler, D. M., & Susi, H. (1986). Examination of the secondary structure of proteins by deconvolved FTIR spectra. *Biopolymers*, *25*(3), 469–487. https://doi.org/10.1002/bip.360250307

Carissimi, G., Baronio, C. M., Montalbán, M. G., Víllora, G., & Barth, A. (2020). On the secondary structure of silk fibroin nanoparticles obtained using ionic liquids: An infrared spectroscopy study. *Polymers*, *12*(6), 1294. https://doi.org/10.3390/POLYM12061294

Carr, A., Bhaskar, V., & Ram, S. (2004). *Monovalent salt enhances solubility of milk protein concentrate* (Patent US2004/0208955A1).

Carter, B. G., Cheng, N., Kapoor, R., Meletharayil, G. H., & Drake, M. A. (2021). Invited review: Microfiltration-derived casein and whey proteins from milk. *Journal of Dairy Science*, *104*(3), 2465–2479. https://doi.org/10.3168/jds.2020-18811

Catarino, M. D., Alves-Silva, J. M., Fernandes, R. P., Gonçalves, M. J., Salgueiro, L. R., Henriques, M. F., & Cardoso, S. M. (2017). Development and performance of whey

protein active coatings with Origanum virens essential oils in the quality and shelf life improvement of processed meat products. *Food Control*, *80*, 273–280. https://doi.org/10.1016/j.foodcont.2017.03.054

Chafidz, A., Jauhary, T., Kaavessina, M., & Latief, F. H. (2018). Formation of fine particles using supercritical fluids (SCF) process: Short review. *Communications in Science and Technology*, *3*(2), 57–63. https://doi.org/https://doi.org/10.21924/cst.3.2.2018.101

Chatzipaschali, A. A., & Stamatis, A. G. (2012). Biotechnological utilization with a focus on anaerobic treatment of cheese whey: Current status and prospects. *Energies*, *5*(9), 3492–3525. https://doi.org/10.3390/en5093492

Chávez, F., Debenedetti, P. G., Luo, J. J., Dave, R. N., & Pfeffer, R. (2003). Estimation of the characteristic time scales in the supercritical antisolvent process. *Industrial and Engineering Chemistry Research*, *42*(13), 3156–3162. https://doi.org/10.1021/ie021048j

Cho, Y., Singh, H., & Creamer, L. K. (2003). Heat-induced interactions of β-lactoglobulin A and κ-casein B in a model system. *Journal of Dairy Research*, *70*(1), 61–71. https://doi.org/10.1017/S0022029902005642

Couto, R., Wong, E., Seifried, B., Yépez, B., Moquin, P., & Temelli, F. (2020). Preparation of PGX-dried gum arabic and its loading with coQ10 by adsorptive precipitation. *Journal of Supercritical Fluids*, *156*, 104662. https://doi.org/10.1016/j.supflu.2019.104662

Curtis, R. A., Ulrich, J., Montaser, A., Prausnitz, J. M., & Blanch, H. W. (2002). Protein-protein interactions in concentrated electrolyte solutions: Hofmeister-series effects. *Biotechnology and Bioengineering*, *79*(4), 367–380. https://doi.org/10.1002/bit.10342

Dahal, Y. R., & Schmit, J. D. (2018). Ion specificity and nonmonotonic protein solubility from salt entropy. *Biophysical Journal*, *114*(1), 76–87. https://doi.org/10.1016/j.bpj.2017.10.040

Danahy, B. B., Minnick, D. L., & Shiflett, M. B. (2018). Computing the composition of ethanol-water mixtures based on experimental density and temperature measurements. *Fermentation*, *4*(3), 1–7. https://doi.org/10.3390/fermentation4030072

Daniloski, D., Petkoska, A. T., Lee, N. A., Bekhit, A. E. D., Carne, A., Vaskoska, R., & Vasiljevic, T. (2021). Active edible packaging based on milk proteins: A route to carry and deliver nutraceuticals. *Trends in Food Science and Technology*, *111*, 688–705. https://doi.org/10.1016/j.tifs.2021.03.024

de Wit, J. N. (1998). Nutritional and functional characteristics of whey proteins in food products. *Journal of Dairy Science*, *81*, 597–608. https://doi.org/https://doi.org/10.3168/jds.S0022-0302(98)75613-9

de Wit, J. N. (2001). *Lecturer's handbook on whey and whey products* (1st ed.). European Whey Products Association.

Deeth, H., & Bansal, N. (2019). Chapter 1 - Whey Proteins: An Overview. In H. C. Deeth & N. Bansal (Eds.), *Whey Proteins* (pp. 1–50). Academic Press. https://doi.org/https://doi.org/10.1016/B978-0-12-812124-5.00001-1

Devries, M. C., & Phillips, S. M. (2015). Supplemental protein in support of muscle mass and health: Advantage whey. *Journal of Food Science*, *80*(S1), A8–A15. https://doi.org/10.1111/1750-3841.12802

Dissanayake, M., & Vasiljevic, T. (2009). Functional properties of whey proteins affected by heat treatment and hydrodynamic high-pressure shearing. *Journal of Dairy Science*, *92*(4), 1387–1397. https://doi.org/10.3168/jds.2008-1791

Drago-Serrano, M. E., De La Garza-Amaya, M., Luna, J. S., & Campos-Rodríguez, R. (2012). Lactoferrin-lipopolysaccharide (LPS) binding as key to antibacterial and antiendotoxic effects. *International Immunopharmacology*, *12*(1), 1–9. https://doi.org/10.1016/j.intimp.2011.11.002

Durham, R. J. (2009). Modern approaches to lactose production. *Dairy-Derived Ingredients: Food and Nutraceutical Uses*, 103–144. https://doi.org/10.1533/9781845697198.1.103

Durling, N. E., Catchpole, O. J., Tallon, S. J., & Grey, J. B. (2007). Measurement and modelling of the ternary phase equilibria for high pressure carbon dioxide-ethanol-water mixtures. *Fluid Phase Equilibria*, *252*(1–2), 103–113. https://doi.org/10.1016/j.fluid.2006.12.014

Dzwolak, W., Kato, M., Shimizu, A., & Taniguchi, Y. (1999). Fourier-transform infrared spectroscopy study of the pressure-induced changes in the structure of the bovine α-lactalbumin: the stabilizing role of the calcium ion. *Biochemica et Biophysica Atcta*, *1433*, 45–55. www.elsevier.com/locate/bba

Eftink, M. R. (2000). Intrinsic Fluorescence of Proteins. In J. R. Lakowicz (Ed.), *Protein Fluorescence* (1st ed., pp. 1–15). Springer. https://doi.org/https://doi.org/10.1007/b115628

Erickson, B. E. (2017). *Acid whey: Is the waste product an untapped goldmine?* Chemical & Engineering News. https://cen.acs.org/articles/95/i6/Acid-whey-waste-product-untapped.html#:~:text=Sweet

Etzel, M. R. (2004). Manufacture and use of dairy protein fractions. *Journal of Nutrition*, *134*(4), 966S-1002S. https://doi.org/10.1093/jn/134.4.996s

Fan, F., & Roos, Y. H. (2015). X-ray diffraction analysis of lactose crystallization in freeze-dried lactose-whey protein systems. *Food Research International*, *67*, 1–11. https://doi.org/10.1016/j.foodres.2014.10.023

Fang, Y., & Dalgleish, D. G. (1997). Conformation of beta-lactoglobulin studied by FTIR: Effect of pH, temperature, and adsorption to the oil-water interface. *Journal of Colloid*

and Interface Science , *196*, 292–298. https://doi.org/https://doi.org/10.1006/jcis.1997.5191

Feng, P., Fuerer, C., & McMahon, A. (2018). Quantification of whey protein content in milk-based infant formula powders by sodium dodecyl sulfate–capillary gel electrophoresis (SDS-CGE): Multilaboratory testing study, final action 2016.15. *Journal of AOAC International*, *101*(5), 1566–1577. https://doi.org/10.5740/jaoacint.18-0057

Feng, Y., Ma, X., Kong, B., Chen, Q., & Liu, Q. (2021). Ethanol induced changes in structural, morphological, and functional properties of whey proteins isolates: Influence of ethanol concentration. *Food Hydrocolloids*, *111*, 106379. https://doi.org/10.1016/j.foodhyd.2020.106379

Food and Agriculture Organization of the United Nations. (2011, December 10). *Global food losses and food waste: extent, causes and prevention*. https://www.fao.org/faostat/en/#data

Fox, P. F., Uniacke-Lowe, T., Mcsweeney, P. L. H., & O'mahony, J. A. (2015). *Dairy Chemistry and Biochemistry Second Edition*. https://doi.org/10.1007/978-3-319-14892-2

Ganju, S., & Gogate, P. R. (2017). A review on approaches for efficient recovery of whey proteins from dairy industry effluents. *Journal of Food Engineering*, *215*, 84–96. https://doi.org/10.1016/j.jfoodeng.2017.07.021

Gaucheron, F. (2013). Milk minerals, trace elements and macroelements. In Y. W. Park & G. F. W. Haenlein (Eds.), *Milk and Dairy Products in Human Nutrition: Production, Composition and Health* (1st ed., Vol. 1, pp. 172–199). John Wiley & Sons, Ltd.

Gerosa, S., & Skoet, J. (2012). *Milk availability -Trends in production and demand and medium-term outlook*. www.fao.org/economic/esa

Glass, L., & Hedrick, T. I. (1977). Nutritional composition of sweet- and acid-type dry wheys. II. Vitamin, mineral, and calorie contents. *Journal of Dairy Science*, *60*(2), 190–196. https://doi.org/10.3168/jds.S0022-0302(77)83853-8

Goulding, D. A., Fox, P. F., & O'Mahony, J. A. (2019). Milk proteins: An overview. In *Milk Proteins: From Expression to Food* (pp. 21–98). Elsevier. https://doi.org/10.1016/B978-0-12-815251-5.00002-5

Gyawali, R., & Ibrahim, S. A. (2016). Effects of hydrocolloids and processing conditions on acid whey production with reference to Greek yogurt. *Trends in Food Science and Technology*, *56*, 61–76. https://doi.org/10.1016/j.tifs.2016.07.013

Haque, M. K., & Roos, Y. H. (2005). Crystallization and x-ray diffraction of spray dried and freeze dried amorphous lactose. *Carbohydrate Research*, *340*(2), 293–301. https://doi.org/10.1016/j.carres.2004.11.026

Heng, M. H., & Glatz, C. E. (1991). Chemical pretreatments and fouling in acid cheese whey ultrafiltration. *Journal of Dairy Science*, *74*(1), 11–19. https://doi.org/10.3168/jds.S0022-0302(91)78138-1

Hinderink, E. B. A., Berton-Carabin, C. C., Schroën, K., Riaublanc, A., Houinsou-Houssou, B., Boire, A., & Genot, C. (2021). Conformational changes of whey and pea proteins upon emulsification approached by front surface fluorescence. *Journal of Agricultural and Food Chemistry*, *69*(23), 6601–6612. https://doi.org/10.1021/acs.jafc.1c01005

Hiraoka', Y., Segawa', T., Kuwajimar, K., Sugai', S., & Murai', N. (1980). α-Lactalbumin: a calcium metalloprotein. *Biochemical and Biophysical Research Communications*, *95*(3), 1098–1104. https://doi.org/https://doi.org/10.1016/0006-291X(80)91585-5

ISO. (2002). ISO 14891. Milk and milk products — Determination of nitrogen content — Routine method using combustion according to the Dumas principle. In *International Organization for Standardization*.

Ivory, R., Delaney, E., Mangan, D., & McCleary, B. V. (2021). Determination of lactose concentration in low-lactose and lactose-free milk, milk products, and products containing dairy ingredients, enzymatic method: Single-laboratory validation first action method 2020.08. *Journal of AOAC International*, *104*(5), 1308–1322. https://doi.org/10.1093/jaoacint/qsab032

Jackman, R. L., & Yada, R. Y. (1989). Ultraviolet absorption and fluorescence properties of whey potato and whey-pea protein composites. *Canadian Institute of Food Science and Technology Journal*, *22*(3), 252–259. https://doi.org/https://doi.org/10.1016/S0315-5463(89)70392-8

Jelen, P. (2002). Whey processing -Utilization and products. In J. W. Fuquay & P. F. Fox (Eds.), *Encyclopedia of Dairy Sciences* (1st ed., pp. 2739–2745).

Jessop, P. G., & Subramaniam, B. (2007). Gas-expanded liquids. *Chemical Reviews*, *107*(6), 2666–2694. https://doi.org/10.1021/cr040199o

Johnson, K.-A. (2018). *Crosslinking and characterization of Pressurized Gas eXpanded liquid polymer morphologies to crease macroporous hydrogel scaffolds for drug delivery and wound healing* [Master's]. McMaster University.

Johnson, K.-A., Muzzin, N., Toufanian, S., Slick, R. A., Lawlor, M. W., Seifried, B., Moquin, P., Latulippe, D., & Hoare, T. (2020). Drug-impregnated, pressurized gas expanded liquid-processed alginate hydrogel scaffolds for accelerated burn wound healing. *Acta Biomaterialia*, *112*, 101–111. https://doi.org/10.1016/j.actbio.2020.06.006

Jost, R., Maire, J. C., Maynard, F., & Secretin, M. C. (1999). Aspects of whey protein usage in infant nutrition, a brief review. *International Journal of Food Science and Technology*, *34*, 533–542. https://doi.org/10.1046/j.1365-2621.1999.00324.x

Jouppila, K., Kansikas, J., & Roos, Y. H. (1997). Glass transition, water plasticization, and lactose crystallization in skim milk powder. *Journal of Dairy Science*, *80*, 3120–3160. https://doi.org/https://doi.org/10.3168/jds.S0022-0302(97)76286-6

Jung, J., & Perrut, M. (2001). Particle design using supercritical fluids: Literature and patent survey. *Journal of Supercritical Fluids*, *20*, 179–219. https://doi.org/https://doi.org/10.1016/S0896-8446(01)00064-X

Kelly, P. (2019). Chapter 3 - Manufacture of whey protein products: Concentrates, isolate, whey protein fractions and microparticulated. In H. C. Deeth & N. Bansal (Eds.), *Whey Proteins* (pp. 97–122). Academic Press. https://doi.org/https://doi.org/10.1016/B978-0-12-812124-5.00003-5

Kilara, A., & Vaghela, M. N. (2017). Whey proteins. In *Proteins in Food Processing, Second Edition* (pp. 93–126). Elsevier. https://doi.org/10.1016/B978-0-08-100722-8.00005-X

Kira, C. S., Maio, F. D., & Maihara, V. A. (2004). Comparison of partial digestion procedures for determination of Ca, Cr, Cu, Fe, K, Mg, Mn, Na, P, and Zn in milk by inductively coupled plasma-optical emission spectrometry. *Journal of AOAC International*, *87*(1), 151–156. https://academic.oup.com/jaoac/article/87/1/151/5657321

Kumar, P., Sharma, N., Ranjan, R., Kumar, S., Bhat, Z. F., & Jeong, D. K. (2013). Perspective of membrane technology in dairy industry: A review. *Asian-Australasian Journal of Animal Sciences*, *26*(9), 1347–1358. https://doi.org/10.5713/ajas.2013.13082

Lefèvre, T., & Subirade, M. (1999). Structural and interaction properties of β-lactoglobulin as studied by FTIR spectroscopy. *International Journal of Food Science and Technology*, *34*(5–6), 419–428. https://doi.org/10.1046/j.1365-2621.1999.00311.x

Legrand, D., Elass, E., Carpentier, M., & Mazurier, J. (2005). Lactoferrin: A modulator of immune and inflammatory responses. *Cellular and Molecular Life Sciences*, *62*(22), 2549–2559. https://doi.org/10.1007/s00018-005-5370-2

Lien, E. L. (2003). Infant formulas with increased concentrations of alpha-lactalbumin. *The American Journal of Clinical Nutrition*, *77*(6), 1555S-1558S. https://doi.org/10.1093/ajcn/77.6.1555s

Liu, N., Couto, R., Seifried, B., Moquin, P., Delgado, L., & Temelli, F. (2018). Characterization of oat beta-glucan and coenzyme Q10-loaded beta-glucan powders generated by the pressurized gas-expanded liquid (PGX) technology. *Food Research International*, *106*, 354–362. https://doi.org/10.1016/j.foodres.2017.12.073

Liu, N., Nguyen, H., Wismer, W., & Temelli, F. (2018). Development of an orange-flavoured functional beverage formulated with beta-glucan and coenzyme Q10-impregnated beta-glucan. *Journal of Functional Foods*, *47*, 397–404. https://doi.org/10.1016/j.jff.2018.05.037

Liu, Z. (2019). *Pressurized Gas eXpanded (PGX) liquid drying of sodium alginate and its loading with coenzyme Q10 by adsorptive precipitation* [Master's]. University of Alberta.

Macwan, S. R., Dabhi, B. K., Parmar, S. C., & Aparnathi, K. D. (2016). Whey and its utilization. *International Journal of Current Microbiology and Applied Sciences*, *5*(8), 134–155. https://doi.org/10.20546/ijcmas.2016.508.016

Madureira, A. R., Pereira, C. I., Gomes, A. M. P., Pintado, M. E., & Xavier Malcata, F. (2007). Bovine whey proteins - Overview on their main biological properties. *Food Research International*, *40*(10), 1197–1211. https://doi.org/10.1016/j.foodres.2007.07.005

Madureira, A. R., Tavares, T., Gomes, A. M. P., Pintado, M. E., & Malcata, F. X. (2010). Invited review: Physiological properties of bioactive peptides obtained from whey proteins. *Journal of Dairy Science*, *93*(2), 437–455. https://doi.org/10.3168/jds.2009-2566

Manzocco, L., Plazzotta, S., Powell, J., de Vries, A., Rousseau, D., & Calligaris, S. (2021). Structural characterisation and sorption capability of whey protein aerogels obtained by freeze-drying or supercritical drying. *Food Hydrocolloids*, *122*, 107117. https://doi.org/10.1016/j.foodhyd.2021.107117

Martins, J. T., Santos, S. F., Bourbon, A. I., Pinheiro, A. C., González-Fernández, Á., Pastrana, L. M., Cerqueira, M. A., & Vicente, A. A. (2016). Lactoferrin-based nanoparticles as a vehicle for iron in food applications – Development and release profile. *Food Research International*, *90*, 16–24. https://doi.org/10.1016/j.foodres.2016.10.027

Mathai, J. K., Liu, Y., & Stein, H. H. (2017). Values for digestible indispensable amino acid scores (DIAAS) for some dairy and plant proteins may better describe protein quality than values calculated using the concept for protein digestibility-corrected amino acid scores (PDCAAS). *British Journal of Nutrition*, *117*(4), 490–499. https://doi.org/10.1017/S0007114517000125

Matthews, M. E., Amundson, C. H., & Hill, C. G. (1976). Changes in distribution of nitrogenous fractions of cheddar cheese whey during ultrafiltration. *Journal of Dairy Science*, *59*(6), 1033–1041.

Mays, T. J. (2005). A new classification of pore sizes. In P. L. Llewellyn, F. Rodriquez-Reinoso, J. Rouqerol, & N. Seaton (Eds.), *Characterization of Porous Solids VII* (Vol. 160, pp. 1–734).

Mehra, R., Kumar, H., Kumar, N., Ranvir, S., Jana, A., Buttar, H. S., Telessy, I. G., Awuchi, C. G., Okpala, C. O. R., Korzeniowska, M., & Guiné, R. F. P. (2021). Whey proteins processing and emergent derivatives: An insight perspective from constituents, bioactivities, functionalities to therapeutic applications. *Journal of Functional Foods*, *87*, 104760. https://doi.org/10.1016/j.jff.2021.104760

Mirabella, N., Castellani, V., & Sala, S. (2014). Current options for the valorization of food manufacturing waste: A review. *Journal of Cleaner Production*, *65*, 28–41. https://doi.org/10.1016/j.jclepro.2013.10.051

Morr, C. V., German, B., Kinsella, J. E., Regenstein, J. M., Van Buren, J. P., Kilara, A., Lewis, B. A., & Mangino, M. E. (1985). A collaborative study to develop a standardized food protein solubility procedure. *Journal of Food Science*, *50*, 1715–1718. https://doi.org/https://doi.org/10.1111/j.1365-2621.1985.tb10572.x

Morr, C. V., & Ha, E. Y. W. (1993). Whey protein concentrates and isolates: Processing and functional properties. *Critical Reviews in Food Science and Nutrition*, *33*(6), 431–476. https://doi.org/10.1080/10408399309527643

Morr, C. V., & Lin, S. H. C. (1970). Preparation and properties of an alcohol-precipitated whey protein concentrate. *Journal of Dairy Science* , *53*(9), 1162–1170. https://doi.org/https://doi.org/10.3168/jds.S0022-0302(70)86362-7

Muzzin, N. (2018). *Evaluating Pressurized Gas eXpanded liquid processed carbohydrates for biomedical and bioseparations applications* [Master's]. McMaster University.

Ney, D. M., Gleason, S. T., van Calcar, S. C., MacLeod, E. L., Nelson, K. L., Etzel, M. R., Rice, G. M., & Wolff, J. A. (2009). Nutritional management of PKU with glycomacropeptide from cheese whey. *Journal of Inherited Metabolic Disease*, *32*(1), 32–39. https://doi.org/10.1007/s10545-008-0952-4

Nijdam, J., Ibach, A., Eichhorn, K., & Kind, M. (2007). An x-ray diffraction analysis of crystallised whey and whey-permeate powders. *Carbohydrate Research*, *342*(16), 2354–2364. https://doi.org/10.1016/j.carres.2007.08.001

Nikolaidis, A., & Moschakis, T. (2018). On the reversibility of ethanol-induced whey protein denaturation. *Food Hydrocolloids*, *84*, 389–395. https://doi.org/10.1016/j.foodhyd.2018.05.051

Nishanthi, M., Chandrapala, J., & Vasiljevic, T. (2017a). Compositional and structural properties of whey proteins of sweet, acid and salty whey concentrates and their respective spray dried powders. *International Dairy Journal*, *74*, 49–56. https://doi.org/10.1016/j.idairyj.2017.01.002

Nishanthi, M., Chandrapala, J., & Vasiljevic, T. (2017b). Properties of whey protein concentrate powders obtained by spray drying of sweet, salty and acid whey under varying storage conditions. *Journal of Food Engineering*, *214*, 137–146. https://doi.org/10.1016/j.jfoodeng.2017.06.032

O'Mahony, J. A., & Fox, P. F. (2014). Milk: An Overview. In *Milk Proteins* (pp. 19–73). Elsevier. https://doi.org/10.1016/b978-0-12-405171-3.00002-7

O'Sullivan, M. (2011). Analytical Methods: Proximate and Other Chemical Analyses. *Encyclopedia of Dairy Sciences: Second Edition*, 76–82. https://doi.org/10.1016/B978-0-12-374407-4.00517-3

Ozel, B., McClements, D. J., Arikan, C., Kaner, O., & Oztop, M. H. (2022). Challenges in dried whey powder production: Quality problems. *Food Research International*, *160*, 111682. https://doi.org/10.1016/j.foodres.2022.111682

Palakodaty, S., York, P., & Pritchard, J. (1998). Supercritical fluid processing of materials from aqueous solutions: The application of SEDS to lactose as a model substance. *Pharmaceutical Research*, *15*(12), 1835–1843. https://doi.org/https://doi.org/10.1023/A:1011949805156

Pan, Y., Rowney, M., Guo, P., & Hobman, P. (2007). Biological properties of lactoferrin: An overview. *Australian Journal of Dairy Technology*, *62*(1), 31–42.

Panghal, A., Patidar, R., Jaglan, S., Chhikara, N., Khatkar, S. K., Gat, Y., & Sindhu, N. (2018). Whey valorization: current options and future scenario – a critical review. *Nutrition and Food Science*, *48*(3), 520–535. https://doi.org/10.1108/NFS-01-2018-0017

Pearce, R. J. (1992). Whey Processing. *Whey and Lactose Processing*, 73–89. https://doi.org/10.1007/978-94-011-2894-0_2

Prosapio, V., Reverchon, E., & De Marco, I. (2014a). Antisolvent micronization of BSA using supercritical mixtures carbon dioxide + organic solvent. *Journal of Supercritical Fluids*, *94*, 189–197. https://doi.org/10.1016/j.supflu.2014.07.012

Prosapio, V., Reverchon, E., & De Marco, I. (2014b). Antisolvent micronization of BSA using supercritical mixtures carbon dioxide + organic solvent. *Journal of Supercritical Fluids*, *94*, 189–197. https://doi.org/10.1016/j.supflu.2014.07.012

Qiu, Y., Smith, T. J., Foegeding, E. A., & Drake, M. A. (2015). The effect of microfiltration on color, flavor, and functionality of 80% whey protein concentrate. *Journal of Dairy Science*, *98*(9), 5862–5873. https://doi.org/10.3168/jds.2014-9174

Rathour, A. K., Rathore, V., Mehta, B. M., Patel, S. M., Chauhan, A., & Aparnathi, K. D. (2017). Standardization and storage study of whey protein concentrate (WPC-70) prepared from buffalo milk using ultrafiltration membrane technology. *Journal of Food Processing and Preservation*, *41*(3), e12882. https://doi.org/https://doi.org/10.1111/jfpp.12882

Roy, D., Ye, A., Moughan, P. J., & Singh, H. (2020). Composition, structure, and digestive dynamics of milk from different species —A review. *Frontiers in Nutrition*, *7*, 1. https://doi.org/10.3389/fnut.2020.577759

Ryan, M. P., & Walsh, G. (2016). The biotechnological potential of whey. *Reviews in Environmental Science and Biotechnology*, *15*(3), 479–498. https://doi.org/10.1007/s11157-016-9402-1

Saito, Z. (1988). Lactose crystallization in commercial whey powders and in spray dried lactose. *Food Structure*, *7*, 75–81. https://digitalcommons.usu.edu/foodmicrostructure/vol7/iss1/9

Saxena, J., Adhikari, B., Brkljaca, R., Huppertz, T., Zisu, B., & Chandrapala, J. (2021). Influence of lactose pre-crystallization on the storage stability of infant formula powder containing lactose and maltodextrin. *Food Hydrocolloids*, *111*, 106385. https://doi.org/10.1016/j.foodhyd.2020.106385

Schuck, P. (2014). Chapter 10 - Effects of Drying on Milk Proteins. In H. Singh, M. Boland, & A. Thompson (Eds.), *Milk Proteins (Second Edition)* (Second Edition, pp. 319–342). Academic Press. https://doi.org/https://doi.org/10.1016/B978-0-12-405171-3.00010-6

Schultz, D. L., & Ashworth, U. S. (1974). Effed of pH, calcium, and heat treatment on curd tension of casein fraction fortified skim milk. *Journal of Dairy Science*, *57*(9), 992–997. https://doi.org/https://doi.org/10.3168/jds.S0022-0302(74)84999-4

Seifried, B. (2010). *Physicochemical properties and microencapsulation process development for fish oil using supercritical carbon dioxide* [PhD]. University of Alberta.

Seifried, B., Yépez, B., Moquin, P., Couto, R., Wong, E. Y., Mahmoudi, J., & Hu, J. (2022). Aerogels & composites: From concept to applications. *13th International Symposium on Supercritical Fluids* , *141*.

Shahidi, F. (2009). Nutraceuticals and functional foods: Whole versus processed foods. *Trends in Food Science and Technology*, *20*(9), 376–387. https://doi.org/10.1016/j.tifs.2008.08.004

Shariati-Ievari, S., Ryland, D., Edel, A., Nicholson, T., Suh, M., & Aliani, M. (2016). Sensory and physicochemical studies of thermally micronized chickpea (*Cicer arietinum*) and green lentil (*Lens culinaris*) flours as binders in low-fat beef burgers. *Journal of Food Science*, *81*(5), S1230–S1242. https://doi.org/10.1111/1750-3841.13273

Shimazaki, K.-I., & Sukegawa, K. (1982). Chromatographic profiles of bovine milk whey components by gel filtration on Fractogel TSK HW55F column. *Journal of Dairy Science*, *65*, 2055–2062. https://doi.org/https://doi.org/10.3168/jds.S0022-0302(82)82461-2

Smithers, G. W. (2008). Whey and whey proteins-From "gutter-to-gold." *International Dairy Journal*, *18*(7), 695–704. https://doi.org/10.1016/j.idairyj.2008.03.008

Temelli, F. (2018). Perspectives on the use of supercritical particle formation technologies for food ingredients. *Journal of Supercritical Fluids*, *134*, 244–251. https://doi.org/10.1016/j.supflu.2017.11.010

Temelli, F., & Seifried, B. (2016). *Supercritical fluid treatment of high molecular weight biopolymers: Vol. US 2013/01* (Patent US009249266B2).

Thomä-Worringer, C., Sørensen, J., & López-Fandiño, R. (2006). Health effects and technological features of caseinomacropeptide. *International Dairy Journal*, *16*(11), 1324–1333. https://doi.org/10.1016/j.idairyj.2006.06.012

Tomasula, P. M., & Parris, N. (1999). *Whey protein fractionation using high pressure or supercritical carbon dioxide* (Patent US005925737A).

Tsermoula, P., Khakimov, B., Nielsen, J. H., & Engelsen, S. B. (2021). Whey - The waste stream that became more valuable than the food product. *Trends in Food Science and Technology*, *118*, 230–241. https://doi.org/10.1016/j.tifs.2021.08.025

Van Calcar, S. C., MacLeod, E. L., & Gleason, S. T. (2010). Improved nutritional management of phenylketonuria by using a diet containing glycomacropeptide compared with amino acids. *American Journal of Clinical Nutrition*, *91*(4), 1072. https://doi.org/10.3945/ajcn.2010.29241

Verlagsgesellschaft, H. (2012). Wellness Foods Europe Dairy products. *Wellness Foods Europe Dairy Products*, 4–8. www.vitafoods.eu.com/well1

Vilchez Athanasopulos, A. C. (2019). *Adsorptive precipitation of vitamin D3 and vitamin E on gum arabic and sodium alginate using supercritical carbon dioxide* [Master's]. University of Alberta.

Walstra, P., Wouters, J. T. M., & Geurts, T. J. (2005). *Dairy Science and Technology Second Edition*.

Wang, T., & Lucey, J. A. (2003). Use of multi-angle laser light scattering and size-exclusion chromatography to characterize the molecular weight and types of aggregates present in commercial whey protein products. *Journal of Dairy Science*, *86*(10), 3090–3101. https://doi.org/10.3168/jds.S0022-0302(03)73909-5

Wehr, H. M., & Frank, J. F. (2004). *Standard Methods For The Examination of Dairy Products* (H. M. Wehr & J. F. Frank, Eds.; 17th ed.). American Public Health Association.

Wen-qiong, W., Yun-chao, W., Xiao-feng, Z., Rui-xia, G., & Mao-lin, L. (2019). Whey protein membrane processing methods and membrane fouling mechanism analysis. *Food Chemistry*, *289*, 468–481. https://doi.org/10.1016/j.foodchem.2019.03.086

Wiercigroch, E., Szafraniec, E., Czamara, K., Pacia, M. Z., Majzner, K., Kochan, K., Kaczor, A., Baranska, M., & Malek, K. (2017). Raman and infrared spectroscopy of carbohydrates: A review. *Spectrochimica Acta Part A: Molecular and Biomolecular Spectroscopy*, *185*, 317–335. https://doi.org/10.1016/j.saa.2017.05.045

Yadav, J. S. S., Yan, S., Pilli, S., Kumar, L., Tyagi, R. D., & Surampalli, R. Y. (2015). Cheese whey: A potential resource to transform into bioprotein, functional/nutritional proteins and bioactive peptides. *Biotechnology Advances*, *33*(6), 756–774. https://doi.org/10.1016/j.biotechadv.2015.07.002

Yang, J., Zamani, S., Liang, L., & Chen, L. (2021). Extraction methods significantly impact pea protein composition, structure and gelling properties. *Food Hydrocolloids*, *117*, 106678. https://doi.org/10.1016/j.foodhyd.2021.106678

Yeo, S. Do, & Kiran, E. (2005). Formation of polymer particles with supercritical fluids: A review. *Journal of Supercritical Fluids*, *34*(3), 287–308. https://doi.org/10.1016/j.supflu.2004.10.006

Yver, A. L., Bonnaillie, L. M., Yee, W., Mcaloon, A., & Tomasula, P. M. (2012). Fractionation of whey protein isolate with supercritical carbon dioxide-process modeling and cost estimation. *International Journal of Molecular Sciences*, *13*(1), 240–259. https://doi.org/10.3390/ijms13010240

Zadow, J. G. (Ed.). (1992). *Whey and Lactose Processing*. Elsevier Applied Science.

Appendix A

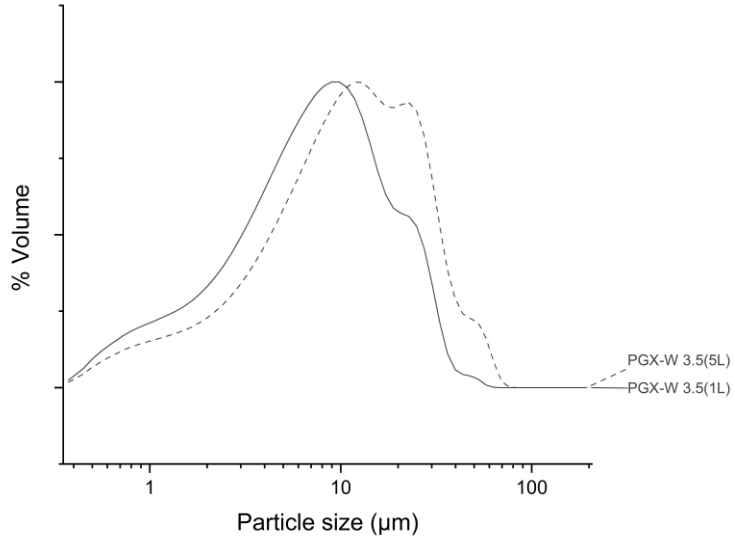

Figure A1. Particle size distributions of PGX-W 3.5(1L) and PGX-W 3.5(5L)

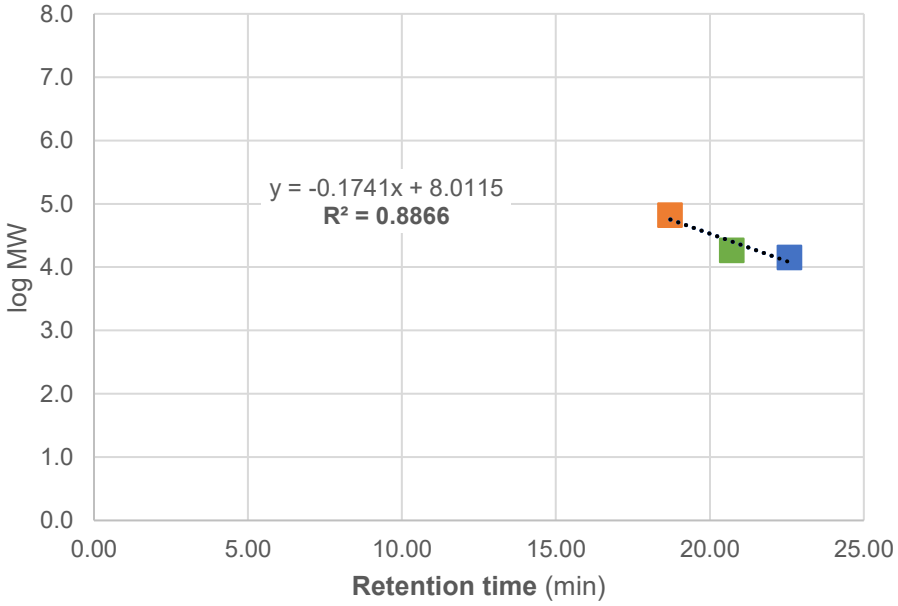

Figure A2. Protein molecular weight calibration curve at 280 nm of whey protein standards: ■:BSA, ■:β-LG and ■:α-LA.